STOCHASTIC SECTION MODULUS REQUIREMENT FOR CARBON FIBRE REINFORCED PLASTIC PULTRUDED BEAMS

BY

Bulus BZIGU

DEPARTMENT OF CIVIL ENGINEERING

AHMADU BELLO UNIVERSITY, ZARIA

NIGERIA

JULY, 2015

STOCHASTIC SECTION MODULUS REQUIREMENT FOR CARBON FIBRE REINFORCED PLASTIC PULTRUDED BEAMS

BY

Bulus BZIGU, B.ENGR. (MAIDUGURI) 2009

(M.Sc./ENG/14950/2011-2012)

A THESIS SUBMITTED TO THE SCHOOL OF POSTGRADUATE STUDIES

AHMADU BELLO UNIVERSITY, ZARIA

IN PARTIAL FULFILLMENT OF THE REQUIREMENT FOR THE AWARD OF

MASTER OF SCIENCE DEGREE IN CIVIL ENGINEERING

DEPARTMENT OF CIVIL ENGINEERING
FACULTY OF ENGINEERING
AHMADU BELLO UNIVERSITY, ZARIA
NIGERIA

JULY, 2015

DECLARATION

I declare that the work in this thesis entitled **Stochastic Section Modulus Requirement for Carbon Fibre Reinforced Plastic Pultruded Beams** has been carried out by me in the Department of Civil Engineering, Ahmadu Bello University Zaria. The information derived from the literature has been duly acknowledged in the text and a list of references provided .No part of this thesis was previously presented for another degree or diploma at this or any other institution.

Bulus BZIGU	_____	_____
Name of Student	Signature	Date

CERTIFICATION

The thesis titled **Stochastic Section Modulus Requirement for Carbon Fibre Reinforced Plastic Pultruded Beams** by **Bulus BZIGU** meets the regulations governing the award of the degree of Master of Science of the Ahmadu Bello University, Zaria, and is approved for its contribution to knowledge and literary presentation.

PROF. O. S. Abejide	_____	_____
Chairman, Supervisory Committee	Signature	Date
DR. J. A. Sadeeq	_____	_____
Member, Supervisory Committee	Signature	Date
DR. Y. D. Amartey	_____	_____
Head of Department	Signature	Date
PROF. A. Z. Hassan	_____	_____
Dean, School of Postgraduate Studies	Signature	Date

DEDICATION

With sincere thanks and profound gratitude, I wish to dedicate this project to God Almighty, the giver of life.

ACKNOWLEDGEMENTS

I am grateful to the Almighty God for giving me life to undertake this programmed. Special appreciation goes to my supervisors Prof. O. S. Abejide and Dr. J. A. Sadeeq for their guidance during the course of this work. I wish to acknowledge the cooperation and numerous supports received from members of my family and the entire staff of Civil Engineering Department, Ahmadu Bello University (ABU) Zaria. I also appreciate my classmates, friends and other members of the postgraduate class for their contributions and support during this research work.

ABSTRACT

Six Carbon Fibre Reinforced Plastic (CFRP) pultruded beam section from The Pultex® Pultrusion Design Manual Volume 4 - Revision 8 Copyright © 2004 by Creative Pultrusions Inc., were assumed to be simply supported doubly symmetric I-section, with uniformly distributed load of $3.5kN/m^2$ applied over the length of $3.050m$ each. A comparative analysis of section modulus effect under the load and resistance factor design (LRFD) and allowable stress design (ASD) was considered based on computer program using FORM5 and ABAQUS 6.10 CAE that was used to generate results for reliability and finite element analysis respectively. Safety indices generated for reliability analysis from FORM5 based on load and resistance factor design (LRFD) and allowable stress design (ASD) format by varying load ratio and section modulus was analyzed. The general conclusion from the results are that, the safety of all the beam section increased with increase in section modulus by average of 1.1% for both load and resistance factor design (LRFD) and allowable stress design (ASD) format. The implication of this is that, when the load and resistance factor design (LRFD) and allowable stress design (ASD) design format is employed, the reserved elastic moment of the carbon fibre reinforced plastic (CFRP) beams are fully utilized, with the possibility of the beam reaching its full elastic moment at higher loading, hence section modulus can be reduced, that would result in lower beam section. Also for finite element analysis (FEA) considered using ABAQUS 6.10 CAE in which the stresses, displacement, strain on the carbon fibre reinforced plastic (CFRP) pultruded beams obtained are analyzed and graphically presented and based on the design parameters, the deformation and the Von Mises stress distribution obtained indicates that, the field of high stress is only shown in Model 1 with $661.2N/mm^2$ which is minimal under the said load when compared to bending and tensile strength of $3300N/mm^2$ for carbon fibre reinforced plastic (CFRP).

TABLE OF CONTENTS

Cover Page	i
Title page	iii
DECLARATION	iv
CERTIFICATION	v
DEDICATION	vi
ACKNOWLEDGEMENTS	vii
ABSTRACT	viii
TABLE OF CONTENT	ix
LIST OF TABLES	xiii
LIST OF FIGURES	xiv
LIST OF SYMBOLS	xvii
CHAPTER ONE: INTRODUCTION	
1.1 General	1
1.2 Problem Statement and Justification of Research	7
1.3 Aim and Objectives	9
1.4 Scope of the Study	10
1.5 Limitations of the Study	10
CHAPTER TWO: LITERATURE REVIEW	
2.1 Overview	11
2.2 Mechanism of Stress Distribution	13
2.3 Elastic State	14
2.4 Mechanical Properties of Carbon Fibre Reinforced Plastic	15

2.5 Material Properties of Carbon Fibre Reinforced Plastic 15

2.6 Challenges in the Design of Fibre Composite Structures 21

2.7 Review of Existing Guidelines Design: Philosophy on FRP Reinforced Concrete Structures 22

2.7.1 European design guidelines 25

2.7.2 Japanese design guidelines 25

2.7.3 Canadian design guidelines 26

2.7.4 American design guidelines 27

2.8 Optimization Methods in Fibre Composite Structural Design 27

2.8.1 Concept of optimization 27

2.8.2 Structural optimization problem 29

2.8.3 Significance of optimization 30

2.8.4 Application of optimization 31

2.8.5 Multi-objective optimization 31

2.8.6 Multi-modal optimization 32

2.9 Design Sensitivity Analysis (DSA) 32

2.10 Reliability Based Design Optimization (RBDO) 34

2.11 Beam 35

2.11.1 Lateral-torsional buckling in simply supported pultruded beams 35

2.12 Structural Reliability 38

CHAPTER THREE: ANALYTICAL TECHNIQUES

3.1 Reliability Concept 42

3.2 Structural Reliability Method 43

3.3 Limit State Functions 46

3.3.1 Bending criterion and applied load 47

3.4 Stochastic Finite Element Method 49

3.5 Finite Element Analysis 51

3.5.1 Model assumptions 52

3.5.2 Modeling the CFRP pultruded beam using ABAQUS 6.10-1 52

3.5.3 Material properties input data for models and flow chart modeling for FEM 53

CHAPTER FOUR: RESULTS AND DISCUSSION

4.1 Model Geometry Description and Loading /boundary condition on the Beam 55

4.2 Finite Element Analysis using ABAQUS 6.10 CAE 57

4.3 Stress and Deformation Pattern in Model 1 57

4.4 Stress and Deformation Pattern in Model 2 59

4.5 Stress and Deformation Pattern in Model 3 60

4.6 Stress and Deformation Pattern in Model 4 62

4.7 Stress and Deformation Pattern in Model 5 63

4.8 Stress and Deformation Pattern in Model 6 65

4.9 Reliability Result from FORM5 for Flexure Failure. 66

CHAPTER FIVE: CONCLUSION AND RECOMMENDATION

5.1 Conclusion 73

5.2 Recommendation 74

REFERENCES 76

APPENDENCES 83

LIST OF TABLES

Table 3.1 Parameter of the Stochastic Model for LRFD and ASD Bending 49

Table 3.2 ABAQUS 6.10-1 Material Properties Input Data Models 53

Table A. Variation of Section Modulus at Various Load Ratios $G(x) = 0.75f_y s_x$ (LRFD-Format) 83

Table A2. Variation of Section Modulus at Various Load Ratios $G(x) = 0.65f_y s_x$ (LRFD-Format) 83

Table A3. Variation of Section Modulus at Various Load Ratios $G(x) = 0.75f_y s_x$ (ASD-Format) 84

Table A4. Variation of Section Modulus at Various Load Ratios $G(x) = 0.65f_y s_x$ (ASD-Format) 84

Table A5. ABAQUS 6.10 CAE Output Field Data for Model 1 85

Table A6. ABAQUS 6.10 CAE Output Field Data for Model 2 85

Table A7. ABAQUS 6.10 CAE Output Field Data for Model 3 86

Table A8. ABAQUS 6.10 CAE Output Field Data for Model 4 86

Table A9. ABAQUS 6.10 CAE Output Field Data for Model 5 87

Table A10. ABAQUS 6.10 CAE Output Field Data for Model 6 87

LIST OF FIGURES

Figure 2.1 Stress-Strain Relationships for Fibre, Matrix, and FRP 13

Figure 2.2 Stress Distributions in Compression Failure showing Force in Stress Block and FRP reinforcement 14

Figure 3.1 Simply Supported Beams with a Symmetric Cross-section Subjected to Uniformly Distributed Loading (Dead load $G_{k,}$ and Imposed load Q_k) 47

Figure 3.2 Sections A - A 47

Figure 3.3 Flow chart modeling for FEM ABAQUS 6.10-1 54

Figure 4.1 Proposed CFRP Pultruded Beams Section for the Models (ABAQUS 6.10 CAE) 56

Figure 4.2 Loading and Boundary Condition on Pultruded CFRP Beam Section in (ABAQUS 6.10 CAE) 56

Figure 4.3 Von Mises Stress Diagram of 76.2x38.1x6.35*mm* (Part# IB340) 1500/1525/1625 Series 58

Figure 4.4 Strain and Displacement Graph of 76.2x38.1x6.35*mm* with Corresponding Stresses under the Applied Load 58

Figure 4.5 Von Mises Stress Diagram of 101.64x50.8x6.35*mm* (Part# IB440) 1500/1525/1625 Series 59

Figure 4.6 Strain and Displacement Graph of 101.6x50.8x6.35*mm* with Corresponding Stresses under the Applied Load 60

Figure 4.7 Von Mises Stress Diagram of 152.4x76.2x6.35*mm* (Part# IB640) 1500/1525/1625 Series 61

Figure 4.8 Strain and Displacement Graph of 152.4x76.2x6.35*mm* with Corresponding Stresses under the Applied Load 61

Figure 4.9 Von Mises Stress Diagram of 152.4x101.6x9.525*mm* (Part# IB660) 1500/1525/1625 Series 62

Figure 4.10 Strain and Displacement Graph of 152.4x101.6x9.525*mm* with Corresponding Stresses under the Applied Load 63

Figure 4.11 Von Mises Stress Diagram of 203.2x101.6x9.525*mm* (Part# IB860) 1500/1525/1625 Series 64

Figure 4.12 Strain and Displacement Graph of 203.2x101.6x9.525*mm* with Corresponding Stresses under the Applied Load 64

Figure 4.13 Von Mises Stress Diagram of 203.2x101.6x12.7*mm* (Part# IB880) 1500/1525/1625 Series 65

Figure 4.14 Strain and Displacement Graph of 203.2x101.6x12.7*mm* with Corresponding Stresses under the Applied Load 66

Figure 4.15 Variation of Safety Index (β) with Load Ratio (α) for $G(X) = 0.75 f_y S_x$ LRFD Format 67

Figure 4.16 Variation of Safety Index (β) with Load Ratio (α) for $G(X) = 0.65 f_y S_x$ LRFD Format 67

Figure 4.17 Variation of Safety Index (β) with Load Ratio (α) for $G(X) = 0.75 f_y S_x$ ASD Format 68

Figure 4.18 Variation of Safety Index (β) with Load Ratio (α) for $G(X) = 0.65 f_y S_x$ ASD Format 68

Figure 4.19 Variation of Safety Index (β)-Von Mises Stress for $G(x) = 0.75 f_y s_x$ LRFD Format 69

Figure 4.20 Variation of Safety Index (β)-Von Mises Stress for $G(x) = 0.75f_ys_x$ ASD Format 70

Figure 4.21 Displacement-Load Ratio Graph under the Applied Load 71

Figure 4.22 Von Mises Stress - Section Modulus Graph under the Applied Load 71

LIST OF SYMBOLS

S_L	*Live load*
S_D	*Dead load*
α	*Dead to live load ratio given by G_k / Q_k*
ϕ	*Partial safety factor*
γ_D	*Partial safety factors for dead load*
γ_L	*Partial safety factors for live load*
A_f	*Area of flange (mm^2)*
A_{fa}	*Net area of one set of flange angle (mm^2)*
A_g	*Gross cross-sectional area of the member*
ASD	*Allowable stress design*
A_w	*Area of web (mm^2)*
b	*Width of the section (mm)*
C_b	*Coefficient that accounts for the moment distribution along the unbraced portion of the beam taken from AISC (2005)*
CFRP	*Carbon Fibre Reinforced Plastic*
C_P	*Load application location constant*
$C\omega$	*Warping constant*
d	*Depth of the section (mm)*
d_i	*Interior depth of a beam (mm)*
d_w	*Web depth measured from angle to angle (mm)*
E_f	*Elastic flexural modulus*

$E(\xi)$	*Estimate of the real response (or error)*
E	*Modulus of elasticity*
E_b	*Full section flexural modulus*
E_L	*Longitudinal compression modulus,*
f_b	*Bending stress (N/mm^2)*
FRP	*Fibre Reinforced Plastic*
G	*Elastic shear modulus*
G_b	*Full section shear modulus*
G_k	*Dead load*
i	*Safety-index*
I	*Second moment of area (mm^4)*
I_y	*Second moment of area about the weak axis of the member*
J	*Torsional constant*
K	*Effective-length factor*
k_f	*Effective length coefficient for flexural buckling about the weak axis*
k_ω	*Effective length coefficient for torsional buckling of the section*
l	*Span of the beam(mm)*
L_b	*Braced length against twist of the cross section*
LRFD	*Load and Resistance Factor Design*
M_A	*Absolute value of moment at quarter point of the unbraced segment*
M_B	*Absolute value of moment at the centerline of the unbraced segment*

M_C	*Absolute value of moment at three-quarter point of the unbraced Segment*
M_{max}	*Absolute value of maximum moment in the unbraced segment*
M_{max}	*Maximum bending moment (N-mm)*
$P(g_i(x) \leq 0)$	*The probability*
$\boldsymbol{\sigma}_{max}$	*Maximum stress (N/mm^2)*
Q_k	*Imposed load*
R	*Member resistance*
r	*Radius of gyration*
S	*Section modulus (mm^3)*
S_x	*Section modulus about the strong axis*
t	*Thickness of the section*
V_{TL}	*Major Poisson's ratio*
w	*Design load*
x	*Design variable*
y	*Distance between the bottom surface of the beam to its centroid (mm)*
β	*Reliability index*
Φ	*Integral value*

CHAPTER ONE

1.0 INTRODUCTION

1.1 General

Structures are designed and constructed to supply sufficient capacity against vertical and lateral load demands with the purposes of providing life safety and preventing collapse. However, many examples of catastrophic results such as failure or damage of buildings, bridge piers, etc., are seen all over the world. These can be due to intentionally or unintentionally created deficiencies during service life and lack of control that needs to be provided both at the design and construction stages (Ümit, 2007). By definition, Fibre Reinforced Plastic (FRP) is a composite of two material groups: (1) reinforcing fibre which provides the strength; and (2) polymer resin matrix such as epoxy, to bind the reinforcements together (Nanni, 1999).

During the last two decades, Fibre Reinforced Polymer (FRP) composite materials have seen a steady increase in their applications for construction. They have been increasingly popular because of their advantages over conventional construction materials including a high strength-to-weight ratio, corrosion resistance leading to increased durability and lower maintenance costs, and their ability to be pultruded into various shapes whose mechanical properties can be custom-tailored for specific applications (Bank, 2006). However, significant barriers for wide-spread adoption still remain which include their high initial cost, the lack of understanding of their physical behaviour by practicing engineers, and the lack of a reliability based on Load and Resistance Factor Design (LRFD) standard governing their design (Ellingwood, 2003).

Carbon Fibre Reinforced Plastic (CFRP) pultruded materials have been around for several decades as an engineering material. They are composed of unidirectional fibres or roving, usually made of glass, which are reinforced with continuous filament mats oriented in different directions and bound together with plastic resin (Michael, 2009).

These materials are pultruded together to form many different types of products including structural shape; these shapes include angles, channels, square tubes, rectangular (box) and round tubes, tees, I-sections and wide-flange sections (W-sections). The final product is a brittle material which tends to have a lower strength and lower modulus of elasticity than a similarly sized steel section (Michael, 2009). Since it is made of a high percentage of unidirectional fibres it is strongest and stiffest in the longitudinal direction of the fibres and weaker in the transverse and shear directions making it an orthotropic material. Also, in an attempt to maximize the efficiency of the section for bending, it is common for more unidirectional material to be put in the flanges and more bi-directional material to be put in the web. This means that in addition to Fibre Reinforced Plastic (FRP) beams being orthotropic due to their different strength and stiffness in different directions they can also be macroscopically non homogeneous because of the different make, up of the flanges and web (Michael, 2009). Fibre Reinforced Plastic (FRP) does have several important advantages over steel; it is approximately 2 to 7 times lighter or less dense, more fire resistant, it is not an electrical conductor, it has good fatigue properties and most importantly it does not corrode.

This means Fibre Reinforced Plastic (FRP) materials require less maintenance, have a long life and low life-cycles costs. Because it was previously not economical to design large scale building frames using Fibre Reinforced Plastic (FRP), it was relegated to smaller scale applications for structures as well as reinforcing existing structures or specific applications where some of its advantages such as corrosion resistance or electrical insulation were required (Michael, 2009). More recently however, Fibre Reinforced Plastic (FRP) materials have begun to be more economically competitive with traditional construction materials and in the near future it may be a reasonable option to design large scale Fibre Reinforced Plastic (FRP) framed structures (Michael, 2009). If this will happen there needs to be a standard that a building code can reference which will govern the design of all aspects of a Fibre Reinforced Plastic (FRP) structure (Michael, 2009).

Luigi *et al.,* (2012) noted that pultruded Fibre Reinforced Polymers (FRP) thin-walled beams are now being used in Civil Engineering for new constructions. According to them the main applications are pedestrian bridges and bridge decks, but there are some applications also in building structures. Due to their longitudinal high strengths and stiffnesses, current Fibre Reinforced Plastic (FRP) profiles are characterized by very slender proportions and high strength to weight ratio. The failure of this kind of structural elements subject to compressive loads is generally caused by instability phenomena. In fact, the thin-walled sectional geometry of the members and the relatively low shear stiffness of the composite materials, given by the resin mechanical properties, may significantly affect the ultimate load of pultruded Fibre Reinforced Plastic (FRP) beams, with it typically being characterized by either local or global buckling load.

Michael, (2009) noted that the first step that should be done is to actually identify all of the limit states that may governed Fibre Reinforced Plastic (FRP) beam in bending, these limit states must account for failure modes due to strength, instability as well as serviceability. He suggested that for beams under flexural stresses, the failure modes to be identified is flexural rupture in tension or compression, local flange buckling, local web buckling and lateral-torsional buckling. For beams under shear stresses, the failure modes were identified as shear rupture and web shear buckling. Flange shear buckling is not a concern because the flange of a section has very low shear stresses compared to the web; so web shear buckling will always occur first. These failure modes for flexure and shear account for all strength failure modes for the section as well as instability failure modes for all elements of the section. For beams with concentrated forces, the failure modes to be identified is rupture of the web due to the concentrated force in tension or compression, bearing failure at supports, web compression buckling and web crippling. These failure modes account for strength failure and global instability of the web (web compression buckling) as well as local instability of web near the location of load application (web crippling). A final limit state to be identified is serviceability due to deflections, in addition to these failure modes which specifically apply to beams in bending, interlaminar shear failure may occur in any pultruded member, this can be addressed, however, by always checking the maximum shear stress in the beam against the interlaminar shear strength (Michael, 2009). Although the Carbon Fibre Reinforced Plastic (CFRP) has the strength comparable to that of steel; its stiffness is only one tenth.

Thus, the design of long-span Carbon Fibre Reinforced Plastic (CFRP) beams will usually be controlled by deflection instead of the strength, resulting in the use of larger sections to satisfy the deflection requirements. This problem will lower the potential of using the Carbon Fibre Reinforced Plastic (CFRP) in the construction market. To adequately serve present and future needs, Carbon Fibre Reinforced Plastic (CFRP) structural members need to be rehabilitated. In view of this problem, the stiffness of Carbon Fibre Reinforced Plastic (CFRP) composite needs to be improved (Seangatith, 2001).

Chikh *et al.*, (2012) has suggested that there is a need to employ innovative materials which can provide quick and reliable solutions to the problems of civil infrastructures that are deteriorating due to environmental effects and steadily increasing load levels. With the recent advances in composite materials technology, Fibre Reinforced Polymers (FRP) have opened new horizons in the civil engineering field to repair and retrofit existing infrastructures or to design new infrastructures. Carbon Fibre Reinforced Plastics sheets or plates are well suited to this application because of their high strength-to weight ratio, good fatigue properties, and excellent resistance to corrosion. Their application in civil engineering structures has been growing rapidly in recent years, and is becoming an effective solution for strengthening deteriorated concrete members. Because Carbon Fibre Reinforced Plastic (CFRP) is quickly and easily applied, their use minimizes labour costs and can lead to significant savings in the overall costs of a project.

Chikh *et al.*, (2012) noted that the compression behaviour of Carbon Fibre Reinforced Plastic (CFRP) wrapped specimens was mostly similar in each experiment series he conducted in terms of stress-strain curves and failure modes of the specimens. No lateral deflection was observed during all tests. All confined concrete columns failed by fracture of the composite wrap in a sudden and explosive way which was preceded by typical creeping sounds. Regarding square columns, failure occurred at one of the corners, because of the high stress concentration. For short specimens, the fibre rupture starts mainly in their central zone and then propagates towards other sections. But for slender specimens, the collapse was mostly concentrated in their end regions, indicating that the greater the slenderness ratio, the smaller the area of Carbon Fibre Reinforced Plastic (CFRP) ruptured (Talat and Ahmed, 2010).

Talat and Ahmed, (2010) concluded in their work that the material properties of Carbon Fibre Reinforced Plastic (CFRP) laminates have been greatly improved over the last few years, with a wide variety of dimensions and strengths required to achieve significant stiffness increases. Carbon Fibre Reinforced Plastic (CFRP) materials with a modulus of elasticity approximately twice that of structural steel have become available, several researchers have indicated that these materials can be used to increase the strength and stiffness of steel-concrete composite beams. The consideration of Carbon Fibre Reinforced Plastic (CFRP) plate end debonding as critical failure mode should be avoided in order to prevent an undesirable failure of the system. Also from their work experimental data and datasheets were developed to catalogue this result, while a commentary was drafted as a supplement to the standard.

1.2 Problem Statement and Justification of Research

In limit state design, the structural inadequacy or failure is expressed through the following equation,

$$\phi R = \gamma_D S_D + \gamma_L S_L \qquad 1.0$$

where R is the member resistance, ϕ is the partial safety factor of R, S_D and S_L are the dead and live load effects respectively γ_D and γ_L are the partial safety factors on S_D and S_L respectively. Equation (1.0) was originally developed during the 1960's for reinforced concrete codes (Melchers, 1987). It enables the live load to have a greater "partial" safety than the dead load, a view of the former greater uncertainty it allowed a measure of workmanship variability and uncertainties about resistance modelling to be associated with the resistance (MacGregor, 1976).

In the Allowable Stress Design (ASD) method, factor of safety is already accommodated in the strength of engineering structures to come up with what is known as permissible stress. Safety factor is not applied to the applied loading and the design is satisfied, when the induced stress is less than the permissible stress. The permissible stress is usually limited to the yield stress.

It is a well-known fact that the maximum stress in a beam is given by;

$$\sigma_m = \frac{M_{\max}}{S} \qquad 1.1$$

where M_{max} the maximum bending moment and S is the section modulus.

For simply supported beam, which is assumed in this work, the maximum bending moment is given by.

$$M_{\max} = \frac{wl^2}{8} \tag{1.2}$$

and, the section modulus is given by;

$$S = \frac{I}{y} \tag{1.3}$$

where, w is the design load; l is the span of the beam; I is the beam second moment of area (moment of inertia); y is the distance between the bottom surface of the beam to its centroid. It is clear that, section modulus play an important role in the strength capacity of beams. The time-rate deterioration of structural members over the years has been a problem that still needs to be properly investigated especially when the said structural members are in use during their designed service life span. The need for a probabilistic check on the structural strength durability and efficiency while in service must be thoroughly defined in order to ascertain the time rate of failure, cause of failure and design life span of the member in question. The concept of service life prediction for Carbon Fibre Reinforced Plastic structures is becoming an area of increasing interest for engineers. Therefore, a good understanding of the concept and its application in structural design is essential to ensure that optimum performance is achieved before a costly repair to the structure becomes necessary (Humphery, 2003).

It is on this basis that the section modulus of pultruded Carbon Fibre Reinforced Plastic (CFRP) beams in a stochastic environment is considered in this work in order to provide greater confidence on the use of this innovative material in civil engineering structures.

The stochastic environment is necessitated by the variability in the production of Carbon Fibre Reinforced Plastic (CFRP) and the loading and construction process that maybe employed. This is exactly the reasons that motivated this work, which is highly justified. However there are no rules yet for Carbon Fibre Reinforced Plastic (CFRP) sections and hence, there is the need to develop one along this line.

1.3 Aim and Objectives

The aim of this research is to ascertain section modulus requirement on the deterministic and probabilistic design of simply supported carbon fibre reinforced plastic (CFRP) pultruded beams sections through application of the Finite Element Method in terms of statistical simulation analyses.

The research objectives include;

1. Stochastic evaluation of flexural capacity of a CFRP pultruded beam only. The limit state functions for pultruded beam sections would be developed with regard to both LRFD and ASD formats.
2. Identify the basic design variables for each of the reliability function, and perform uncertainty modelling to generate the statistics of the basic variables, that include mean, coefficient of variations and distributions models.
3. Perform reliability analysis of the beam subjected to uniformly distributed loading using First Order Reliability Method (FORM) through FORTRAN computer program to be developed with the view to generate safety indices for varying dead to live load ratios and section modulus.

4. Assess the effect of varying load ratios and sections modulus of the CFRP beams design based on Load and Resistance Factor Design (LRFD) and Allowable Stress Design (ASD) formats.

1.4 Scope of the Study

In this study, a CFRP pultruded beam with doubly symmetrical section will be analysed. Only uniformly distributed load would be considered. And the beam failure is assumed when its flexural capacity is exceeded. First Order Reliability Method would be used with parametric stochastic models generated from secondary sources. Also Finite Element model will be observed using ABAQUS 6.10 CAE.

1.5 Limitations of the Study

This study is limited only to the evaluation of section modulus in the performance for structural safety in flexure of CFRP pultruded beams. The data employed are as obtained from literature and without any experimental verification of authentic publication.

CHAPTER TWO

2.0 LITERATURE REVIEW

2.1 Overview

For a structure to remain safe or serviceable throughout its design period, its safety is determined by the magnitude of deformation that can be tolerated. No matter the magnitude of deformation that can be allowed, other important parameters that need to be taken into account when designing a structure include tensile strength, yield strength, young modulus, ductility and most importantly section modulus which is directly related to the strength of the structure (Ibrahim, 2003).

In structural engineering, the section modulus of a beam is the ratio of a cross section second moment of area to its greatest distance from the neutral axis and which is the measure of the ability of the beam to resist bending moment (Ibrahim, 2003).

In AISC document "Basic design values (available at www.aisc.org/2005 spec); placed the LRFD values for bending as F_yS_y rather than F_yZ_y which shows translation between the elastic modulus (S_y) and plastic modulus (Z_y) for steel. It is on this basic that this work, which is "comparison of section modulus effect in deterministic and probabilistic design of Carbon Fibre Reinforced Structures", is thought very essential. As earlier stated the ability of Carbon Fibre Reinforced Plastic to resist bending moment about a given axis depends on its section modulus. The value is given as;

$$M\left(\frac{m_i}{y_e}\right) = \frac{M}{S} \qquad 2.0$$

where m_i = second moment of area in mm^4

If a beam is subjected to some bending moment, the stress at the extreme fibre of the given steel and Carbon Fibre Reinforced Plastic is given by;

$$F_b = M\left(\frac{mi}{y_e}\right) = \frac{M}{S} \qquad 2.1$$

where; F_b = induced stress in the extreme fiber of the shape in N/mm^2

M = moment force applied to the shape in *N-mm*

y_e = distance from the neutral axis to the shape in *mm*.

S = section modulus of the shape in mm^3

m_i = cross section moment of area in mm^4.

The following equation can be used to approximate the section modulus of beams and girders (Deduct the area of the rivet or bolt hole from the used area).

$$S = d_w\left(A_f + \frac{A_f}{6}\right) + d_i A_{fa} \qquad 2.2$$

where; S = the section modulus in mm^3

d_w = the web depth measured from angle to angle in *mm*

A_f = the area of flange inmm^2

A_w = the area of web in mm^2

d_i = the interior depth of a beam in *mm*

A_{fa} = the net area of one set of flange angle in mm^2

2.2 Mechanism of Stress Distribution

Fibre Reinforced plastic (FRP) materials are composed of high strength fibres embedded in a polymer matrix. The fibers, which have very small diameters and are generally considered continuous which provide the strength and stiffness of the composite, while the matrix, which has comparatively poor mechanical properties, separates and disperses the fibres. The primary function of the matrix is to transfer loads to the fibres through shear stresses that develop at the fibre-matrix interface, although it is also important for environmental protection of the fibres. In concrete reinforcing applications, the fibres are generally carbon (graphite), glass, or aramid (Kevlar), and the matrices are typically epoxies or vinyl esters. The Figure 2.1 below shows typical stress-strain curves for fibres, matrices, and the FRP materials that result from the combination of fibres and matrix. (ISIS, 2011)

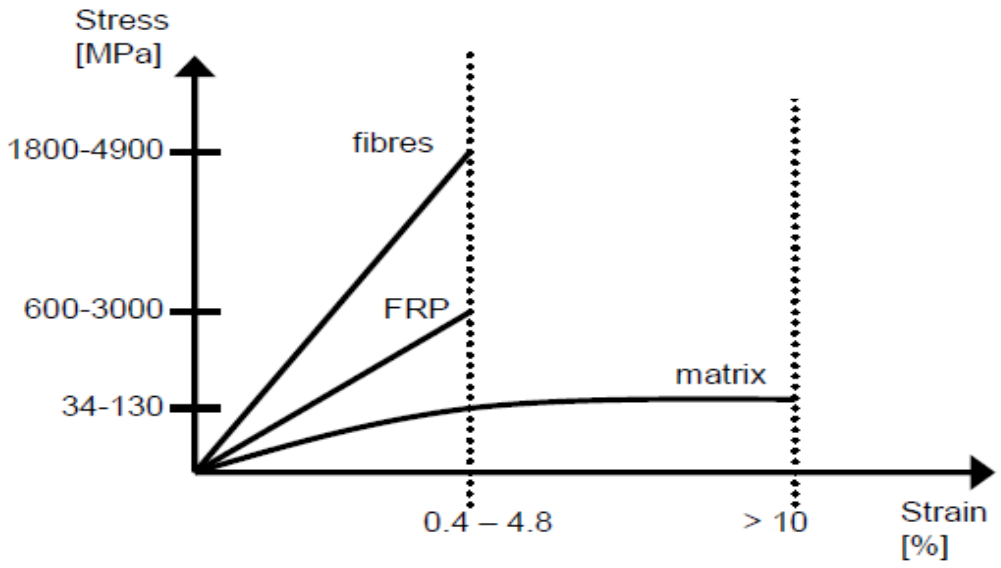


Figure 2.1 Stress-Strain Relationships for Fibre, Matrix, and FRP

Similarly, the stress distribution in compression failure showing forces in stress block and FRP reinforcement of beam section is shown below in Figure 2.2.

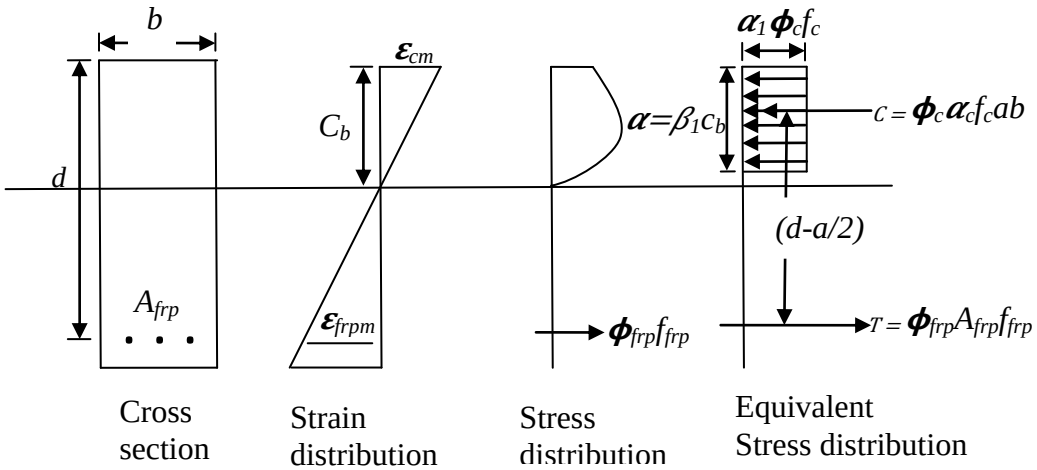


Figure 2.2 Stress Distributions in Compression Failure showing Forces in Stress Block and FRP Reinforcement.

2.3 Elastic State

For low values bending moments, the maximum extreme fiber stress will be within the elastic range as indicated in Figure 2.2 the limiting condition for elastic behavior will be reached when the maximum stress reaches the value $\sigma_{\max}$

Maximum elastic response;

M_y = (Yield)(Area)(Lever arm)

$$= \sigma_{\max}\left(\frac{bd}{4}\right)\left(\frac{2d}{3}\right)$$

$$= \sigma_{\max}\left(\frac{bd^2}{6}\right)$$

$$= \sigma_{\max}\varepsilon_e \qquad 2.3$$

$$\varepsilon_e = \left(\frac{bd^2}{6}\right) \qquad 2.4$$

where; b = width of the section in *mm*, d = depth of the section in *mm*, σ_{max} = maximum stress in *N/mm* and ε_e = elastic modulus in mm^3.

2.4 Mechanical Properties of Carbon Fibre Reinforced Plastic

The ultimate strength of FRP is stronger than that of steel for same diameter; however unlike steel the compression strength is less than the tensile strength. The strength is close to 7-10 times that of steel. The stress-strain diagrams for FRP show it is linearly elastic to rupture. The stresses in Glass FRP (GFRP) bars are well below ultimate when failure occurs. The modulus of elasticity is twenty to twenty-five percent of that of steel, lower modulus of elasticity of FRP may lead to the deflection; lower stiffness produces load deflection that is almost linear. At ultimate load, deflection in GFRP is double that of steel, but due to the higher strength and ductility at failure, deflection of the steel reinforcing is greater (Saadatmanesh, 1994). The specific gravity of FRP material is a quarter of that of steel which makes it easier to handle. FRP and concrete have similar coefficients of thermal expansion which will aid in its use. The bond strength of FRP reinforcement is not as high as steel reinforcing bars, but then again epoxy coated bars reduce bond strength (Bedard, 1992). The bond strength has been determined to be two-thirds that of steel reinforcement (Brown, 1993).

2.5 Material Properties of Carbon Fibre Reinforced Plastic

The use of FRP as reinforcement has the following advantages of light weight, high tensile strength, corrosion resistance, flexibility, and electromagnetic resistance (Khalifa *et al.*, 1993). The disadvantages of FRP are low modulus of elasticity, higher cost, low failure strain, anchorage methods, bond to concrete, and ultraviolet light sensitivity.

Fibre Reinforced Plastic (FRP) can be made of carbon, aramid or glass, fibre reinforced plastics are often made by the pultrusion process. The fibers are impregnated with a resin and pulled through a dye that forms the geometry of the section. The sections can be hollow tubes, I-shape or round rods. The round rods are wrapped with additional fiber to form ribs which aids in the bonding to concrete (Saadatmanesh, 1994). Hooks and bends are difficult to make, it may be necessary to make connections like plumbing or use grids where straight sections will not work (Bedard, 1992). Carbon and aramid FRP can have high fatigue characteristics, three times more than steel, glass fatigue characteristics are generally less than steel. Of the three types of FRP, mentioned here, Carbon Fibre Reinforced Plastic (CFRP) has the highest tensile properties. Aramid FRP (AFRP) has the higher strain at failure, but also is most affected by water. Glass FRP (GFRP) is the least expensive and is sand finished for better bonding properties (Erki and Rizkalla, 1993). FRP material resists temperatures as high as 225°F (107.2°C). At temperatures in excess of 400°F (204.4°C), FRP reinforcement loses some of its flexural capacity, high temperature areas could prevent the use of FRP in bridges (Brown *et al.,* 1993). With increasing popularity of the carbon fibre reinforced polymers in structural engineering projects, vast amount of studies have been conducted all over the world. In this section, some of the important studies in literature, as they relate to this study, are presented.

De Loranzis *et al*. (2001) conducted beam tests to examine the flexural bond capacity of FRPs and to determine the effects of bond length, size effect, FRP stiffness, and sheet width on the FRP bond capacity. As a result, design expressions for peeling stresses, effective bond length, and FRP ultimate strain, which can be used in controlling bond failure, was proposed. They pointed out that failure occurred at concrete adhesive interface without any significant damage of concrete and added that the concrete strength did not affect the ultimate load.

Seangatith (2001) conducted a study on optimization of pultruded GFRP beam bonded with CFRP Plates. In his study, the geometric variables of the beam are the optimized design variables, and the rest of the design variables including the material properties of both GFRP and CFRP, types of loading, and allowable deflection are fixed. Based on the ASCE (1984), Structural Plastic Design guideline, the assumptions and constraint equations can be written in the following mathematics forms:

1. The allowable deflection constraint.

$$g(1) = \frac{-I_{x.opt}}{I_{x.\min}} + 1 \qquad 2.5$$

where $I_{x,opt}$ and $I_{\text{x,min}}$ are the optimized moment of inertia and minimum moment of inertia of the beams cross-section about the *x*-axes, respectively. The shear deformations and thick-walled correction factors can be included in the calculation of $I_{x,opt}$. The term $I_{x,min}$ is determined based on the allowable deflection.

2. The allowable ultimate stress constraint.

$$g(2) = \frac{f_b}{F_b} - 1 \qquad 2.6$$

where $f_b = M_x / S_x$ is tensile or compressive stresses, M_x is the bending moment, S_x is the minimum elastic section modulus of the beam's cross section, F_b is allowable tensile or compressive stress of the GFRP.

Bank (1989), evaluated the flexural and shear moduli of full section fibre reinforced plastic (FRP) pultruded beams with the use of full section tests to characterize the mechanical properties of thin-walled fibre composite material beams. Full section tests were performed to verify structural behavior that is predicted from analysis based on composite material properties. An experimental methodology was described which allows simultaneous determination of the flexural section and the section shear modulus full section beams for use in a shear deformation beam theory. ASCE has issued a structural plastic design manual (ASCE structural plastic design manual, 1984) which was intended to be a guideline for engineers who work with structural plastics (Seangatith, 2004). The manual recommends that the buckling resistance of single angle member subjected to axially compressive load can be approximated by the lower value determined from the flexural buckling and torsional buckling equations. For the members failing in flexural buckling, the flexural buckling strength $\sigma_{xc,F1}$ can be calculated from Euler's flexural buckling equation:

$$\sigma_{xc,F1} = \frac{\pi^2 E}{(KL/r)^2} \qquad 2.7$$

where, E is the modulus of elasticity for bending in the direction of buckling, L is the length, K is the effective-length factor, and r is the radius of gyration in that direction. For the members failing in torsional buckling, the torsional buckling strength $\sigma_{xc,T}$ can be estimated from the torsional buckling equation for linearly elastic isotropic materials:

$$\sigma_{xc,T} = \frac{E_L}{2(1+V_{LT})}\left(\frac{t}{b}\right)^2 \qquad 2.8$$

where E_L is the longitudinal compression modulus, V_{TL} is the major Poisson's ratio, and t and b are the leg thickness and the leg width of the section, respectively. It is well known that the value of the term E_L / [2(1+V_{LT})] for GFRP is always greater than that of the in-plane shear modulus G_{LT}, by over two times (Seangatith, 2004). Thus, Equation (2.8) always overestimates the torsional buckling strength of the GFRP structural members. For the members failing in flexural-torsional buckling, the buckling strength can be approximated by using an interaction relationship between the flexural and torsional buckling strength equations. A few forms of the relationship are proposed, but is not specified, being left to the judgement of the designer.

Zureick and Steffen (2000) presented the results of a study on the short term behavior of concentrically loaded single angle members; made of pultruded glass fibre reinforced polymeric materials. A total of 25 specimens were tested with KL/r ratios ranging from 30 to 105 and b/t ratios of 8, 10.7, 12, 16, and 24. Under axial compression, the GFRP angle members buckle in either flexural or flexural torsional mode. Analytical equations that describe the buckling behavior of especially orthotropic, centrally loaded, equal-leg angle section were derived. The compression and in-plane shear coupon tests of the material from each specimen were also conducted. The results were statistically analyzed to obtain the 95% lower confidence limit on the fifth percentile strength and modulus values. These material properties were used in the analytical buckling equations to correlate the test results to the analytical results in order to obtain the design strength, ϕP_n, of the angle members.

It is proposed that the nominal strength, P_n, of the members, can be taken as the lowest value determined in accordance with the limit states of the flexural buckling, the flexural-torsional buckling, and the material compression strength. For the limit state of the flexural buckling, the nominal buckling load is determined by using the Equation (2.9).

$$P_n = \frac{\pi^2 E_L}{(KL/R)^2} A_g \qquad 2.9$$

where E_L is the longitudinal compressive modulus of elasticity and A_g is the gross cross-sectional area of the member. It should be noted that Equation (2.9) is similar to Equation (2.7), except that E is replaced by E_L. For the limit state of the flexural-torsional buckling the nominal buckling load is determined by using the Equation (2.10)

$$P_n = 0.9 \frac{G_{LT}}{(b/\mathrm{t})^2} A_g \qquad 2.10$$

Equation (2.10) is similar to Equation (2.8), except that the term E / [2(1 + V_{LT})] is replaced by the in-plane shear modulus, G_{LT}, obtained experimentally from the in-plane shear coupon test, and the factor of 0.9 was proposed based on the approximation that the flexural-torsional buckling load is approximately equal to 90% of the torsional buckling. For the limit state of the material compressive failure, the nominal strength is determined by

$$P_n = \sigma_L^C A_g \qquad 2.11$$

where σ_L^C is the ultimate longitudinal compressive strength of the GFRP material, by using Monte Carlo simulation, the resistance factor, $\boldsymbol{\phi}$, was proposed as follows: $\boldsymbol{\phi}$ = 0.65 for the flexural buckling limit state; for the flexural torsional buckling limit state; and for the

material compressive limit state. It can be seen that Equation (2.9) and (2.10) are a better-developed form of Equation (2.7) and (2.8) respectively.

It is well-known that a number of design equations for the concentrically loaded GFRP equal-leg angle members have been proposed by the GFRP manufacturers. Most of these equations are practical and easy to use. They have been developed based on full-scale test results of the structural members and curve fitting, these equations are, however, recommended to be used only for their products. From the review of the previous research works, it is believed that the buckling strength equations of the GFRP equal-leg angle structural member subjected to the concentric axial compression can be derived in a well-developed form without introducing any curve-fit-based coefficients or flexural-torsional buckling related factors. In addition, since the GFRP material has a high E_L/G_{LT} ratio or high orthotropy, which is usually in the range of two to four times as high as that of the steel (Zureick and Scott 1997; Seangatith, 1999; Mottram 2004), it exhibits a larger effect from shear deformation when compared with that of the isotropic material. Therefore, the effect of the transverse shear should be included into the buckling stress equations, and hence a more realistic behavior of the structural member can be determined.

2.6 Challenges in the Design of Fibre Composite Structures

Many researchers have accepted that the traditional materials such as wood, steel and concrete lose the battle against corrosion. New construction technologies have been trailed using FRP materials as an alternative to traditional steel, concrete, and wood materials (Daly and Duckett, 2002). In addition, it use has been increasing for the repairing, strengthening and replacement of old structures. Therefore, the evaluation of fibre

composites in civil engineering applications is important to justify whether it is reliable enough to be used as a construction material.

Steel is a homogenous material with constant stiffness in all directions, while the FRP composite material has different stiffness in different directions. The fibre composite member designed for tension cannot be loaded with torsion forces (Loughlan, and Ahmed, 2008). Therefore, fibre composites are generally anisotropic, brittle, low modulus, and are highly dependent on the properties of its components matrix and fibre. The design of fibre composite structure is not only a shape or geometry design, the material itself should be included in the design process. Any design method for fibre composite structure has to consider the fibre plies design level and the overall geometry level of the structure.

2.7 Review of Existing Guidelines Design: Philosophy on FRP Reinforced Concrete Structures

Design guidelines for FRP reinforced concrete structures have been developed in Japan (JSCE, 1997), Canada (ISIS, 2001; CSA-S806, 2002), USA (ACI 440.1R-01, 2001; ACI440.1R-03, 2003; ACI 440.1R-06, 2006;ACI 440.1R-08, 2008), and Europe (Clarke *et al*., 1996); when dealing with FRP reinforcement the amount of reinforcement to be used has to be determined by a different approach, due to the lower stiffness and the high strength of composite materials. In fact, for FRP reinforcement, the strength to stiffness ratio in an order of magnitude is greater than that of steel, and this affect the distribution of stresses along the section. Hence, when considering a balanced section, a condition desired for steel reinforced concrete design, the neutral axis depth for FRP reinforced concrete sections would be very close to the compressive end. This implies that for such a section, large amount of the cross section is subjected to tensile stress and the compressive zone is

subjected to greater strain gradient. Hence, for similar cross section to that of steel, large deflection and less shear strength is expected (Pilakoutas *et al*., 2002).

The following sentence reported in the (ACI 440.1R-06 2006) can be considered as a principle that is universally accepted by the referenced guidelines: "These design recommendation are based on limit state design principles and that of FRP reinforced concrete member is designed based on its required strength and then checked for fatigue endurance, creep rupture endurance, and serviceability criteria. In many instances, serviceability criteria or fatigue and creep rupture endurance limit may control the design of concrete members reinforced for flexure with FRP bars (especially AFRP and GFRP that exhibit low stiffness)". Nevertheless, also significant differences occur among the available FRP reinforced concrete documents; for example, when considering the limit state philosophy, two main design approaches may be distinguished; if one takes into account the inequality:

$$R \geq S \tag{2.12}$$

where R is the resistance of member and S is the load effect, the two different design approaches are:

The American-like design approach, where Equation (2.12) becomes;

$$\varnothing R_n \geq S_u \tag{2.13}$$

R_n being the nominal strength of member (depending on the characteristic strength of materials); $\varnothing$ is a strength reduction factor and S_u is the corresponding design load effect, obtained by amplifying the applied loads by appropriate coefficients, α;

The Eurocode-like design approach, where Equation (2.12) becomes;

$$R_n \geq S_d \tag{2.14}$$

where R_u is the ultimate resistance of member, computed as a function of the design strength of material, derived by multiplying the characteristic materials strength by the material safety factors; and S_d is the design load effect, analogous to S_u. In conclusion the reduction applied on the resistance by the American Standards through the ∅ factor in the Eurocode-like Standards corresponds to the reduction applied on the materials resistance; in other words the nominal value of resistance computed in the American Standard is a function of the Eurocode-like characteristic (namely guaranteed in ACI codes) values of material strengths. In particular for the flexural design, all available guidelines on FRP reinforced concrete structures distinguish between two types of flexural failure, depending on the reinforcement ratio of balanced failure, ρ_{fb}, to be checked in the design procedure; if the actual reinforcement ratio, ρ_f, is less than ρ_{fb}, it is assumed that flexural failure occurs due to rupture of FRP reinforcement, where as if ρ_f is greater than ρ_{fb}, then it is assumed that the element will fail due to concrete crushing. In the ideal situation where ρ_f is equal to ρ_{fb}, the concrete element is balanced and hence, flexural failure would occur due to simultaneous concrete crushing and rupture of the FRP reinforcement. It should be noted that, for FRP reinforced concrete structures, the concept of balanced failure is not the same as in steel reinforced concrete construction, since FRP reinforcement does not yield and, hence, a balanced FRP reinforced concrete element will still fail in a sudden, brittle manner; accordingly, a concrete crushing failure can be considered as the ductile mode of failure of an FRP reinforced concrete section (Fico, 2007). A brief overview of the aforementioned guidelines is given.

2.7.1 European design guidelines

The European design guidelines by Clarke *et al* (1996) are based on modifications to British (BS8110, 1997) and European RC codes of practice (ENV 1992-1-1, 1992). The guidelines include a set of partial safety factors for the material strength and stiffness that take into consideration both the short and long term structural behavior of FRP reinforcement; and hence, the adopted values are relatively high when compared with the values adopted by other guidelines. The guidelines do not make any distinction between the two types of flexural failure and in addition, they do not provide clear indications about the predominant failure mode, which would result from the application of these partial safety factors.

2.7.2 Japanese design guidelines

The Japan Society of Civil Engineers (JSCE) design guidelines (JSCE, 1997) are based on modifications of the Japanese steel RC code of practice, and can be applied for the design of concrete reinforced or prestressed with FRP reinforcement; the analytical and experimental phases for FRP construction are sufficiently complete (ACI 440.1R-06, 2006). The JSCE places in between the two design philosophies reported, considering both material and member safety factors, that are slightly higher than the ones used for steel reinforcement; although the model adopted for the flexural design covers both types of flexural failure, there is no information about the predominant mode of flexural failure that would result from the application of the proposed partial safety factors. The guideline may also be utilized as a reference document, since it gives general information about different types of FRP reinforcement, quality specifications, and characterization tests for FRP materials.

2.7.3 Canadian design guidelines

The Canadian Standard Association (CSA) design guidelines CAN/CSA-S806-02 (2002) are the most recently issued Canadian guidelines on the design and construction of building components with FRP. In addition to the design of concrete elements reinforced or prestressed with FRP, the guidelines also include information about characterization tests for FRP internal reinforcement. The guideline was approved, in 2004, as a national standard of Canada, and is intended to be used in conjunction with the national building code of Canada (CSA A23.3, 2004). The document prescribes that ‘‘the factored resistance of a member, its cross sections, and its connections shall be taken as the resistance calculated in accordance with the requirements and assumptions of this Standard, multiplied by the appropriate material resistance factors. Where specified, the factored member resistance shall be calculated using the factored resistance of the component materials with the application of an additional member resistance factor as appropriate’’. In other words, the Canadian approach is that of material safety factors, with the exception of special cases (i.e. stability in compressed members; sway resisting columns; and flexure and axial load interaction and slenderness effects). As for the predominant mode of failure, the CSA S806-02 remarks that “all FRP reinforced concrete sections shall be designed in such a way that failure of the section is initiated by crushing of the concrete in the compression zone”. The Canadian network of centers of excellence on intelligent sensing for innovative structures has also published a design manual that contains design provisions for FRP reinforced concrete structures (ISIS, 2001).

The guidelines also provide information about the mechanical characteristics of commercially available FRP reinforcement. This guideline is also based on modifications to existing steel reinforced concrete codes of practice, assuming that the predominant mode of failure is flexural, which would be sustained due to either concrete crushing (compressive failure) or rupture of the most outer layer of FRP reinforcement (tensile failure).

2.7.4 American design guidelines

The American Concrete Institute (ACI) design guidelines for structural concrete reinforced with FRP Bars (ACI 440.1R-06, 2006) are primarily based on modifications of the ACI-318 steel code of practice (ACI 318-02, 2002). The document only addresses non-prestressed FRP reinforcement (concrete structures prestressed with FRP tendons are covered in ACI 440.4R).

2.8 Optimization Methods in Fibre Composite Structural Design

This section reviews the most popular optimization methods used in the design of fibre composite structures for civil engineering applications. The design optimization of civil engineering structures has specific design requirements or constraints regarding the serviceability of the structure during its design life.

2.8.1 Concept of optimization

The concept of optimization is basic in much of what we do in our daily lives: a desire to do better or be the best in one field or another. In engineering we wish to produce the best possible result with the available resources. In a highly competitive modern world it is no longer sufficient to design a system whose performance of the required task is just satisfactory, it is essential to design the best system.

Thus in “designing” new product in any field: aerospace, automotive, chemical, electrical, biomedical, agriculture, etc., we must use design tools which provide the desired results in a timely and economical fashion. Numerical optimization is one of the tools at our disposal (Vanderplaats, 2011).

Optimization is the most powerful design improvement tool that is available today. It is not debatable that optimization is useful. It has been successfully worked for many years. However, at the same time it is by no means a replacement for designer. It is also not a “push-button” tool that instantly produces the best result without human intervention. It is a process that reduces the design time, improves the design quality, and free engineers and designers for creative work by taking over tedious operations. Optimization is a very general automated design technique. In studying this technique it is determining the response of the specified system to the certain combination of input parameters. For example, calculating stresses in structures as a result of certain loads. Design on the other hand, means the process of defining a system. For example designing a structure would mean selecting specific dimensions and location of the structural members that will allow the structure to withstand the specific load. The alternative designs of the same system differ from each other because some parameters of the system are not the same. The parameters that could be changed in the system while searching for the best design are called design variables. Although we may not always think of it this way, design process may be defined as the process of finding the minimum or maximum of some characteristics, which may be called the objective function. For the design to be acceptable it must also satisfy certain requirements.

These requirements are called constraints. Optimization automatically changes the design variables in order to help us find the minimum or maximum of the objective function, while satisfying all the required design constraints (Vanderplaats, 2011).The optimization process may be broken down into the following steps (Vanderplaats, 2011).

(i) Find a research direction that will improve the objective.

(ii) Search in this direction until no more improvement can be made.

(iii) Repeat the process, until no search direction can be found that improves the objective.

The optimization problem formulation and the optimization process presented above are very general and can be applied to any design problem in any field (Vanderplaats 2011).

2.8.2 Structural optimization problem

The structural optimization problem can be posed as (Iyengar and Curtin, 1997); Minimize or maximize.

$$F = F(X_1, X_2, X_3 \ldots\ldots\ldots\ldots\ldots\ldots\ldots\ldots, X_n)$$

Subject to

$$C_1 = C_1(X_1, X_2, X_3 \ldots\ldots\ldots\ldots\ldots\ldots\ldots\ldots, X_n) = 0$$

$$C_2 = C_2(X_1, X_2, X_3 \ldots\ldots\ldots\ldots\ldots\ldots\ldots\ldots, X_n) = 0$$

$$C_3 = C_3(X_1, X_2, X_3 \ldots\ldots\ldots\ldots\ldots\ldots\ldots\ldots, X_n) = 0$$

and

$$\boldsymbol{\phi}_1 = \boldsymbol{\phi}_1(X_1, X_2, X_3 \ldots\ldots\ldots\ldots\ldots\ldots\ldots\ldots, X_n) \geq 0$$

$$\boldsymbol{\phi}_n = \boldsymbol{\phi}_n(X_1, X_2, X_3 \ldots\ldots\ldots\ldots\ldots\ldots\ldots\ldots, X_n) \geq 0$$

$X_1, X_2, X_3, \ldots\ldots\ldots\ldots\ldots, X_n$ the design variable, $C_1, C_2, C_3, \ldots\ldots, C_n$ are equality constraints and $\boldsymbol{\phi}_1$, $\boldsymbol{\phi}_2$, $\boldsymbol{\phi}_3$ …… $\boldsymbol{\phi}_n$ are the inequality constraints.

The nature of the mathematical programming that can be employed depends on the functional form of *F, C* and, if these are linear functions of design variables, then the mathematical programming problem may be treated as a linear programming problem. On the other hand if any one of them is a nonlinear function of the design variable, then one maybe is classified as a nonlinear programming problem. By and large, most of the structural design problems belong to the later (Iyengar and Curtin, 1997). They are nonlinear functions since they are subject to variability in design, loading, construction and use.

2.8.3 Significance of optimization

Although the potential of modern structural optimization techniques has been realized by aeronautical, automotive, and mechanical industries, they are still viewed by civil engineers as academic exercises. It should be esteemed; however, that structural optimization can be much more than weight savings. Structural optimization techniques can be used to find better topologies and shapes for the design of civil engineering structures. The load transfer mechanism of a reinforced concrete member is not the function of a single variable, and it depends on the geometry, loading, and support conditions of the member. It is time consuming and difficult for the structural designer to find appropriate strut-and-tie models in complex members by using conventional methods. Therefore, the proposed automatic design optimization procedure is not only helpful for concrete researchers to understand the shear resistance mechanism, but also a valuable design tool for concrete designers in the design and detailing of reinforced concrete members using the strut-and-tie modeling (Liang *et al.*, 2000).

2.8.4 Application of optimization

Optimization is a very important tool and is used to reduce cost and simultaneously provide reliable quality of products. In civil engineering, cost can be greatly reduced and material saved using this tool (Nocedal and Wright, 2006). Since it provide safe structures and durable results, there need be no fear as to the reliability of the tool during any construction project (Nocedal and Wright, 2006). Economics also relies heavily on optimization techniques. An often studied problem in microeconomics, the utility maximization problem, and its dual problem, is economic optimization problems (Nocedal and Wright, 2006).

2.8.5 Multi-objective optimization

Adding more than one objective to an optimization problem adds complexity. For example, if you wanted to optimize a structural design, you would want a design that is both light and rigid, because these two objectives conflict, a trade-off exists. There will be one lightest design, one stiffest design, and an infinite number of designs that are some compromise of weight and stiffness. This set of trade-off designs is known as a "Pareto set". The curve created by plotting weight against stiffness of the design is known as the Pareto frontier. A design is judged to be Pareto optimal if it is not dominated by other designs: a Pareto optimal design must be better than another design in at least one aspect. If it is worse than another design in all respects, then it is dominated and is not Pareto optimal (Papalambros and Wilde, 2000).

2.8.6 Multi-modal optimization

Optimization problems are often multi-modal, that is, they possess multiple good solutions (Papalambros and Wilde, 2000). They could all be globally good (same cost function value) or there could be a mix of globally good and good solutions. Obtaining all (or at least some) of the multiple solutions is the goal of a multi-modal optimizer. Classical optimization techniques due to their iterative approach do not perform satisfactorily when they are used to obtain multiple solutions, since it is not guaranteed that different solutions will be obtained even with different starting points in multiple runs of the algorithm. Evolutionary algorithms are however very popular approaches to obtaining multiple solutions in multi-modal optimization task (Papalambros and Wilde, 2000).

2.9 Design Sensitivity Analysis (DSA)

Design sensitivity method has been used in the last two decades in automotive optimization due to the increase of hardware capability. Design sensitivity method requires the calculation of the gradient of the objective and the constraints with respect to the design variables. There are two methods used to find the variation of the objective function and the constraints: the finite difference method and the response surface method (RSM). The simple form of the finite difference for function *f(x)* and *x* variable is (Chiandussi *et al*., 1998).

$$\frac{df}{dx} \approx \frac{\Delta f}{\Delta x} = \frac{\left[f\left(x+\Delta x\right) - f\left(x\right) \right]}{\Delta x} \qquad 2.15$$

The RSM is a statistical method and it depends on an approximation function to simulate the response of the variables. The relation between variables x and the real response ξ is;

$$\xi = f(x) \quad 2.16$$

$$E(\xi) = f(x) + \varepsilon \quad 2.17$$

where, E (ξ) is an estimate of the real response and is the error.

Optimum design of FRP composite shell has been studied by using DSA method. Analytical, semi-analytical, and finite difference methods were used in the analysis. The conclusion was made that different optimization objectives could be used with DSA method. In addition, using a higher order discrete model could enhance the accuracy (Mota *et al*., 1995; Correia *et al.*, 1997).

Wu and Burgueño (2006) studied the optimum shape and stacking sequence design of FRP composite shells using FE and DSA. Lindgaard and Lund (2010) studied the non-linear buckling optimization of fibre composite shells. The bucking behavior was improved by using DSA method. FRP composite box beam was studied to minimize the weight of the structure. The design constraints were stress, displacement, critical load, and natural frequency. The optimization variables were layer thicknesses and layer orientations of the rectangular beam section (Cardoso *et al*., 2002). The geometrical non-linearity was included in the design and optimization of composite beam dome and the optimum size of the dome was 42.23*m* in span and 6.1*m* height (Valido and Cardoso, 2003).

2.10 Reliability Based Design Optimization (RBDO)

Reliability-Based Design Optimization (RBDO) method is different to the normal optimization method and it is called non-deterministic method or probabilistic method. The objective function is limited by probabilistic constraints instead of conventional deterministic constraints. It considers the uncertainty of the optimization design in fibre composite structural problem. The mathematical form of the RBDO is described below (Thompson *et al.*, 2006).

Find x

Minimizing $f(x)$ 2.18

Subject to constraints $P\,(g_i(x) \leq 0 - (-\beta_I) \leq 0\ (i = 1, 2, \ldots, k)$ 2.19

$$x_{lower} \leq x \leq x_{lower} \quad 2.20$$

where, x is any design variable, $P\,(g_i(x) \leq 0)$ is the probability, Φ is the integral of the (0, 1) standardized normal distribution and i is the so-called safety-index. Since the application of FRP composite structures are new, the ultimate load and risk assessment in the optimum design of FRP composite structure have become a critical consideration for engineers. Furthermore, there is a limitation in a full-scale testing due to the cost issue, and there is a lack of the result for construction of probability distributions. The probability design methods have a target for the research to fill the design gap in the new technology. Thompson *et al.* (2006) used the RBDO to design FRP composite bridge deck panel. The objective function was to minimize the weight of the panel. Two types of constraints were used in the design; deterministic stress constraints and two probabilistic deflections constrains. The design optimization achieved 55% weight saving compared to the initial design.

António and Hoff Bauer (2009) carried out a research on the optimization of FRP composite shallow shell reinforced with a composite beam including a geometrical non-linearity. The objective function was a weight minimization; the RBDO included the probabilistic stress, deflection, and buckling constraints.

2.11 Beam

Beams are structural elements that are capable of withstanding load primarily by resisting bending. The bending forces are induced into the material of the beam as a result of the external loads, own weight, span and external reactions. Loads carried by beams are transferred to columns, walls or girder which then transfers the forces to adjacent compression structural members. Beams are characterized by their profile (shape of their cross section), their length, and their material. There are different types of beam designs and materials to choose from when designing a structure. Beam types and end conditions could either be cantilever, simply supported, fixed ended or continuous (Chanaky, 2009)

2.11.1 Lateral-torsional buckling in simply supported pultruded beams

It is generally accepted that the well-known equation that is used for simply supported isotropic beam sections can be used for conventional pultruded I-shaped profiles provided the appropriate values of E and G are used in the equations (Bank, 2006). Inclusion of the effects of shear deformation on lateral-torsional buckling of conventional pultruded profiles is small and, as shown by Robert (2002), can generally be neglected. The effects of shear deformation are greater for beams with short spans or when a beam has a low shear modulus compared to its longitudinal elastic modulus (Sapkás and Kollár, 2002).

Pultruded cross-sections can be divided into two groups based on their warping resistance; open and closed. Open cross-sections have unstiffened outstanding elements, such as the flanges of I-shaped, channel or Tee sections. Closed cross-sections do not have any unstiffened elements and all of the elements of the cross-section connect together to form a "closed" geometry. Tube sections are examples of closed cross-sections. The critical stress for lateral-torsional buckling of a doubly symmetric open cross-section subjected to flexural loads is given by Equation (2.21) (Timoshenko and Gere, 1961). This equation was derived assuming that the,

$$f_{cr} = \frac{1}{S_x}\frac{\pi}{L_b}\sqrt{EI_y\left(1+\frac{C_1\pi^2}{CL_b^2}\right)} \qquad 2.21$$

where, S_x = Section modulus about the strong axis

L_b = Length between points that are either braced against lateral displacement of the compression flange or braced against twist of the cross section

E = Elastic flexural modulus

I_y = Second moment of area about the weak axis of the member

$C = GJ$

$C1 = EC\omega$

G = Elastic shear modulus

J = Torsional constant

$C\omega$ = Warping constant

The beam was isotropic, subjected to pure bending; the load was applied at the shear center on the cross-section; the beam was simply supported and the ends were permitted to freely rotate about the strong and weak axes of the cross-section (warping). In order to make the equation more general, the previous assumptions need to be accounted for by variables which may change depending on the beam being designed. After substitution and rearrangement Equation (2.22) is arrived at with the addition of terms which account for the assumptions made in Equation (2.21). The terms in Equation (2.22) are described and explained below.

$$f_{cr} = \frac{C_b C_p}{S_x} \sqrt{\frac{\pi^2 J E_b I_y G_b}{\left(K_f L_b\right)^2} + \frac{\pi^2 E_b^2 I_y C_w}{\left(K_f L_b\right)^2 \left(K_w L_b\right)^2}} \qquad 2.22$$

where,

C_b = Moment modification factor for unsupported spans with both ends braced

$$C_b = \frac{12.5 M_{\max}}{2.5 M_{\max} + 3M_A + 4M_B + 3M_C} \leq 3.0 \qquad 2.23$$

where;

M_{max} = absolute value of maximum moment in the unbraced segment

M_A = absolute value of moment at quarter point of the unbraced segment

M_B = absolute value of moment at the centerline of the unbraced segment

M_C = absolute value of moment at three-quarter point of the unbraced Segment

C_b is permitted to be conservatively taken as 1.0 for all cases. For cantilevers or overhangs where the free end is unbraced, C_b= 1.0.

C_P = load application location constant

k_f = effective length coefficient for flexural buckling about the weak axis

k_ω = effective length coefficient for torsional buckling of the section

E_b = full section flexural modulus

G_b = full section shear modulus

C_b is a coefficient that accounts for the moment distribution along the unbraced portion of the beam taken from AISC (2005). Equation (2.21) was derived assuming a uniform bending moment along the entire span, so C_b is introduced to account for different moment distributions caused by loading configurations other than pure bending. The location of the load placement on the cross section of the beam can affect the lateral-torsional buckling capacity of the beam (Timoshenko and Gere, 1961). C_P is a coefficient which accounts for the height of the load relative to the neutral axis of the beam (Timoshenko and Gere, 1961). When the load acts on the compression flange (above the neutral axis) the beam is more susceptible to lateral torsional buckling than if the load is applied through the shear center. When the load acts on the tension flange (below the neutral axis) the beam is less susceptible to lateral torsional buckling than if the load is applied through the shear center.

2.12 Structural Reliability

Sorensen (2003) defined reliability of structural systems as the probability that the structure under consideration has a proper performance throughout its lifetime. The reliability of a structure could be defined as the ability that the structure fulfils its design purpose for some specified reference period (Togan and Daloglu, 2006).

Computer techniques of structural analysis have improved the accuracy of representing the actual behavior of bridge components (Nowak, 2004). Advanced programs (e.g. ABAQUS, NASTRAN, and ANSYS) are available for linear and nonlinear analysis of complex structural systems. A dense element mesh allows for an accurate determination of strain/stress at almost any point in the structure. One major problem that remains is how to represent boundary conditions and material properties. For example, the actual support in-situ is often different from an idealized type, and strength of material and modulus of elasticity can be different from what is assumed in design (Nowak, 2004). The study of structural reliability is concerned with the calculation and prediction of the probability of a limit state violation for engineered structures at any stage during their life. In particular, the study of structural safety is concerned with the violation of the ultimate or safety limit state for the structure. The violation of a limit state is the attainment of an undesirable condition for the structure, that is, damage to a part of the structure or total collapse of the structure which could lead to loss of human lives (Melcher's, 1987). Society expects structures for example buildings and bridges to be designed with a reasonable safety level. In practice, these expectations are achieved by following code requirements specifying design values for minimum strength, maximum allowable deflection and so on. Code requirements have evolved to include design criteria that take into account some of the sources of uncertainties in design. Such criteria are often referred to as reliability-based design criteria. The reliability of a structure is its ability to fulfill its design purpose for some specified design lifetime. Reliability is often understood to equal the probability that a structure will not fail to perform its intended function.

The term failure does not mean catastrophic failure but is used to indicate that the structure does not perform as desired. The reliability of a structure can be considered as a rational evaluation criterion. It provides a good basis for decision about repair, rehabilitation, or replacement (O'Connor, 1990).

A structure is said to have failed when the nominal value of load exceeds the nominal value of load carrying capacity. But in most cases, a structure is a system of components, and failure of one component does not necessarily mean failure of the structural system. When a component reaches its ultimate capacity, it may continue to resist the load while loads are redistributed to other components. System reliability provides a methodology to establish the relationship between the reliability of an element and the reliability of the system. Reliability based design, which accounts for uncertainties in design variables can be used as an essential means for checking the consistency of existing codes, with the view of optimizing the code so as to produce more consistent and economic codes for a better design (Nowak and Collins, 2000; Melchers, 1987; 1999; Ellingwood, 1994). The probability of occurrence of an event such as limit state violation is a numerical measure of the chance of its occurrence. This measure either may be obtained from the measurement of the long-term frequency of occurrence of the event for generally similar structures, or may be simply subjective estimation of the numerical value. In practice, it is not usually possible to observe for a sufficiently long period of time, a combination of subjective estimation and frequency observations for structural components and properties used to predict the probability of a limit state violation for the structure as a whole.

Structural reliability with respect to some limit states is quantitatively expressed by a number on a suitable scale being related to a given time period (Augusti *et al.,* 1984). Taking for granted that the reliability evaluation is based on probabilistic modeling, the reliability measure scale is in one-to-one correspondence with the probability that the adverse event occurs within the considered time period (Ditlevsen and Madsen, 2005). Lately, the use of reliability in structural assessments improved the quality of bridges concerning safety, serviceability, and durability (Nowak and Collins, 2000). Partial safety factors based on load and resistance uncertainties were proposed in the United States for building design codes not before the late 1970‘s (Galambos and Ravindra, 1978; Ellingwood *et al*., 1980). New bridge design codes are based on probabilistic methods (Nowak, 1999) and load and resistance factor parameters are considered as random variables. The reliability index, β, is used to measure the reliability of structural member as well as structural systems. This index accounts for the margin of safety implied by the design procedure as well as the uncertainties in estimating the member strengths and the applied loads; it is related to the probability of failure (Nowak and Collins, 2000). These optimization techniques will be applied to section modulus of CFRP pultruded beams in order to determine the structurally safe values for designs since the variables are of a stochastic nature. The methods applied herein are described in chapter three; these include reliability and finite element methods.

CHAPTER THREE

3.0 ANALYTICAL TECHNIQUES

3.1 Reliability Concept

Reliability of structural systems can be defined as the probability that the structure under consideration has a proper performance throughout its lifetime. For many years it has been assumed in design of structural systems that all loads and strengths are deterministic. The strength of an element was determined in such a way that it exceeded the load with a certain margin. The ratio between the strength and the load was denoted by the safety factor. This number was considered as a measure of the reliability of the structure. In codes of practices for structural systems, values for loads, strengths and safety factors are prescribed. These values are traditionally determined on the basis of experience and engineering judgment. However, in new codes partial safety factors are used. Characteristic values of the uncertain loads and resistances are specified and partial safety factors are applied to the loads and strengths in order to ensure that the structure is safe enough. The partial safety factors are usually based on experience or calibrated to existing codes or to measures of the reliability obtained by probabilistic techniques (Sorensen, 1999). The study of structural reliability is concerned with the calculation and prediction of the probability of limit state violation for engineering structures (Melchers, 1987).

Ditlevsen and Madsen (2005) considered structural reliability as a method that attempt to treat rationally, the various sources of uncertainties. According to Tsopanakis and Papadrakakis (2002) structural reliability analysis is a tool that assists the design engineer to take into account all possible uncertainties during the design and construction phases and the lifetime of a structure in order to calculate its probability of failure.

Reliability-based design is a probabilistic design process where the loads, strengths of materials and sections are represented by their known or postulated distributions and are defined in terms of distribution types, means and standard deviations. The probability of failure *(P_f)* for a specific design case is calculated as the probability that the maximum total load effect exceeds the resistance to failure. This is opposed to limit state design (LSD) method, which is a semi-statistical design process in which the probabilistic aspect are treated at the code development stage (Kadry and Smail, 2001), in order to define characteristic value and partial safety factors for load and resistance that are used to ensure, on average an acceptably low probability of failure across a full spectrum of design cases. In the current design codes in Europe, LSD is used as a practical method of incorporating reliability methods in the normal design process. This approach failed to fully address the statistical nature of basic design variable. Issues of uncertainties are lumped conservatively within partial safety factors. A limit state code is calibrated to ensure that selected appropriate reliability levels called target values, are attained in design (Zimmerman *et al.*, 1998).

3.2 Structural Reliability Method

The basic reliability problem considers only one load effect S and resisted by resistance *R* both load and resistance *S* and *R*, are described by a known probability density function, $f_s()$ and $f_r()$ respectively. As noted, *S* can be obtained from the applied loading through a structural analysis. It is important to make sure that *S* and *R* are expressed in the same unit. Considering the safety of a structural element here only and as usually, it can be said that a structural element will fail if its resistance *R* is less than the applied load *S* acting on it

(Melchers, 1987). The probability of failure of the structural element can be stated in any of the following ways;

$$P_f = P(R - S) \tag{3.0}$$

where, R = Resistance and S = Loading on structure.

The structural failure in this case is defined as the region where $(R - S)$ is less than zero:

$$P_f = P\,[(R - S) \leq 1] \tag{3.1}$$

an alternative approach to Equation (3.1), the performance function can also be given as:

$$P_f = P[(R/S) \leq 0] \tag{3.2}$$

That is the failure region in this case is defined as where R/S is less than one or R is less than S and $P_f < 1$

It can also be expressed as:

$$P_f = P\left[(\mathrm{InR} - \mathrm{InS}) \leq 1\right] \tag{3.3}$$

Or in general;

$$P_f = P\,[G(R, S)] \leq 0 \tag{3.4}$$

where $G(X)$ is the 'limit state function' and the probability of failure is identical with the limit state violation. For any random variable X, the cumulative distribution function is given by:

$$F_x(\mathrm{X}) = P(X) = \int_{-x}^{x} f_x(X)dy \tag{3.5}$$

Provided that $X \geq Y$

It follows that for the common, but special case when R and S are independent, the expression for the probability of failure is:

$$P_f = P(R - S) = \int_{-\infty}^{+\infty} \int_{-\infty}^{s \geq r} f_r(R)\, f_s(S)drds \tag{3.6}$$

Equation (3.6) can be written as;

$$P_f = P\left[(R-S) \le 0\right] = \int_{-\infty}^{+\infty} f_r(X)\, f_s(X) dr ds \qquad 3.7$$

This integral is known as 'convolution integral' and $F_x(X)$ is the probability that $R \geq X$, or is the probability of the actual resistance R of the member less than some values of X. The term $F_s(X)$ represent the probability that the load effect S acting on the member has a value between X and $X = X + \Delta X$ in limit as $\Delta X \to 0$. Considering the possible value of x, the total failure probability is obtained by;

$$P_f = \int_{-\infty}^{+\infty} \left[1 - f_s(X)\right] f_r(X) dx \qquad 3.8$$

This is the sum of all cases of resistance in which the applied load exceeds the resistance. The convolution integral may be integrated for a few distributions of R and S. This is easy when R and S are normal random variables with means μ_R, μ_S and variance σ_R^2, σ_S^2 respectively. The safety margin will be:

$$G = R - S \qquad 3.9$$

Therefore, the mean and variance will be given by;

$$\mu_X = E(x) = \mu_R - \mu_S \qquad 3.10$$

$$\sigma_X^2 = \text{var}(\mu) = \sigma_R^2 + \sigma_S^2 \qquad 3.11$$

$$\sigma_Z = \sqrt{\sigma_R^2 + \sigma_S^2} \qquad 3.12$$

Using the well-known rule for addition and subtraction of normal random variable

Equation (3.7) becomes;

$$P_f = P\left[(R-S) \le 0\right] = P(Z \le 0) = \phi\left(\frac{\mu_Z}{\mu_S}\right) \qquad 3.13$$

where ϕ is the standard normal distribution function and reliability index, β, is defined as the ratio μ_Z / σ_Z

$$P_f = \phi(\mu_Z / \sigma_Z) = \phi(-\beta) \quad 3.14$$

Hence, P_f increases with decrease in resistance.

3.3 Limit State Functions

The limit state function gives a descriptive assessment of the state of a structure or structural element as being failed or safe. It is obtained from traditional deterministic analysis but uncertain parameters are treated statistically.

The limit state function is given as,

$$G(X) = R - S \quad 3.15$$

where R is a function of material properties and S is a function of applied loads, densities and dimensions. The limit state function is usually expressed in terms of basic random variables $\bar{X}$ which affects the structural performance. That is,

$$\bar{X} = (X_1, X_2, X_{3 \ldots} X_n) \quad 3.16$$

and

$$G(X) = F(X) = f(X_1, X_2, X_{3 \ldots\ldots} X_n) \quad 3.17$$

where $G(X)$ is performance function (safety margin) and the limit state equation is represented as:

$G(X) < 0$ Corresponds to a failure.

$G(X) = 0$ Correspond to limit state attainment.

$G(X) > 0$ Corresponds to safety.

Therefore the probability of failure is given as $P\,[G(X) < 0]$.

3.3.1 Bending criterion and applied load

In this work, simply supported CFRP pultruded beam is considered for investigation. The structural configuration of the CFRP beam is as follows,

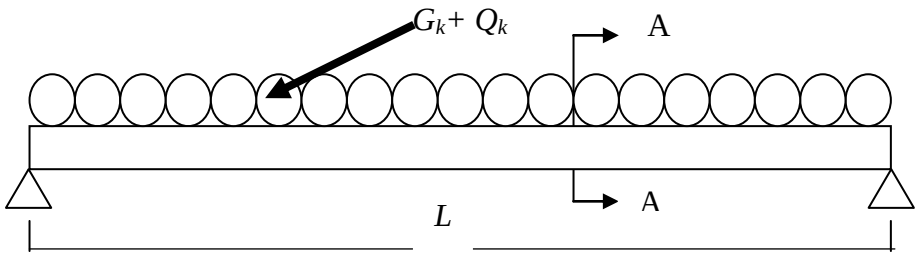


Figure 3.1 Simply Supported Beam with a Symmetric Cross-section Subjected to Uniformly Distributed Loading (Dead load, G_k and Imposed load, Q_k)

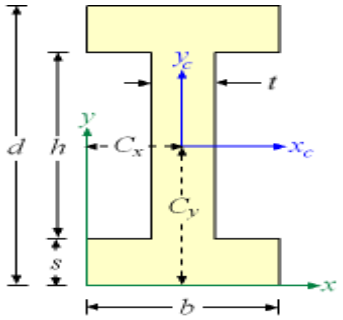


Figure 3.2 Section A-A

The beam is assumed to have failed when its flexural capacity is exceeded. The maximum applied bending is given by;

$$w = Q_K(\alpha\gamma_G + \gamma_Q)$$

where, w = design uniformly distributed load

Q_k = imposed load and G_k the dead load

α = dead to live load ratio given by G_k/Q_k

γ_G = partial safety factor for dead load, equal to 1.4 for LRFD, and 1.0 for ASD

γ_Q = partial safety factor for imposed load, equal to 1.6 for LRFD, and 1.0 for ASD

The generalized reliability index is given by Equation (3.15) (Melchers, 1987). An assessment made on a simply supported beam assuming ACI 318 (2005) design code for loading, considering maximum moments occurring at the mid span is given as:

$$M_a = \frac{wl^2}{8} = (\mathrm{S}) = \frac{w_u l^2}{8},\ S = \frac{q_k l^2(\alpha\gamma_G + \gamma_Q)}{8} = 0.125 q_k l^2(\alpha\gamma_G + \gamma_Q) \qquad 3.18$$

Hence, the moment of resistance (M_R), for the section may be evaluated as:

$M_r = 0.75 f_y S_x$ for LRFD and $M_r = 0.65 f_y S_x$ for ASD

The limit state function for flexure mode is given as:

$$G(X) = R - S \qquad 3.19$$

where, $R = M_r$ and $S = M_a$

Therefore, the expression for the performance function for compression failure G(X), in the limit state of bending would be:

$$G(X) = M_r - M_a \quad \text{i = 1, 2,…...,n.} \qquad 3.20$$

This, on substitution of values, gives:

$G(X) = 0.75 f_y S_x - 0.125 q_k l^2(\alpha\gamma_G + \gamma_Q)$ for LRFD and

$G(X) = 0.65 f_y S_x - 0.125 q_k l^2(\alpha\gamma_G + \gamma_Q)$ for ASD 3.21

Equation (3.19) provides the expectation that the resistance moment is greater than the applied moment. Expectation of a variable X, that is, $E(X)$ is the weighted average or mean of all the values that the random variable may take. Consequently, it indicates the value or level of safety attained in the structural member.

Table 3.1 Parameter of the stochastic model for LRFD and ASD bending

S/No.	Variable	Meaning	Distribution type	Expected value	Coefficient of variance
1	f_y	Yield stress	Lognormal	$3300 N/mm^2$	0.05
2	l	Span	Normal	$3050 mm$	0.027
3	q_k	Imposed load	Gumbel	$3.5 kN/m^2$	0.15
4	S_x	Section modulus	Normal	Varies	0.15

3.4 Stochastic Finite Element Method

Stochastic finite element methods have recently become an active area of research. As the name suggests, researchers in this field attempt to combine two crucial methodologies developed to deal with the complex problems of modern engineering. The stochastic analysis refers to the explicit treatment of uncertainties in any quantity entering the corresponding deterministic analysis at a specific period of time. The exact values of these quantities are usually unknown because they cannot be precisely measured (Klieber and Hein, 1992). It is used to describe the merging of advanced reliability methods with the finite element method to obtain probability estimates for predefined performance criteria. These methods are generally applicable to both linear and non-linear problems. Stochastic finite element method is the generalization of the deterministic finite element method to incorporate the random fluctuations in material and geometric properties of the model and the random forces that may act on it (Shaker *et al*., 2007) .The aim of stochastic finite element is two folds, first, to compute the variability of the response of a random system and subsequently, using these results to estimate the structural reliability (Shaker *et al*., 2007).

The key steps involved in the analysis of the system using stochastic finite element method are;

(1) Selection of appropriate probability models to describe the uncertainties in the system parameters and the boundary conditions.

(2) Discretization of the random fields that is, the replacement of these random fields by an equivalent set of random variables.

(3) Formulation of finite element equations, using standard methods like energy method, virtual work method or weighted residual method and its solution.

(4) Estimation of system response statistic, which involves the inversion of random matrix operators.

(5) Using these results to make a safety assessment of the structure.

Stochastic Finite Element Method (SFEM) combines areas of finite element analysis and that of reliability. The distinguishing feature of stochastic finite element method, which is based on the perturbation approach, is treating probabilistic non-linear problem with deterministic computational techniques of the mathematical properties of linear operators (Raji, 2003). SFEM is an extension of the classical deterministic Finite Element approach to the stochastic framework that is, to the solution of stochastic (static and dynamic) problems involving finite elements whose properties are random. From a mathematical point of view, SFEM can be seen as a powerful tool for the solution of stochastic partial differential equations (PDEs) and it is treated as such in numerous studies where convergence and error estimation issues are examined in detail (Stefanou, 2008).

In order to apply the finite element technique, the region of interest is discretized by a finite element mesh. The basic idea of the mean-based, second-moment analysis as used in stochastic finite element analysis is to expand, via Taylor series, the entire vector and the matrix stochastic field variables typical of deterministic finite element method about the mean values of the random variables, to retain only up to second order method terms and to use in the analysis only the first tier statistical moments. In this way, equations for the expectation and cross-covariance of the nodal displacement can be obtained in terms of the nodal displacement derivatives with respect to the random variables (Kleiber and Hein, 1992; Raji, 2003; Musa, 2003; Stefanou, 2008).

3.5 Finite Element Analysis

This approach discretizes the structure into small divisions (elements) where each element is defined by a specified number of nodes. The behavior of each element (and ultimately the structure) is assumed to be a function of its nodal quantities (displacements and/or stresses), that serve as the primary unknowns in this formulation. This is one of the most general and accurate methods to use, because it does not put any limitation on the geometry, loads, or boundary conditions, and can be applied to open/closed girders and static/dynamic analysis. Additionally, the structures response can always be improved by refining the mesh and increasing the number of nodes (or degrees of freedom) for each element. However, the rather involved modeling and analysis efforts required by this method may in some cases make it impractical for preliminary analysis (Benetti and Tralli, 1989).

3.5.1 Model assumptions

1) The entire structure remains elastic prior to bending, that is members are long and rigid.

2) The members have symmetric cross sections.

3) The cross sections of the members do not distort in their own plane after bending.

4) The members are perfectly horizontal.

5) Local torsion or buckling does not occur.

3.5.2 Modeling the CFRP pultruded beam using ABAQUS 6.10-1

ABAQUS is a general finite element package with capability to solve nonlinear problems. In particular, whenever a material definition is not supported, the user is provided with the ability to use external subroutines. Taking advantage of the ability to script within ABAQUS, using the Python language (http://www.python.org/) an algorithm taking into account the progressive damage within the constituents is proposed. To account for the different material properties in tension and compression, a linear elastic analysis with homogeneous properties is first run to identify stress states within the beam. Material properties are then assigned correspondingly. Because of changes in the model, caused by modeling the damage at different parts of the beam throughout the analysis, this process is updated in each iteration depending on the stress states obtained at the previous iteration. The cracking in the core material is modeled using a smeared crack approach. When the strain in the core material exceeds a limiting value, the elastic modulus is put to zero at the offending Gauss point. The peel-off of the laminate from the core material is not modeled as the interaction behavior between core material and laminates is yet to be quantified, and is the subject of continuing investigation. Damage in the laminates is modeled by means of

an external FORTRAN subroutine implementing the damage model of Chang *et al*., (1989).

3.5.3 Material properties input data for models and flow chart modeling for FEM

Modeling started by create geometry model of rough surface and rigid plat. Model of the geometry refer to author analysis regarding topography of real surface. Material definition is according to reference from Table 3.2 and Figure 3.3 below.

Table 3.2 ABAQUS 6.10-1 Material Properties Input Data Models

1500/1525/1625 Series(*mm*)	**Model 1**	**Model 2**	**Model 3**	**Model 4**	**Model 5**	**Model 6**
Depth(*mm*)	76.2	101.6	152.4	152.4	203.2	203.2
Width(*mm*)	38.1	50.8	76.2	101.6	101.6	101.6
Thickness(*mm*)	6.35	6.35	6.35	9.525	9.525	12.7
Young modulus (N/mm^2)	400000	350000	300000	250000	200000	150000
Density (g/cm^3)	1400	1400	1400	1400	1400	1400
Poisson's ratio	0.34	0.34	0.34	0.34	0.34	0.34
Section modulus (mm^3)	20000	40000	90000	130000	230000	300000

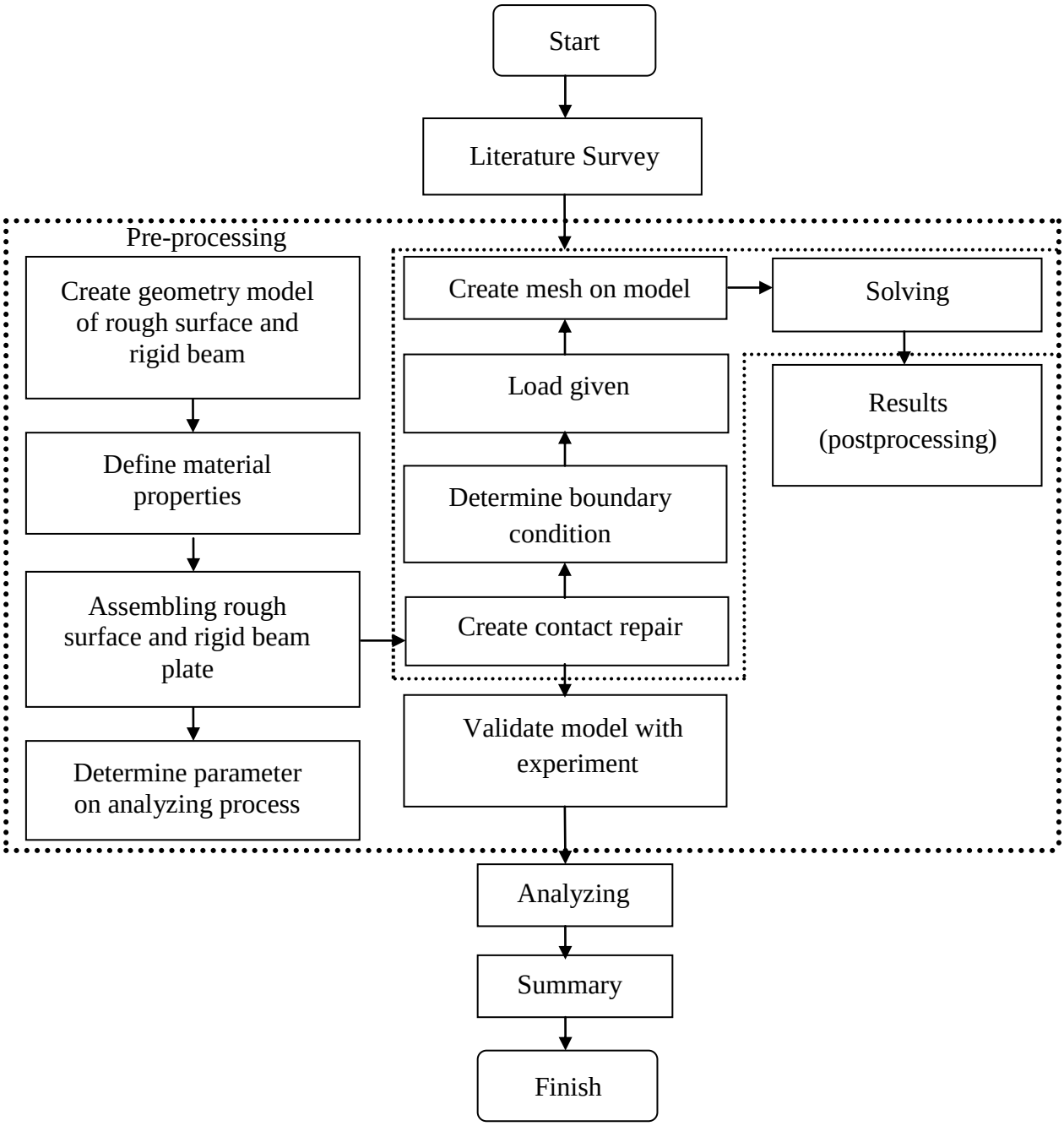


Figure 3.3: Flow chart modeling for FEM ABAQUS 6.10-1

CHAPTER FOUR

RESULTS AND DISCUSSION

4.1 Model Geometry Description and Loading/boundary condition on the Beam

Figure 4.1 shows the six CFRP pultruded beam sections which were stochastically selected for this study. The material properties for finite element analysis used for the models are from Table 3.2 and Figure 3.3 discussed in chapter three. The beams section were assumed to be simply supported and loaded with $3.5 kN/m^2$ as imposed load having length of $3.050 m$ each. The proposed pultruded beams section is assumed symmetrical about the horizontal plane in which it will accommodate both positive and negative bending moments. The strength limit state is considered for the design, with load being represented by applied moment and the resistance by the moment carrying capacity. The mode of failure considered in this work would be governed by *ASCE Standard 7-10* (2010) standard of design for the FRP beams section, although safety checks will be made on the beams section. The reliability analysis is performed using First Order Reliability Method as proposed by Gollwitzer *et al*., (1988).

Figure 4.2 defines the loading and restraint/boundary conditions for each model used in ABAQUS 6.10 CAE. The ABAQUS 6.10 CAE executions were terminated when the deflection exceeded $2.5 mm$. The detailed boundary conditions as well as the total number of nodes are shown in Appendix C. The FEA results include Von Mises stress, displacement, and strain in the beam sections from the FEA ABAQUS program are shown below.

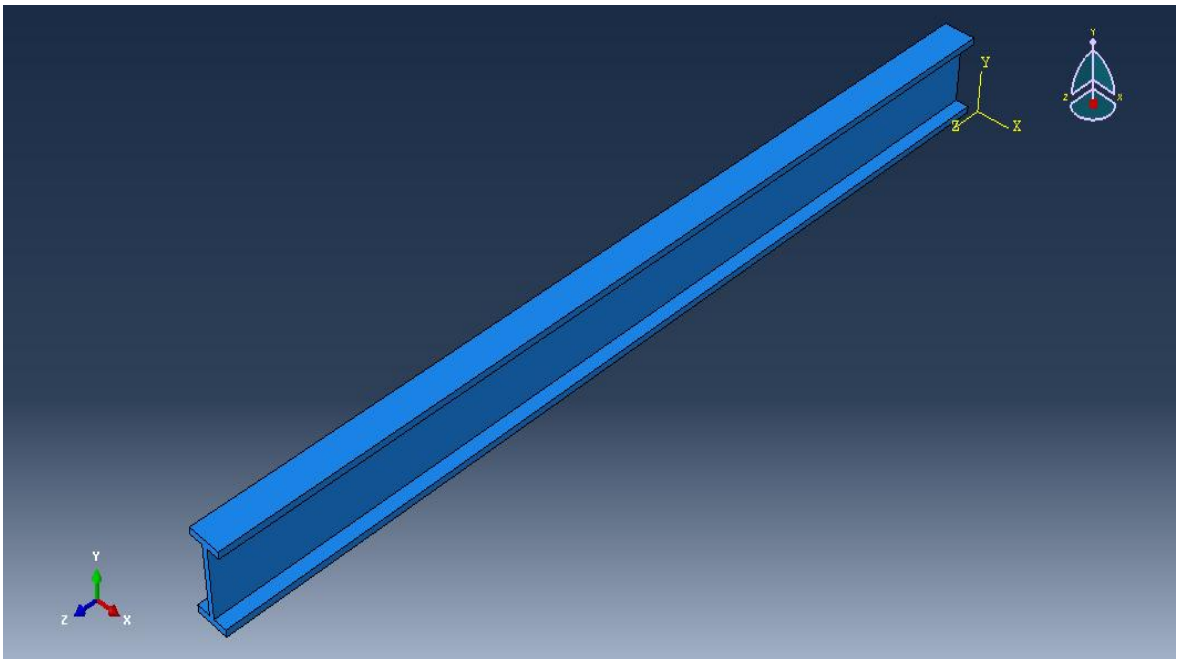


Figure 4.1 Proposed Carbon Fibre Reinforced Plastic Pultruded Beams Section for the Models: (ABAQUS 6.10)

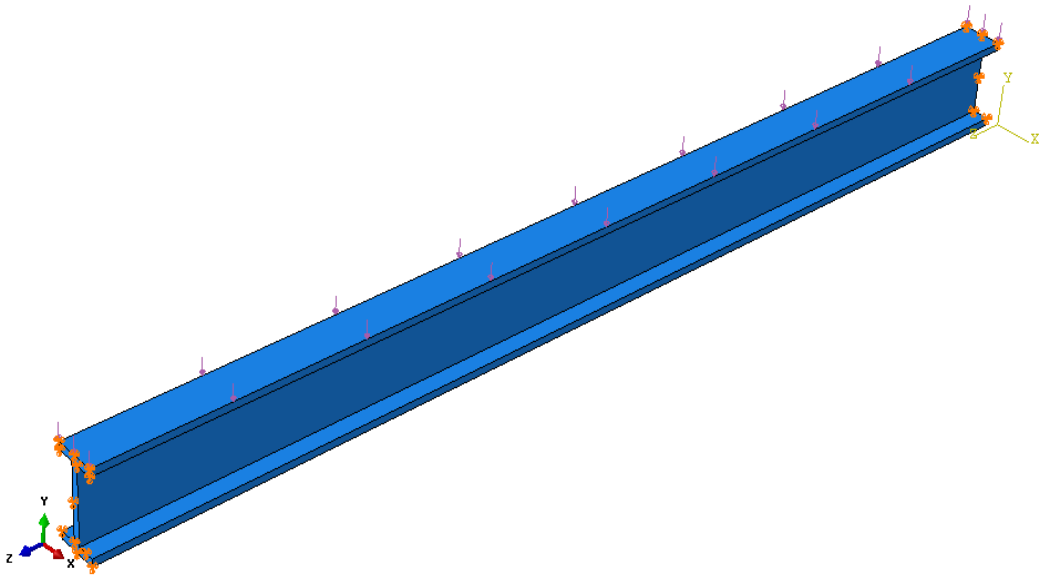


Figure 4.2 Loading and Boundary Condition on Pultruded CFRP Beam Section in ABAQUS 6.10 CAE

4.2 Finite Element Analysis using ABAQUS 6.10 CAE

The finite element model was developed using ABAQUS 6.10 CAE. Due to the symmetry of the loading configuration as well as of the beam's cross-sectional dimensions, the entire pultruded beam section was modeled. The 76.2x38.1x6.35*mm* section was meshed using overall mesh size of 3.175 which generated 27720 elements on part, 101.6x50.8x6.35*mm* section the mesh size of 3.175 was used and generated 37800 elements on part, 152.4x76.2x6.35*mm* the mesh size was 5.0 and generated 11600 elements on part, 152.4x101.6x9.525*mm* section with mesh size of 5.0 which generated 26800 element on part, 203.2x101.6x9.525*mm* section with mesh size of 5.0 which generated 30800 element on part, and finally 203.2x101.6x12.7*mm* section with mesh size of 6.35 which generated 20480 elements on beam part**.**

4.3 Stress and Deformation Pattern in Model 1

Figure 4.3 shows the Von Mises stress diagram of 76.2x38.1x6.35*mm* (Part# IB340) beam section analyzed and calculated in FEA ABAQUS. Fields of high stress are formed in the beam near the both top end of the flange and web edge of the section. The contour red indicates high Von Mises stress of 661.2N/mm^2 with the displacement of 1.448*mm* caused by the applied load which is due to the small nature of sectional modulus of the section. Since stress is a function of force over the area so as the cross-sectional area of the beam increases which by default increases the section modulus, the Von Mises stress will decreases which could be due to the increase in surface area of contact under the applied load. Figures 4.4 shows the graph of the stress-displacement and stress-strain of the section with a linear relationship up to 661.2N/mm^2 (stress point) and the corresponding strain of 0.0017 then become nonlinear as the section starts to deflect due to increase in stress.

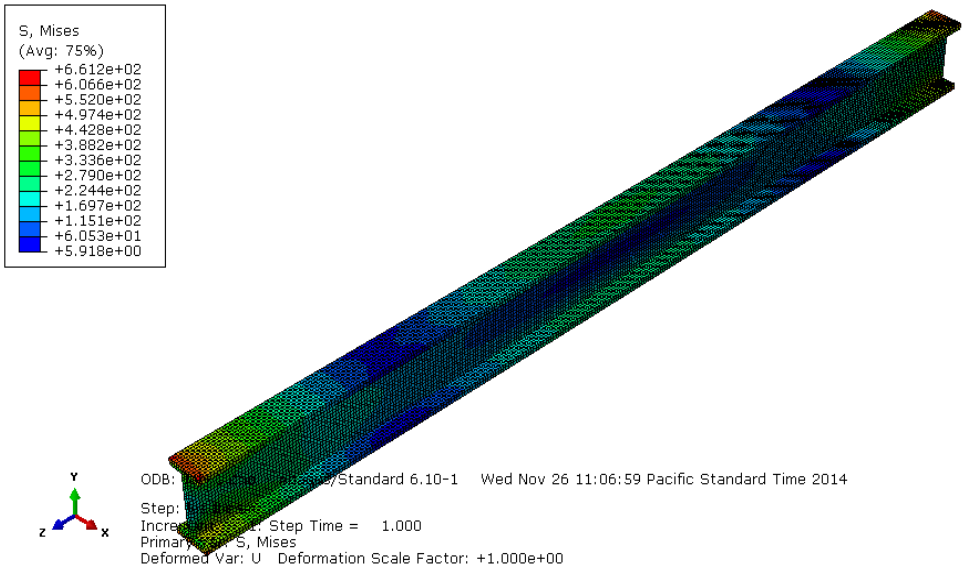


Figure 4.3 Von Mises Stress Diagram of 76.2x38.1x6.35*mm* (Part# IB340) 1500/1525/1625 Series

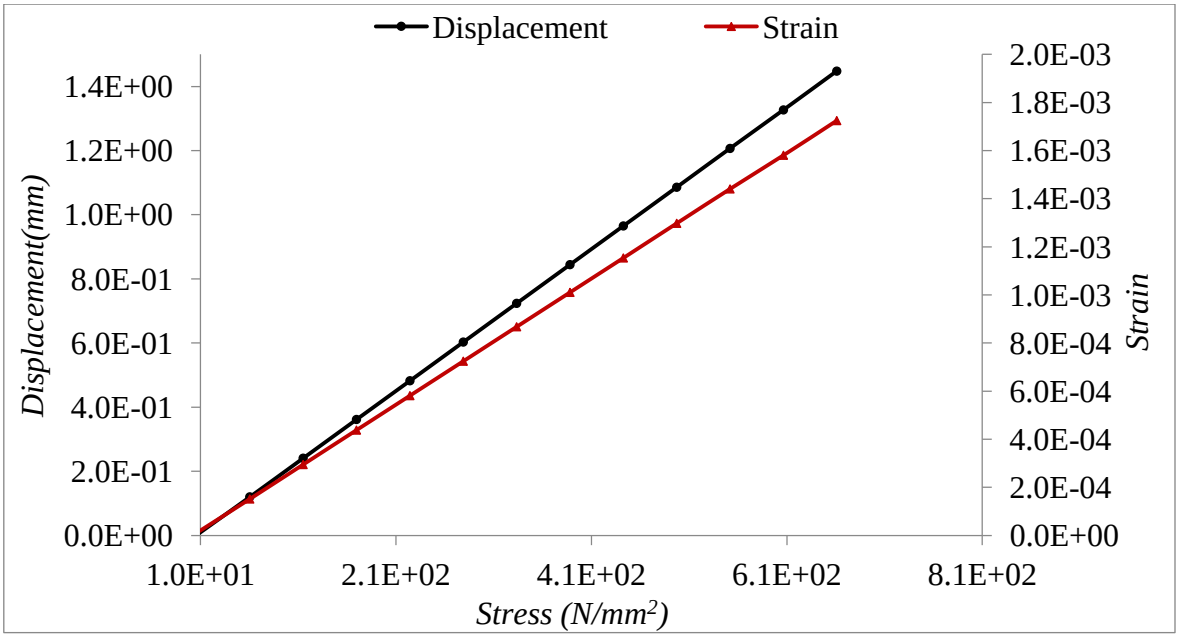


Figure 4.4 Strain and Displacement Graph of 76.2x38.1x6.35*mm* with Corresponding Stresses under the Applied Load

4.4 Stress and Deformation Pattern in Model 2

The Von Mises stress pattern obtained after the analysis of the CFRP beam section can be seen in the deformed diagram of the 101.6x50.8x6.35*mm* (Part# IB440) model shown in Figure 4.5. Fields of high stress are formed in the beam near the both top end of the flange and web edge of the section, the contour red indicates 518.6N/mm^2 Von Mises stress and hence it is an indication that the beam section is stable when compared to first model, due to increase in section modulus with increase in size of the beam section, the stress decreases which could be due to the increase in surface area of contact under the applied load. Figure 4.6 shows the graph of stress-displacement and stress-strain which show a linear relationship in the beam section to a point of 1.029*mm* displacement and strain of 0.0016.

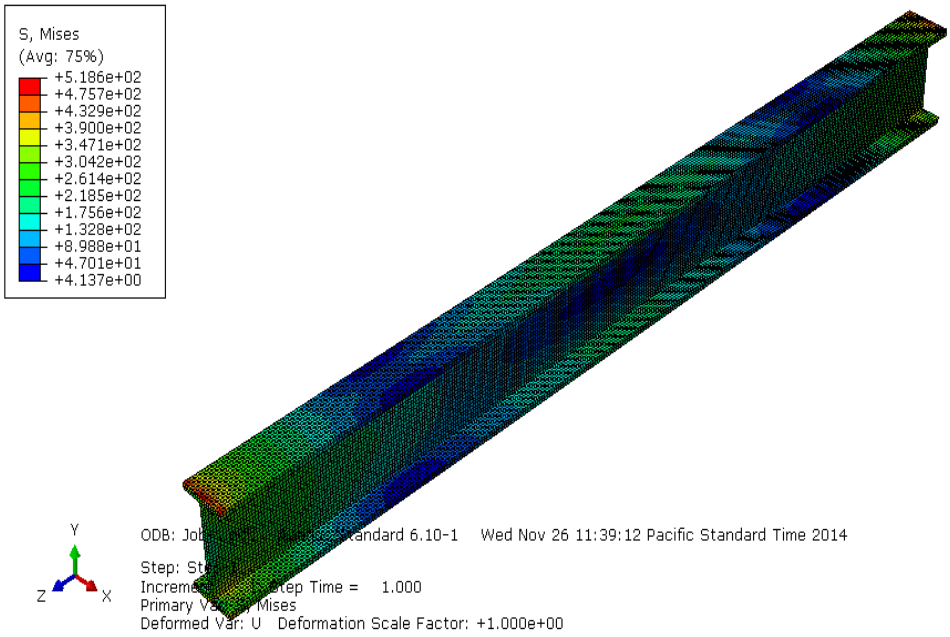


Figure 4.5 Von Mises Stress Diagram of 101.64x50.8x6.35*mm* (Part# IB440) 1500/1525/1625 Series

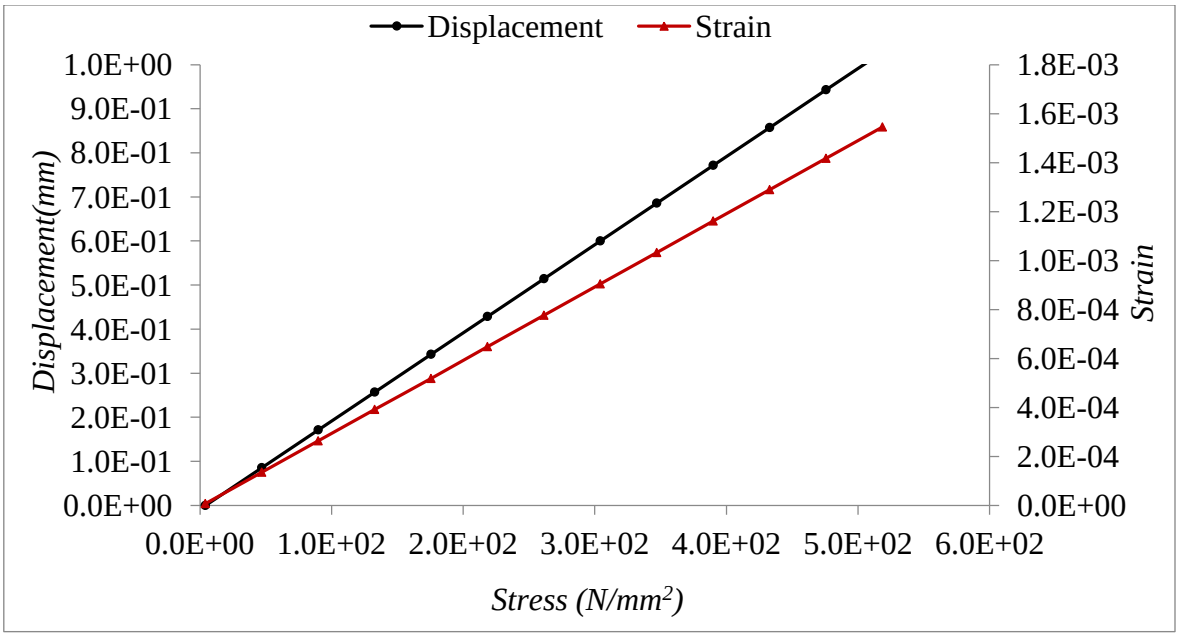


Figure 4.6 Strain and Displacement Graph of 101.6x50.8x6.35*mm* with corresponding Stresses under the Applied Load

4.5 Stress and Deformation Pattern in Model 3

The Von Mises stress pattern obtained after the analysis of the CFRP beam section can be seen in the deformed diagram of 152.4x76.2x6.35*mm* (Part# IB640) model shown in Figure 4.7. Fields of high stress are formed in the beam near the top end of the flange and web edge of the section, the contour red indicates 342.8N/mm^2 Von Mises stress and hence it is an indication that the beam section is stable when compared to second model, due to increase in section modulus with increase in size of the beam section, the stress decreases which could be due to the increase in surface area of contact under the applied load. Figure 4.8 shows the graph of stress-displacement and stress-strain with a linear relationship in the section to a point of 0.981*mm* displacement and strain of 0.0014.

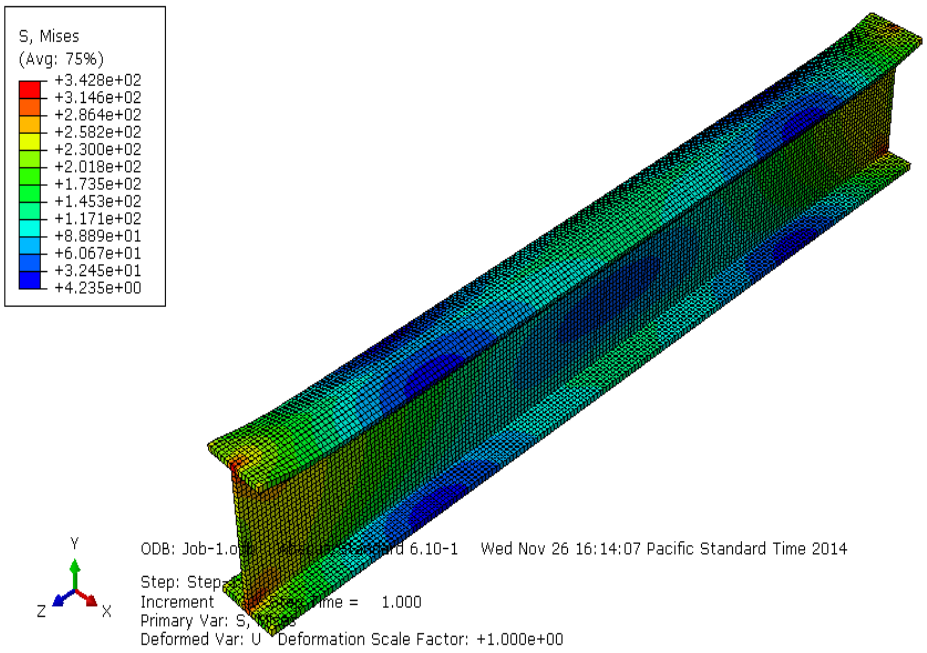


Figure 4.7 Von Mises Stress Diagram of 152.4x76.2x6.35*mm* (Part# IB640) 1500/1525/1625 Series

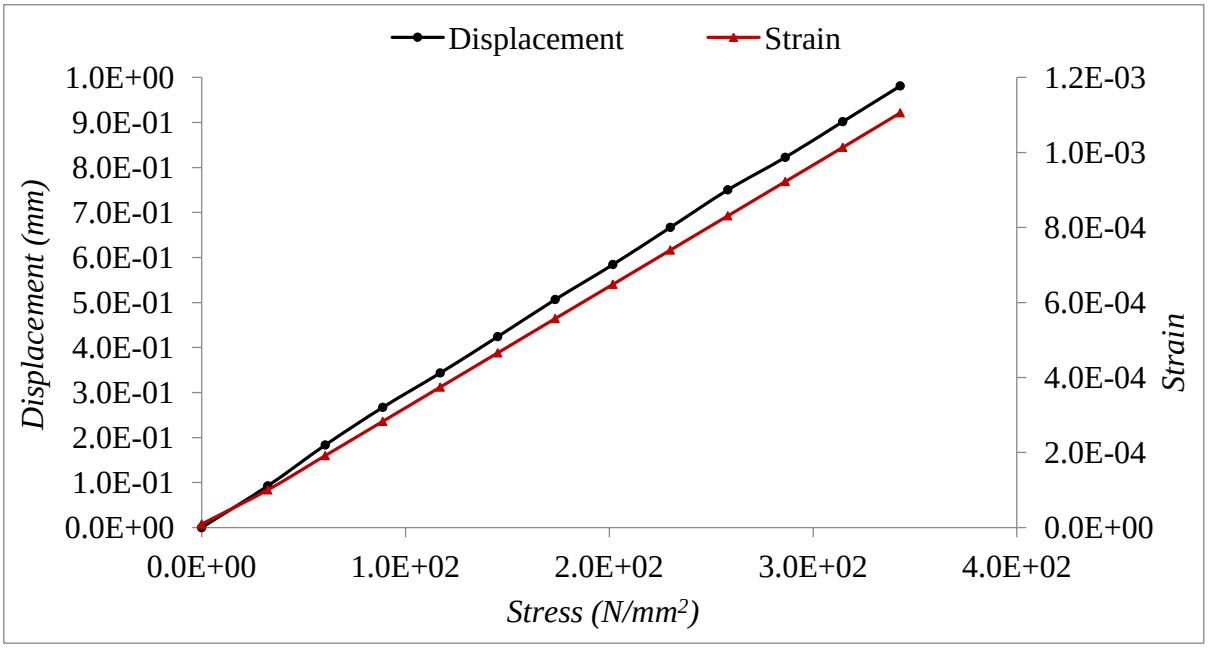


Figure 4.8 Strain and Displacement Graph of 152.4x76.2x6.35*mm* with corresponding Stresses under the Applied Load

4.6 Stress and Deformation Pattern in Model 4

Figure 4.9 shows the Von Mises stress diagram of 152.4x101.6x9.525*mm* (Part# IB660) beam section under the same loading as the first three models. Fields of high stress zone formed in the beam are near the top end of the flange and web edge of the section, the contour red indicates 317.1N/mm^2 Von Mises stress and hence it is an indication that the beam section is more stable when compared to the first three models, due to increase in section modulus and increase in beam size, the stress decreases which could be due to the increase in surface area of contact under the applied load. Figure 4.10 shows the graph of stress-displacement and stress-strain with a linear relationship in the section to a point of 0.866*mm* displacement and strain of 0.0013.

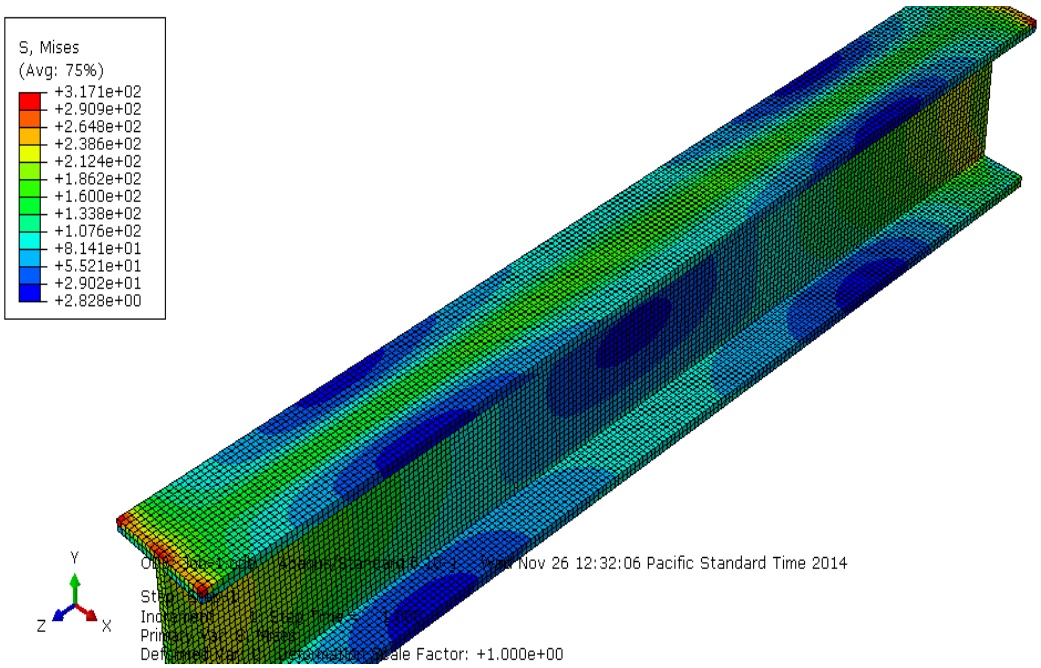


Figure 4.9 Von Mises Stress Diagram of 152.4x101.6x9.525*mm* (Part# IB660) 1500/1525/1625 Series

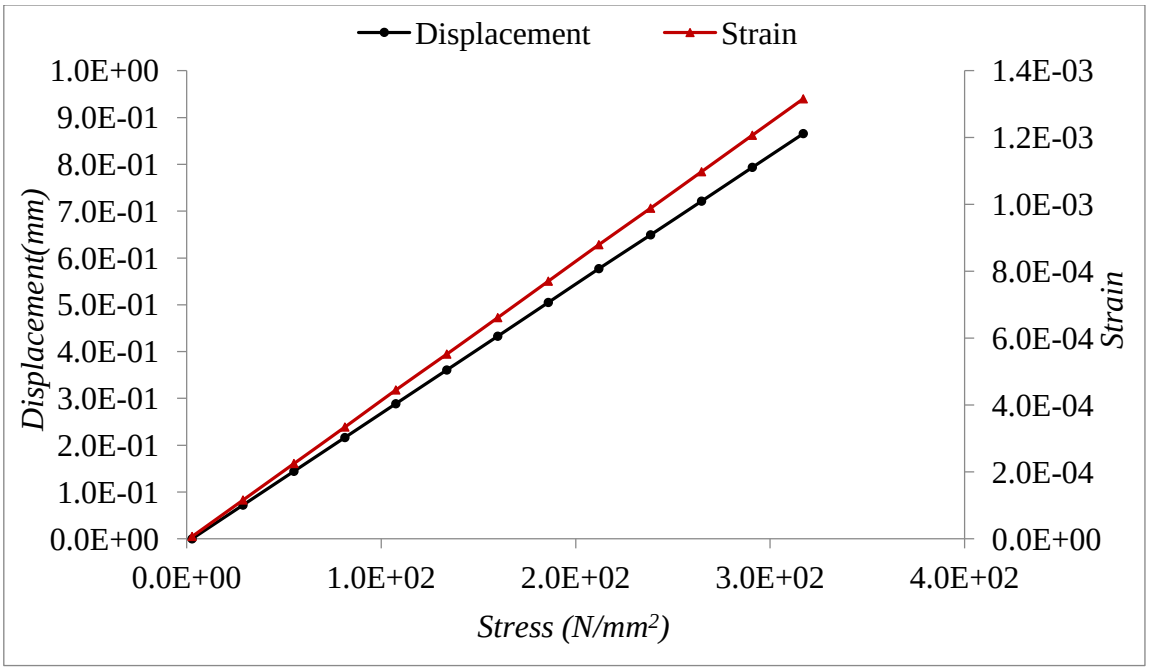


Figure 4.10 Strain and Displacement Graph of 152.4x101.6x9.525*mm* with Corresponding Stresses under the Applied Load

4.7 Stress and Deformation Pattern in Model 5

The Von Mises stress pattern obtained after the analysis of the CFRP beam section can be seen in the deformed diagram of the 203.2x101.6x9.525*mm* (Part# IB860) model shown in figure 4.11. Fields of high stress are formed in the beam near the top end of the flange and web edge of the section, the contour red indicates 254.3N/mm^2 Von Mises stress and hence it is an indication that the beam section is stable when compared to the models above, due to increase in section modulus with increase in size of the beam section, the stress decrease which could be due to the increase in surface area of contact under the applied load. Figure 4.12 shows the graph of stress-displacement and stress-strain which shows a linear relationship in the beam section to a point of 0.761*mm* displacement and strain of 0.0013.

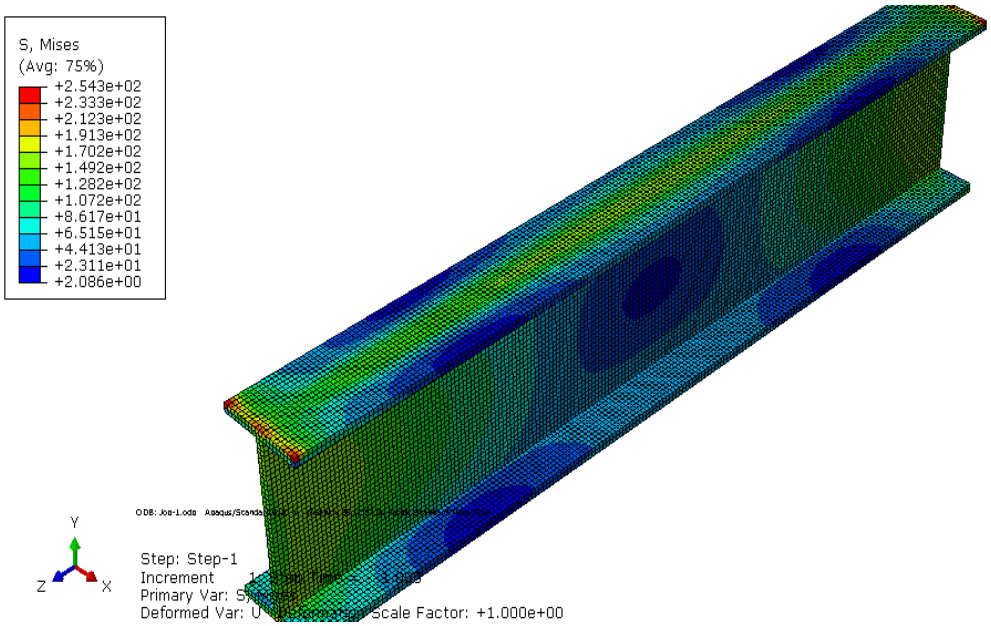


Figure 4.11 Von Mises Stress Diagram of 203.2x101.6x9.525*mm* (Part# IB860) 1500/1525/1625 Series

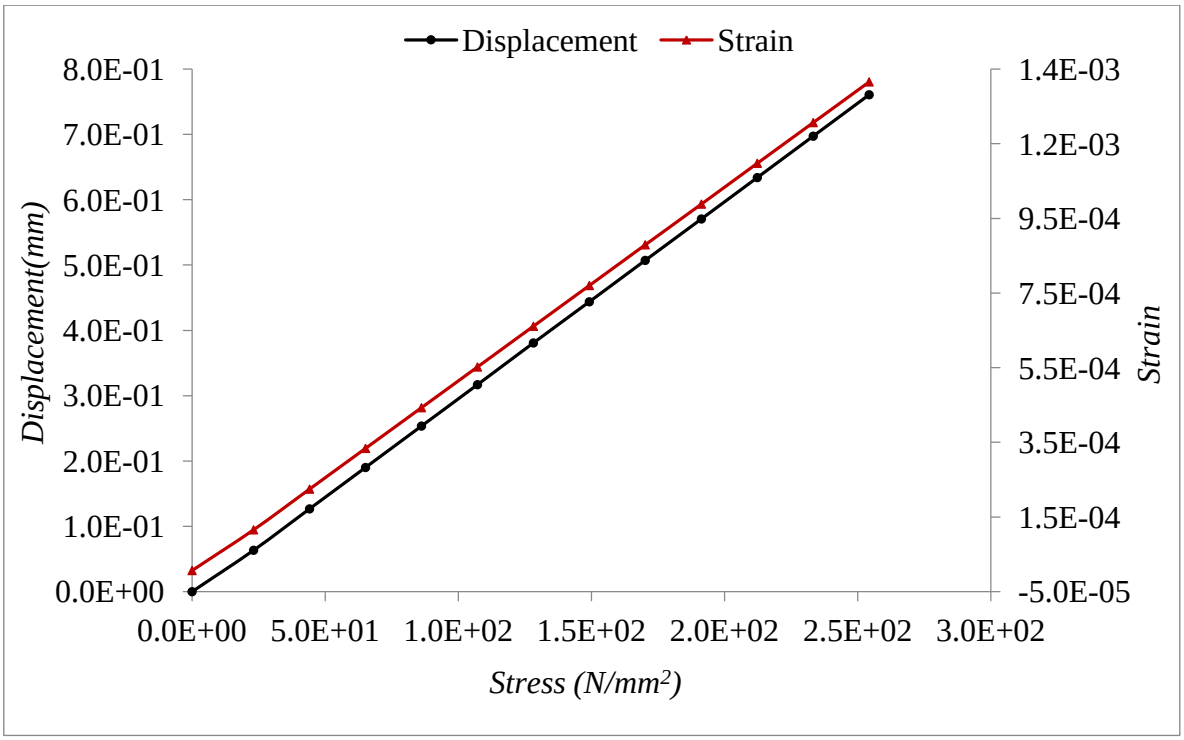


Figure 4.12 Strain and Displacement Graph of 203.2x101.6x9.525*mm* with corresponding Stresses under the Applied Load.

4.8 Stress and Deformation Pattern in Model 6

The Von Mises stress pattern obtained after the analysis of the CFRP beam section can be seen in the deformed diagram of the 203.2x101.6x12.7*mm* (Part# IB880) model shown in Figure 4.13. Fields of high stress are formed in the beam near the top end of the flange and web edge of the section, the contour red indicates 171.9N/mm^2 Von Mises stress and hence it is an indication that the beam section is stable when compared to the other models above, due to increase in section modulus with increase in size of the beam section, the stress decreases which could be due to the increase in surface area of contact under the applied load. Figures 4.14 shows the graph of stress-displacement and stress-strain which shows a linear relationship in the beam section to a point of 0.672*mm* displacement and strain of 0.0012.

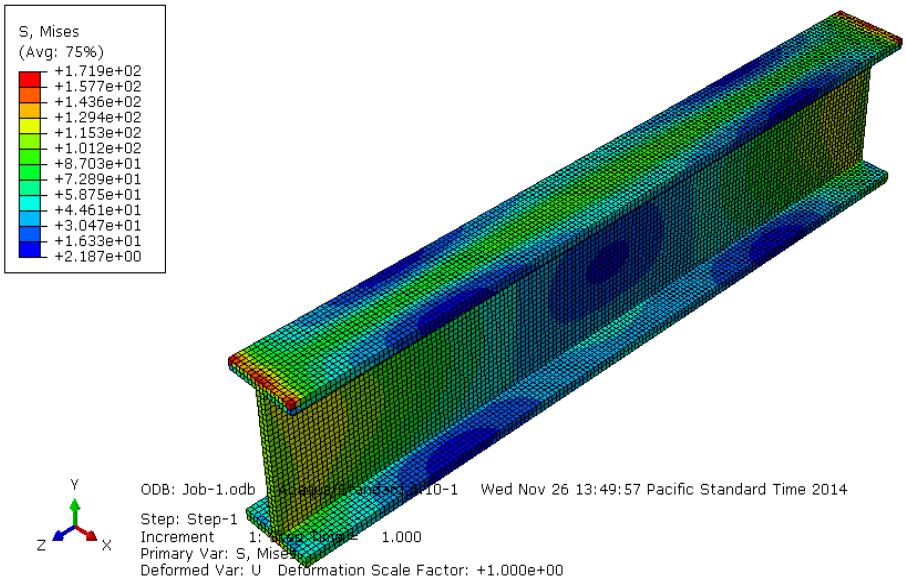


Figure 4.13 Von Mises Stress Diagram of 203.2x101.6x12.7*mm* (Part# IB880) 1500/1525/1625 Series

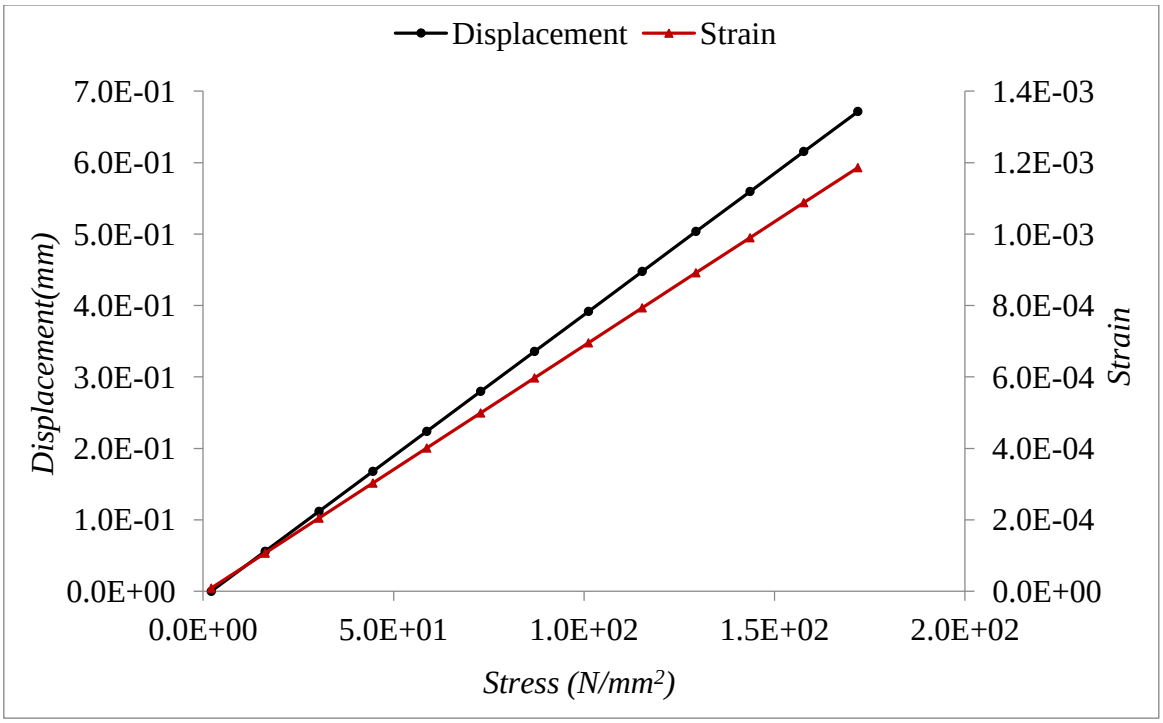


Figure 4.14 Strain and Displacement Graph of 203.2x101.6x12.7*mm* with Corresponding Stresses under the Applied Load

4.9 Reliability Result from FORM5 for Flexure Failure

The stochastic models generated in Table 3.0 are analyzed using the First Order Reliability Method to give values of safety indices (β) for the six (6) pultruded CFRP beam sections are shown below in Figures 4.15 to 4.18. Also, the relationship between the Von Mises stresses and reliability or safety indices is plotted in Figures 4.19 and 4.20 while Figure 4.21 shows the relationship of load ratio to displacement.

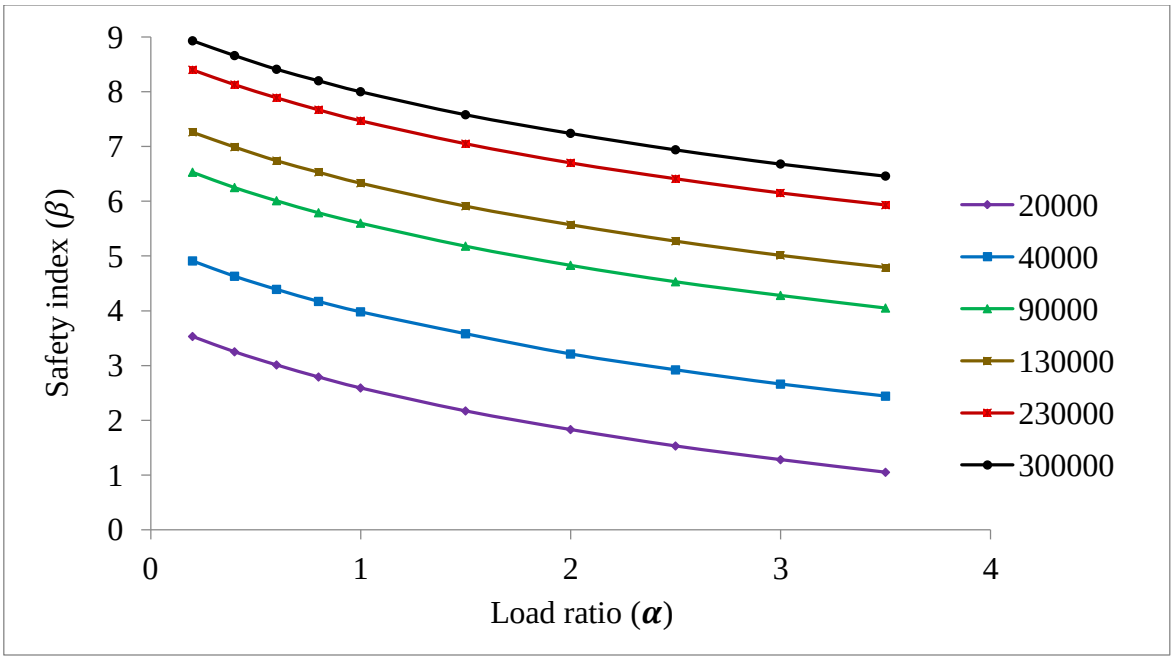


Figure 4.15 Variation of Safety Index (β) with Load Ratio (α) for $G(X) = 0.75 f_y S_x$ LRFD Format

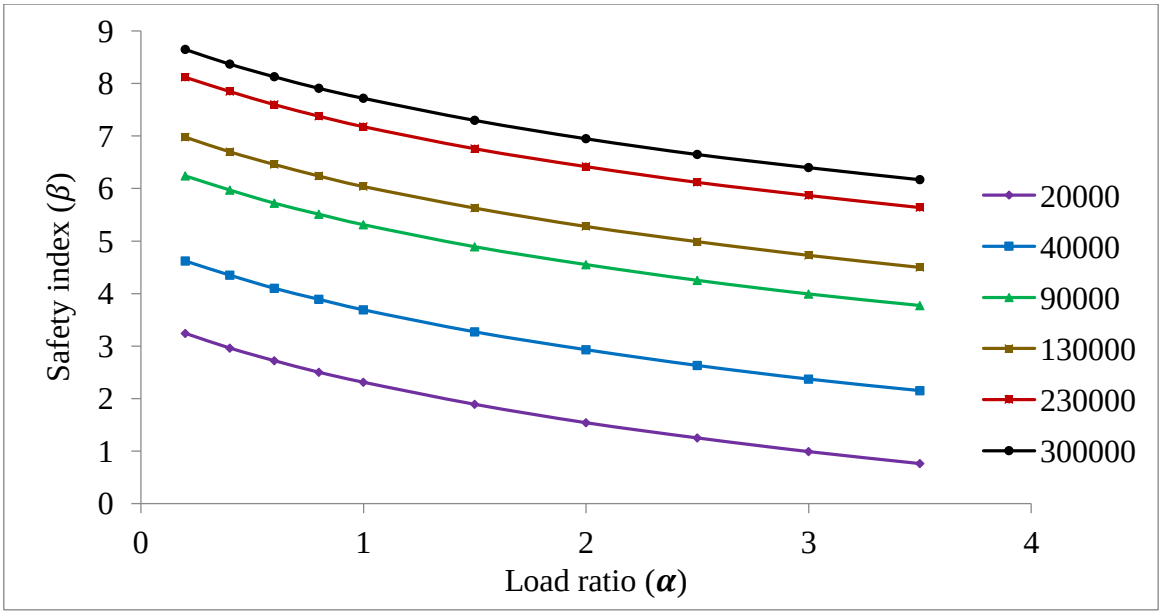


Figure 4.16 Variation of Safety Index (β) with Load Ratio (α) for $G(X) = 0.65 f_y S_x$ LRFD Format

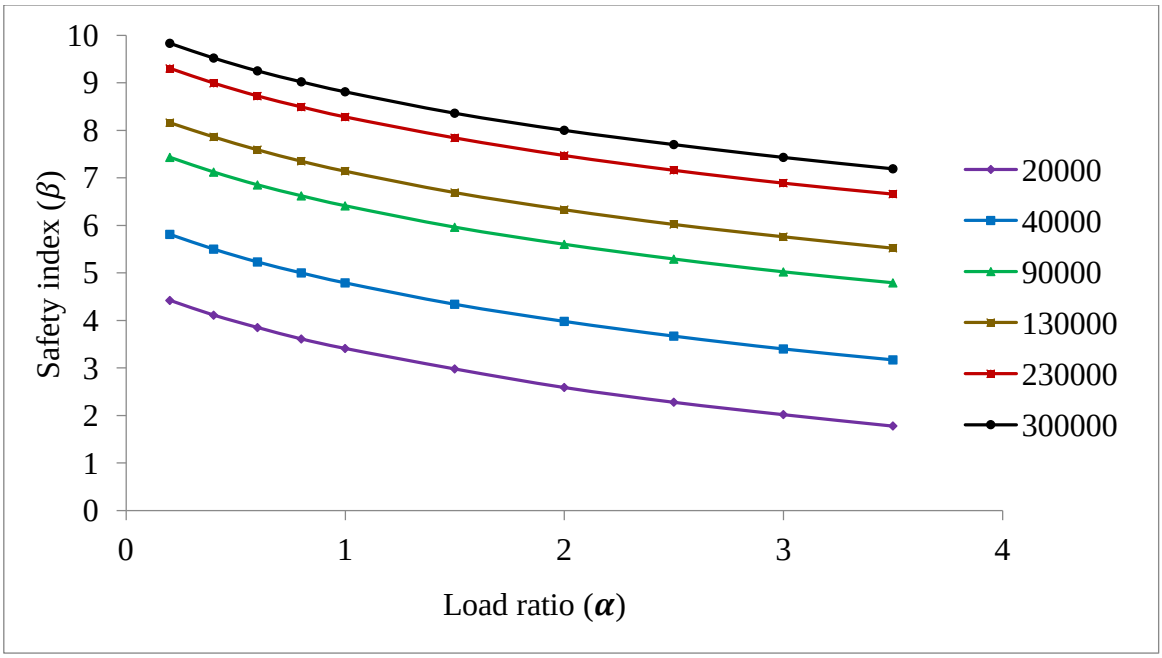


Figure 4.17 Variation of Safety Index (β) with Load Ratio (α) for $G(X) = 0.75 f_y S_x$ ASD Format

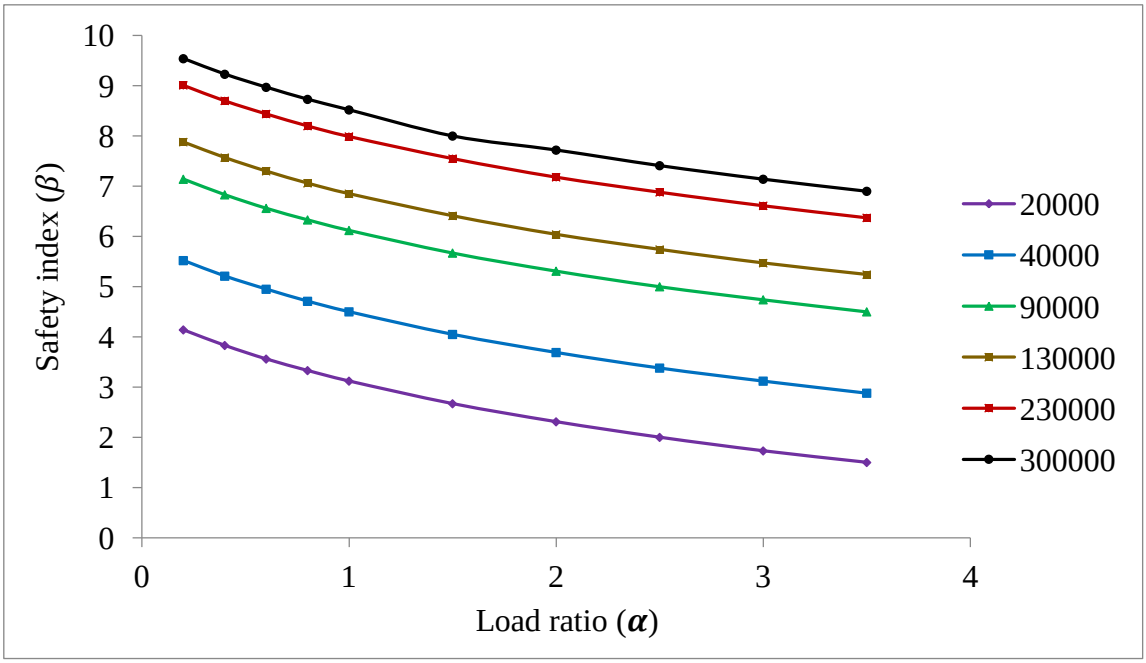


Figure 4.18 Variation of Safety Index (β) with Load Ratio (α) for $G(X) = 0.65 f_y S_x$ ASD Format.

In figures 4.15 to 4.18, the effects of section modulus of the CFRP beam section with the safety indices are presented for both LRFD and ASD format. It is shown that based on LRFD and ASD format, structural safety indices increase with increasing section modulus; since section modulus is a function of strength, as the section modulus increases the stresses in the members are reduced hence the increase in safety index, these results agree with the findings of Roberts and Masri (2003) on Section properties and buckling behavior of pultruded FRP profiles .The only situation that does not guarantee the safety of the beam is when the section modulus is less than $2.0x10^4 mm^3$. When the section modulus is less than $2.0x10^4 mm^3$ these beams are unsafe since the safety indices are negative thus signifying failure. Also, an increase in load ratio goes with a decrease in safety index, based on these results there is nonlinear relationship between safety indices and section modulus, higher load ratio results to low structural safety level.

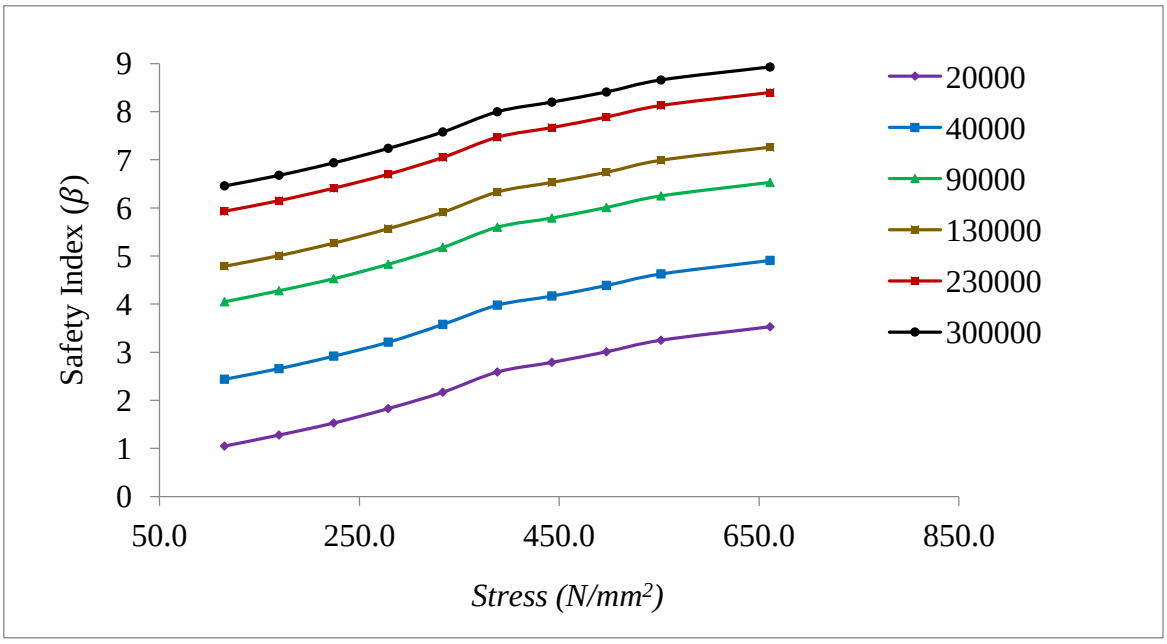


Figure 4.19 Variation of Safety Index (β)-Von Mises Stress for $G(x) = 0.75f_y s_x$ LRFD Format.

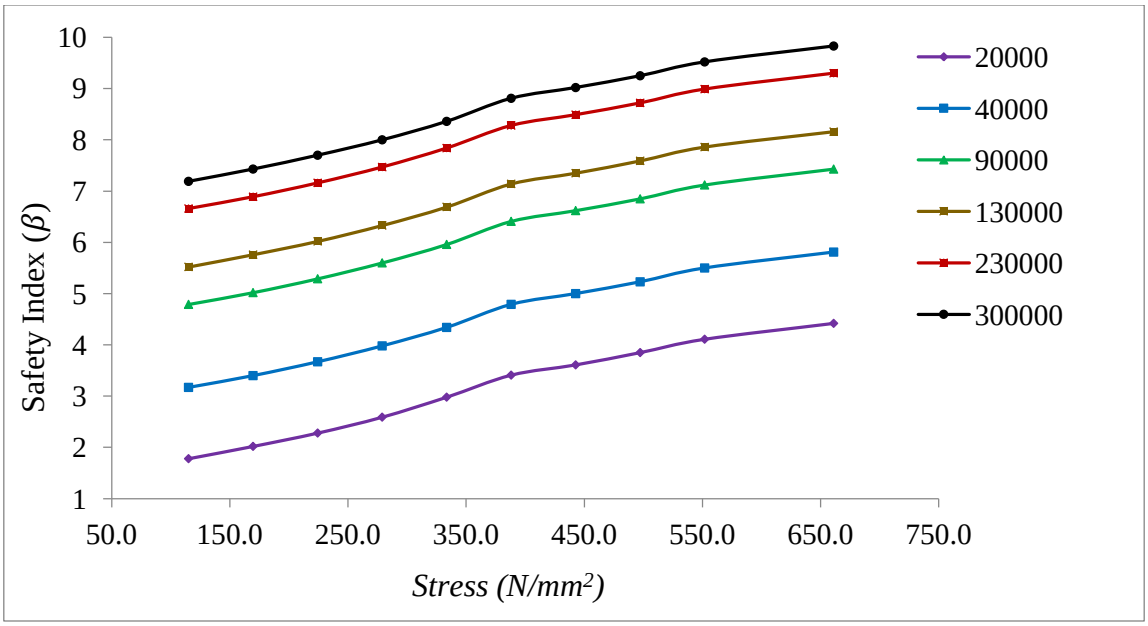


Figure 4.20 Variation of Safety Index (β)-Von Mises Stress for $G(x) = 0.75fysx$ ASD Format.

The results shown in Figure 4.19 and Figure 4.20 indicates that the lower the section modulus and increasing load ratios the more the stresses is being observed which may result to the failure of the beam, consequently with lower FRP tensile strength. However, increase in section modulus as well as increase in CFRP strength increases safety index greatly and the beam is more stable and can also withstand increasing load ratio up to a value of 3.5 at a tensile strength of $3300 N/mm^2$ before failure. Thus, the safety margin of the modeled beam is adequate.

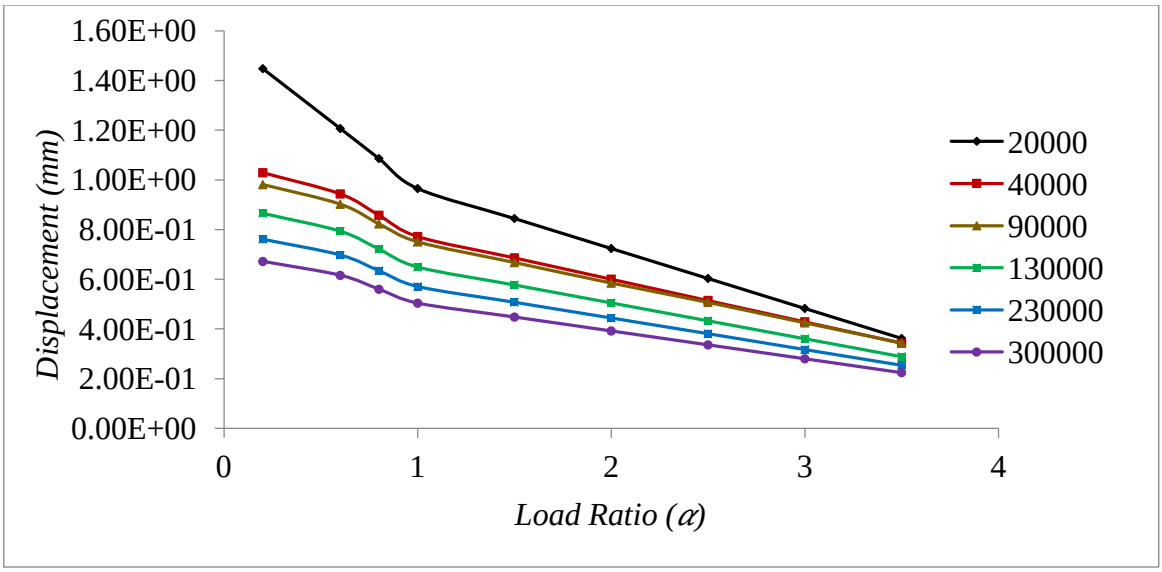


Figure 4.21 Displacement-Load Ratio Graph under the Applied Load

Figure 4.21 shows the displacement-load graph under the applied load, section modulus increases, displacement in the member decreases with increase in load ratio, the more stable is CFRP pultruded beams, these results agree with the findings of Ümit (2007) on, anchorage strength of fibre reinforced polymers.

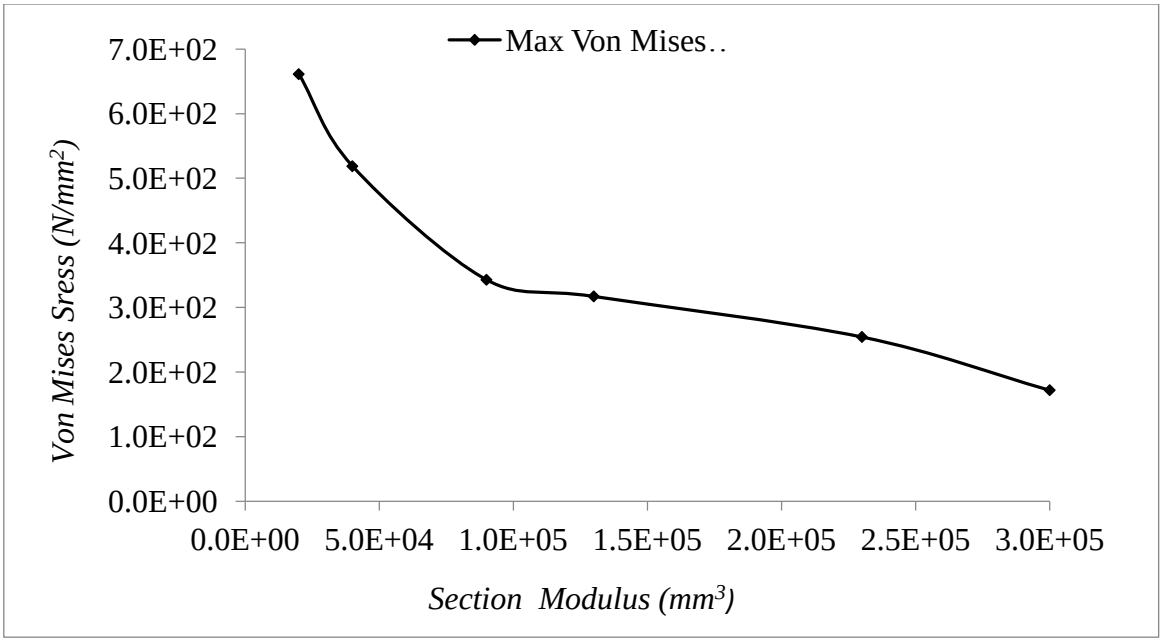


Figure 4.22 Von Mises Stress - Section Modulus Graph under the Applied Load

Figure 4.22 shows the maximum Von Mises stresses in all the models used in ABAQUS 6.10 CAE analysis, when the section modulus is $2.0x10^4 mm^3$ the stress is $661.2 N/mm^2$ which will continue to decrease until the stress is $171.9 N/mm^2$ when the section modulus is $3.0x10^5 mm^3$ which could be due to the increase in surface area of contact under the applied load, the only condition under which the members will not be stable is when the section modulus is less than $2.0x10^4 mm^3$. In summary the stresses in the beams section increases when the section modulus decreases with increase in load ratio. The results from FEA ABAQUS 6.10 CAE and FORM5 analysis are as shown in APPENDICE.

CHAPTER FIVE

5.0 CONCLUSION AND RECOMMENDATION

5.1 Conclusion

From the Finite Element Analysis (FEA) and reliability analysis results, it can be clearly seen that the CFRP pultruded beam sections did not suffer both deformation and displacement due to the material properties provided. Also, the overall member stiffness of the entire section is efficient to sustain the ultimate loads during the service life time. Consequently, based on the design parameters, the deformation obtained and the Von Mises stress distribution indicates that, the field of high stress shown in Model 1 with $661.2 N/mm^2$ and a corresponding displacement of $1.448 mm$ which is minimal under the said load. Also, the Von Mises stress, strain and displacement were reduced with less than 0.001% for strain and 0.1% for displacement on average, when section modulus increases.

The analysis generated by the FORM shows that, with lower load ratios and increasing section modulus the beam performance criteria is adequate resulting to a positive safety index (β) increase with 1.1% that is of greater structural safety. The theoretical framework for risk assessment based on the Joint Council for Structural Safety JCSS (2005) illustrates that the output of a quantitative risk analysis is generally a quantitative measure of consequences and associated probabilities, (Inger *et al*., 2008). Thus the design of an element based on uncertainties such as Quantitative Risk Analysis (QRA) and Structural Reliability Analysis (SRA) indicates that; the reliability indices of epistemic uncertainties for structural safety should be taken as ($\beta = 3$) corresponding to a failure probability of 10^{-3} (Faber *et al*, 2008). From the design model of the CFRP beam section using FORM, the maximum safety index given as ($\beta = 9.83$) which is higher than the limit set by the JCSS

(2005) specification, hence the beam is adequately reliable to a probability of > 10^{-3}; and conforms to the standard specified by the JCSS (2005). Thus CFRP pultruded beam sections possess adequate rigidity for flexural resistance as simply supported beams.

5.2 Recommendation

Based on the result obtained from the analysis in ABAQUS 6.10 CAE and First Order Reliability Method (FORM), the following recommendations are made;

1. CFRP pultruded sections are structurally adequate and safe for use as simply supported beams as per their section modulus.
2. The current load and resistance factor design (LRFD), which is known as limit state design in the United Kingdom, is semi-probabilistic. The is because no guidance is provided for the determination of the extent of the safety achieved in this work, even though the likelihood of failure is recognized and addressed through the use of partial factor of safety. In design of CFRP structures a fully probabilistic method should be employed in order to accommodate all the uncertainties associated with the design variables and measure the extent of the structural reliability through the safety index.
3. An experimental based approach analysis similar to this work is recommended as a means of checking the reliability of CFRP sections in order to trade-off safety and economy.
4. Since no information or guidelines are available in the codes of practice for CFRP materials, therefore further research is recommended to obtain more appropriate result on the deformation, failure and the load carrying capacities of these pultruded beam sections which are used in structural system.

5. Further research is needed to be carried out to study the effect of special loads such as seismic loading and superficial vibration when CFRP beam section in compression is integrated into structural systems. Static loading was considered in this work.
6. It is also recommended that, CFRP pultruded beams should be used more in offshore environment where steel is prone to corrosion.

REFERENCES

ACI 440.1R-03 (2003) *Guide for the Design and Construction of Concrete Reinforced with FRP Bars.* Detroit: American Concrete Institute, USA pp. 42

ACI 440.1R-06 (2006) *Guide for the Design and Construction of Concrete Reinforced with FRP Bars,* Detroit: American Concrete Institute, USA.

ACI 318-02, (2002) *Guide for the Design and Construction of Concrete Reinforced with FRP Bars*. Detroit: American Concrete Institute, USA.

ACI 318-02 and ACI 318R-02, (2002) *Building codes Requirement for structural concretes and commentary*, American Concrete Institute, Farmington Hills; Michigan, USA

ACI 318-05, (2005) *Building code requirements for structural concrete*. Detroit: American Concrete Institute, USA.

ACI 440.1R-06 (2006) *Guide for the design and construction of concrete reinforced with FRP bars*. Detroit: American Concrete Institute, USA.

ACI Committee 318 (1999) *Building Code Requirements for Reinforced Concrete* (ACI 318-99) American Concrete Institute, Farmington Hills

AISC (2005) *Specification for Structural Steel Buildings and Commentary* ANSI/AISC 360-05, American Institute of Steel Construction, Chicago www.aisc.org/2005 spec

Alsayed, S. H., Al-Salloum, Y. A., and Almusallam, T. H. (1997) Shear Design for Beams Reinforced by GFRP Bars. *Third International Symposium on Non-Metallic (FRP) Reinforcement for Concrete Structures,* Sapporo Japan p. 285-292

António C. C. and Hoff Bauer L. N. (2009) An approach for reliability-based robust design optimization of angle-ply composites *Journal of Composite Structures,* Vol. 90(1):53-9.

ASCE (1984) *Structural Plastics Design Manual* ASCE Manuals and Reports on Engineering Practice No. 63, American Society of Civil Engineers, Reston VA.

ASCE (2003) *Minimum Design Loads for Building and other Structures* American Society of Civil Engineers Baltimore, USA pp.7 -20

ASCE (2005) *Minimum Design Loads for Buildings and Other Structures*. ASCE/SEI 7-05 USA

ASCE Standard 7-10 (2010) *Minimum Design Loads for Buildings and Other Structures*. Copyright © 2010 by the American Society of Civil Engineers, ISBN 978-0-7844-10851 Published by American Society of Civil Engineers 1801 Alexander Bell Drive Reston, Virginia 20191 www.pubs.asce.org

Augusti, G., A Baratta, and F. Casciati (1984) *Probabilistic Methods in Structural Engineering* London: Chapman and Hall.

Bank L.C. (1989) Flexural and Shear Moduli of Full-Section Fibre Reinforced Plastic (FRP) Pultruded Beams. *Journal of Testing and Evaluation, ITEVA* Vol. 17(1) Philadelphia

Bank, L. C. (2006) *Composites for Construction Structural Design with FRP Materials*, Hoboken N. J., John Wiley & Sons

Bedard Claude (1992) Composite Reinforcing Bars: Assessing Their Use in Construction. *Concrete International: Design and Construction*, Vol. 14(1):55-59

Benedetti A. and Tralli, A. (1989) New hybrid FE model for arbitrarily curved beam, Linear analysis. *Journal of Composite and Structure*, Vol. 33(6):1437-1449

Brown, Vicki L., Charles L., and Bartholomew (1993) FRP Reinforcing Bars in Reinforced. *ACI Materials Journal* Vol. 1 pp.34-39

BS8110: Part 1(1997*) structural use of concrete: part 1, code of practice for Design and construction,* British Standards Institution, London.

Cardoso B., Sousa L. G., Castro J. A. and Valido A. J. (2002) Optimal design of laminated Composite beam structures. Structural and Multidisciplinary Optimization, Vol. 24(3):205- 11

Chanakya Arya (2009). *Design of Structural Element*: *Concrete, Steelwork, Masonry and* Timber *Design to British Standards and Euro codes*. 2nd Edition Taylor and Francis 2 Park Square, Milton Park, Abingdon, Oxon OX14 4RN

Chang F., Lessard L., Chang K., and Liu S., (1989) Damage tolerance of laminated composites containing a hole and subjected to tension or compression. *34th International SAMPE Symposium and Exhibition-Tomorrow's Materials*: Today. SAMPE, Covina CA, USA pp 559-568. 52

Chiandussi, G., Fontana R., and Urbinati, F. (1998) Design sensitivity analysis method for multidisciplinary shape optimization problems with linear and non-linear responses *Journal of Engineering Computations*, Vol. 15 (2):391-417

Chikh N., M. Gahmous, and R. Benzaid (2012) Structural Performance of High Strength Concrete Columns Confined with CFRP Sheets. *Proceedings of the World Congress on Engineering* Vol. 3 WCE July 4 - 6, London, U.K

Clarke, J. L., (1996) *Structural Design of Polymer Composites, Eurocomp Design Code and Handbook* E & FN Sons, London.

CNR-DT 203 (2006) Guide for the Design and Construction of Concrete Structures Reinforced with Fibre Reinforced Polymer Bars National Research Council, Rome, Italy.

Correia V. M. F., Soares C. M. M., and Soares, C. A. M. (1997) Design sensitivity analysis and optimal design of composite structures using higher order discrete models. *Engineering Optimization*, Vol. 29(1):85-111.

Creative Pultrusions, Inc. (2004). *The New and Improved Pultex® Pultrusion Design Manual of Standard and Custom Fibre Reinforced Polymer Structural Profiles*. Imperial Version Vol. 4 Revision 8

CSA-S806-02 (2002) *Design and Construction of Building Components with Fibre-Reinforced Polymers,* Canadian Standards Association, Ontario, Pp.177

CSA A23.3 (2004) *Design of Concrete Structures* Canadian Standards Association, Ontario

Daly, A. and Duckett W. (2002) *Design and testing of an FRP composite highway deck* ACIC: Thomas Telford; Pp.501

De Lorenzis L., Miller B. and Nanni A. (2001) Bond of FRP Laminates to Concrete. *ACI, Materials Journal* Vol. 98(3), Pp 256-264

Ditlevsen L. and Madsen H. O. (2005) Proposal for a Direct Use of Reliability Methods in Structural Design *Document of the Committee of Structural Safety*, Crystal Magazine.

Ditlevsen, O., & Madsen, H. O. (2005a) *Structural Reliability Methods, Coastal, Maritime and Structural Engineering, Department of Mechanical Engineering*, Technical University of Denmark

Ellingwood, B.R. (1994) Probability-Based Codified Design: Past Accomplishments and Future Challenges. *Journal of Structural Safety*, Vol. 13(3):159-176.

Ellingwood B. R. (2003) Toward Load and Resistance factor Design for Fibre Reinforced Polymer Composite Structures *Journal of Structural Engineering* Vol. 129(4):449-458

Ellingwood B., Galambos T.V., MacGregor J.G. and Cornell C.A. (1980) Development of a probability based load criterion for American national standard A58 building code requirements for minimum design loads in buildings and other structures. *Special Publication* 577, Washington D.C.: National Bureau of Standards, USA.

Erki, M.A. and S.H. Rizkalla, (1993) Anchorages for FRP Concrete *International Design and Construction* Vol. 15(6):54-59.

Eurocode 2: Part 1-1(1992-1-2:2008): *Design of Concrete structures*. CEN, Rue de Stassart, Brussels

Faber M., D. Straub and M. Maes (2006) A computational framework for risk assessment of Reinforced Concrete Structures using indicators *Journal of Computer-aided Civil and Infrastructure Engineering* Vol. 21(3):216–230

Fico, R., Prota, A. and Manfredi, G. (2007) Assessment of Eurocode-like Design Equations for the Shear Capacity of FRP RC Members. *Journal of Composites Part B: Engineering,* Article in Press.

Galambos, T. V. and Ravindra, M. K. (1978) Load and Resistance Factor Design *Journal of Structural Division*, ASCE, ST9, proc. 14008 53

Galambos, T. V., Ellingwood, B., MacGregor, J. G., and Cornell, C. A. (1982) Probability Based Load Criteria: Assessment of Current Design Practice. *ASCE Journal of Structural Division*, Vol. 108(5):959-977

Gollwittzer, S., T. Abdo and R. Rackwitz, (1988) *First Order Reliability Method: (FORM).* User Manual RCP-GMBH, Munich Germany, p.134

Humphrey, M (2003) *Development and Structural Investigation of Monoque Fibre Composite Trusse*s Queensland University of Technology

Ibrahim A. (2003) *Mechanics of Material Advance Topic in Mechanics* 3rd Edition, McGraw Hill Companies, Maryland USA

Iyengar, N. and Curtin, W. A. (1997) Time-dependent failure in fibre reinforced Composites by fibre degradation, *Act a Material* Vol. 45(4): 1489-1507.

Jorge Nocedal and Stephen J. Wright (2006) *Numerical Optimization* 2nd Edition, Springer Series in Operations Research, Springer Verlag,

Kadry S, and Smail K. (200l). An Effective Method for Exact Reliability Analysis *Journal of Applied Sciences*, Vol. 7(16):2333-2338 Asian Network for Science Information

Khalifa, Maghi A., Kuska, Sharon S. B., and Krieger James, (1993) Bridges Constructed Using Fibre Reinforced Plastics. *Concrete International Design and Construction*, Vol. 15(6):43-47

Klieber .M and Hein .T. D (1992) *The stochastic finite element method* John wiley and sons, USA

Liang, Q. Q., Xie, Y. M. and Steven, G. P. (2000) Optimal topology selection of Continuum structures with displacement constraints. *Journal of Computers and Structures*, Vol.77 (6):635-644

Lindgaard E. and Lund, E (2010) Nonlinear buckling optimization of composite Structures *Computer Methods in Applied Mechanics and Engineering*, Vol. 199(37-40):2319-30.

Loughlan J, and Ahmed M. N. (2008). Multi-cell carbon fibre composite box beams subjected to torsion with variable twist. *Thin-Walled Structures* Vol. 46:914-24.

Luigi Ascione, Valentino P. Berardi, Antonella Giordano and Saverio Spadea (2012) Buckling Behavior of FRP pultruded Beams. *Conference of Civil Engineering Infrastructure Based on Polymer Composites* CECOM, 22nd-23rd November, Krakow, Poland

MacGregor, J. (1976) Safety and limit states design for reinforced concrete, *Canadian Journal of Civil Engineering* Vol. 3(4):484-513

Melchers, R. E. (1987) *Structural Reliability, Analysis and Prediction* John Wiley New York, USA

Melchers, R. E. (1999) *Structural Reliability Analysis and Prediction*. Ellis Horwood Limited, Great Britain.

Michael Joseph McCarthy (2009*) Professional Factors for an LRFD Standard for Pultruded Beams.* A Thesis Submitted to the Department of Civil and Environmental Engineering for the Degree of Master of Science in Civil Engineering, Department of Civil and Environmental Engineering, University of Wisconsin – Madison

Mota Soares C. M., Marques Cordeiro, N. M. and Barbosa, J. I. (1995) Discrete model for the design sensitivity analysis of multi-layered composite shells of revolution *Journal of Composites Engineering*, Vol. 5(5):533-50. 54

Mottram, J. T. (2004) Determination of Critical Load for Flange Buckling in Concentrically Loaded Pultruded Columns. *Journal of Composites Part B: Engineering*, Vol. 35(1):35-47.

Musa, M. N., (2003) *Probabilistic Finite Element Analysis of Horizontally Curved Reinforced Concrete Waffle Slab*. A Thesis Submitted to the Postgraduate School, Ahmadu Bello University Zaria, for the Award of Master of Science Degree, Department of Civil Engineering, Ahmadu Bello University Zaria.

Nanni, A., (1999). Composites: Coming on Strong *Journal of Concrete Construction* Vol. 44 Pp. 120

Nocedal j. and S. J. Wright (2006) *Numerical Optimization* 2nd Edition Springer ISBN 0387303030 New York pp.5

Nowak, A.S. (1999). Report 368: Calibration of LRFD Bridge Design Code. National Academy Press Washington D.C

Nowak, A. S. (2004). System Reliability Models for Bridge Structures‖. *Bulletin of the Polish Academy of Sciences*, Vol. 52(4):321.

Nowak, A. S. and Collins, K. R., (2000) *Reliability of Structures* 1st Edition McGraw Hill Co Inc. USA

Panos Y. Papalambros and Douglas J. Wilde, (2000) *Principles of Optimal Design: Modeling and Computation*. 2nd Edition ISBN: 978-0521627276 Cambridge University Press pp.416

Raji, H. O., (2003) *Reliability Assessment of Timber Shell Roof Forms*. A Thesis Submitted to the Postgraduate School, Ahmadu Bello University Zaria, for the Award of Master of Science Degree, Department of Civil Engineering, Ahmadu Bello University Zaria

Roberts, T. M., (2002). Influence of shear deformation on buckling of pultruded fibre Reinforced plastic profiles *Journal of Composite Construction* ASCE Vol. 64:241-248

Roberts T.M. and Masri H.M.K.J.A.H. (2003) Section properties and buckling behavior of pultruded FRP profiles *Journal of Reinforced Plastics and Composites* Vol. 22(14):1305-1313

Saadatmanesh, H., (1994) Fibre Composites for New and Existing Structures *ACI Structural Journal*, Vol. 91(3):346-354

Sapkás, Á and L.P. Kollár (2002) Lateral-torsional buckling of composite beams with shear deformation. *International Journal of Solids and Structures*, Vol. 39:2939-2963

Seangatith, Sittichai (1999) Mechanical Properties and Behavior of Glass Fiber-Reinforced Plastic Composite Material *The Fifth National Convention on Civil Engineering*, Chonburi, Thailand, Vol. 1, pp. 202-207.

Seangatith Sittichai (2001) *Optimization of Pultruded GFRP Beams Bonded with CFRP Plates*. School of Civil Engineering, Institute of Engineering Suranaree, University of Technology, Nakhonratchasima 30000 Thailand

Seangatith Sittichai (2004) Buckling strength of GFRP equal-leg angle structural members under concentric axial compression *Journal of Science Technology* Vol. 11:230-242 School of Civil Engineering, Institute of Engineering, Suranaree University of Technology, Nakhon Ratchasima 30000, Thailand

Sorensen, J. D., (2003). *Note 1&2: Structural Reliability*. Institute of Building Technology and Structural Engineering Aalborg University, Sohngaardsholmsvej 57, DK-9000 Aalborg, Denmark 105

Stefanou, I., Sulem, J. and Vardoulakis I. (2008) Three-dimensional Cosserat homogenization of masonry structures: elasticity, *ACTA Geotech*. Vol. 3(1):71-83.

Talat Salama and Mr. Ahmed Abd-El-Meguid (2010) *Strengthening Steel Bridge Girders using CFRP* Department of Civil Construction and Environmental Engineering, University of Alabama, Birmingham Prepared by UTCA University Transportation Center for Alabama The University of Alabama, The University of Alabama at Birmingham, and The University of Alabama in Huntsville UTCA Report Number 06217 June

Thompson M. D., Eamon C. D. and Rais-Rohani M., (2006) Reliability-based Optimization of fiber-reinforced polymer composite bridge deck panels *Journal of Structural Engineering,* Vol. 132(12):1898-906

Timoshenko S.P. and Gere J. M. (1961) *Theory of Elastic Stability* McGraw-Hill, New York, USA

Togan V. and Daloglu, A. (2006) Reliability and Reliability - Based Design Optimization *Journal of Engineering Environmental Science* Vol. 30:237-249.

Tsopanakis and Papadrakakis (2002) Robust and Efficient Method for Reliability Based Structural Optimization.

ÜMİT SERDAR ÇAMLI, (2007) *Anchorage Strength of Fibre Reinforced Polymers*. A Thesis Submitted to the Graduate School of Natural and Applied Sciences of Middle East Technical University in Partial Fulfillment of the Requirement for the Degree of Master of Science in Civil Engineering

Valido A. J. and Cardoso B. (2003) Geometrical nonlinear composite beam structures: Optimal design. *Engineering Optimization,* Vol. 35(5):553-60.

Wu J. and Burgueño R. (2006) An integrated approach to shape and laminate stacking sequence optimization of free-form FRP shells *Journal of Computer Methods in Applied Mechanics and Engineering,* Vol. 195(33-36):4106 - 23.

Zimmerman T. I. E., Hopkins P. and Sanderson N. (1998) Can Limit State Design Be Used to Design a Pipeline above 80% SMYS. Offshore Mechanics and Acetic Engineering OMAE Vol. 5-A

Zureick A. and Scott D. (1997) Short-term Behavior and Design of Fibre Reinforced Polymeric Slender Members under Axial Compression. *Journal of Composite Construction*, Vol.1 (4):140-149

Zureick A. and Steffen R. (2000) Behavior and Design of Concentrically Loaded Pultruded Angle Struts *ASC E Journal of Structural Engineering*, Vol. 126(3):406-416

APPENDIX A

Table A. Variation of Section Modulus at Various Load Ratios G(x) = $0.75f_y s_x$ (LRFD-Format)

Section Modulus (mm^3)	Load Ratio (α)									
	0.2	0.4	0.6	0.8	1	1.5	2	2.5	3	3.5
20000	3.53	3.25	3.01	2.79	2.59	2.17	1.83	1.53	1.28	1.05
40000	4.91	4.63	4.39	4.17	3.98	3.58	3.21	2.92	2.66	2.44
90000	6.53	6.25	6.01	5.79	5.6	5.18	4.83	4.53	4.28	4.05
130000	7.26	6.99	6.74	6.53	6.33	5.91	5.57	5.27	5.01	4.79
230000	8.4	8.13	7.89	7.67	7.47	7.05	6.7	6.41	6.15	5.93
300000	8.93	8.66	8.41	8.2	8	7.58	7.24	6.94	6.68	6.46

Table A2. Variation of Section Modulus at Various Load Ratios G(x) = $0.65f_y s_x$ (LRFD-Format)

Section Modulus (mm^3)	Load Ratio (α)									
	0.2	0.4	0.6	0.8	1	1.5	2	2.5	3	3.5
20000	3.24	2.96	2.72	2.5	2.31	1.89	1.54	1.25	0.99	0.762
40000	4.62	4.35	4.1	3.89	3.69	3.27	2.93	2.63	2.37	2.15
90000	6.24	5.97	5.72	5.51	5.31	4.89	4.55	4.25	3.99	3.77
130000	6.98	6.7	6.46	6.24	6.04	5.63	5.28	4.99	4.73	4.5
230000	8.12	7.85	7.6	7.38	7.18	6.76	6.42	6.12	5.87	5.64
300000	8.65	8.37	8.13	7.91	7.72	7.3	6.95	6.65	6.4	6.17

Table A3. Variation of Section Modulus at Various Load Ratios G(x) = $0.75f_y s_x$ (ASD-Format)

Section Modulus (mm^3)	Load Ratio (α)									
	0.2	0.4	0.6	0.8	1	1.5	2	2.5	3	3.5
20000	4.42	4.11	3.85	3.61	3.41	2.98	2.59	2.28	2.02	1.78
40000	5.81	5.5	5.23	5	4.79	4.34	3.98	3.67	3.4	3.17
90000	7.43	7.12	6.85	6.62	6.41	5.96	5.6	5.29	5.02	4.79
130000	8.16	7.86	7.59	7.35	7.14	6.69	6.33	6.02	5.76	5.52
230000	9.3	8.99	8.72	8.49	8.28	7.84	7.47	7.16	6.89	6.66
300000	9.83	9.52	9.25	9.02	8.81	8.36	8.0	7.7	7.43	7.19

Table A4. Variation of Section Modulus at Various Load Ratios G(x) = $0.65f_y s_x$ (ASD-Format)

Section Modulus (mm^3)	Load Ratio (α)									
	0.2	0.4	0.6	0.8	1	1.5	2	2.5	3	3.5
20000	4.14	3.83	3.56	3.33	3.12	2.67	2.31	2	1.73	1.5
40000	5.52	5.21	4.95	4.71	4.5	4.05	3.69	3.38	3.12	2.88
90000	7.14	6.83	6.56	6.33	6.12	5.67	5.31	5.0	4.74	4.5
130000	7.88	7.57	7.3	7.06	6.85	6.41	6.04	5.74	5.47	5.24
230000	9.01	8.7	8.44	8.2	7.99	7.55	7.18	6.88	6.61	6.37
300000	9.54	9.23	8.97	8.73	8.52	8	7.72	7.41	7.14	6.9

Table A5. ABAQUS 6.10 CAE Output Field Data for Model 1

Stress (N/mm^2)	Strain (mm)	Reaction force (kN)	Displacement (mm)
6.61E+02	1.73E-03	6.13E+03	1.45E+00
6.07E+02	1.58E-03	5.62E+03	1.33E+00
5.52E+02	1.44E-03	5.11E+03	1.21E+00
4.97E+02	1.30E-03	4.60E+03	1.09E+00
4.43E+02	1.15E-03	4.09E+03	9.65E-01
3.88E+02	1.01E-03	3.58E+03	8.45E-01
3.34E+02	8.68E-04	3.07E+03	7.24E-01
2.79E+02	7.25E-04	2.55E+03	6.03E-01
2.24E+02	5.82E-04	2.04E+03	4.83E-01
1.70E+02	4.39E-04	1.53E+03	3.62E-01
1.15E+02	2.95E-04	1.02E+03	2.41E-01
6.05E+01	1.52E-04	5.11E+02	1.21E-01
5.18E+00	8.96E-06	0.00E+00	0.00E+00

Table A6. ABAQUS 6.10 CAE Output Field Data for Model 2

Stress (N/mm^2)	Strain (mm)	Reaction force(kN)	Displacement (mm)
5.19E+02	1.55E-03	4.92E+03	1.03E+00
4.76E+02	1.42E-03	4.51E+03	9.44E-01
4.33E+02	1.29E-03	4.10E+03	8.58E-01
3.90E+02	1.16E-03	3.69E+03	7.72E-01
3.47E+02	1.03E-03	3.28E+03	6.86E-01
3.04E+02	9.05E-04	2.87E+03	6.00E-01
2.61E+02	7.77E-04	2.46E+03	5.15E-01
2.19E+02	6.49E-04	2.05E+03	4.29E-01
1.76E+02	5.19E-04	1.64E+03	3.43E-01
1.33E+02	3.92E-04	1.23E+03	2.57E-01
8.99E+01	2.64E-04	8.21E+02	1.72E-01
4.70E+01	1.36E-04	1.10E+02	8.58E-02
4.14E+00	7.37E-06	0.00E+00	0.00E+00

Table A7. ABAQUS 6.10 CAE. Output Field Data for Model 3

Stress (N/mm^2)	Strain (mm)	Reaction force (kN)	Displacement (mm)
3.43E+02	1.11E-03	7.77E+03	9.81E-01
3.15E+02	1.01E-03	7.30E+03	9.02E-01
2.86E+02	9.23E-04	6.64E+03	8.23E-01
2.58E+02	8.31E-04	5.97E+03	7.51E-01
2.30E+02	7.40E-04	5.31E+03	6.67E-01
2.02E+02	6.49E-04	4.65E+03	5.85E-01
1.74E+02	5.57E-04	3.98E+03	5.07E-01
1.45E+02	4.66E-04	3.32E+03	4.24E-01
1.17E+02	3.75E-04	2.66E+03	3.44E-01
8.89E+01	2.83E-04	1.99E+03	2.67E-01
6.07E+01	1.92E-04	1.33E+03	1.84E-01
3.25E+01	1.01E-04	6.64E+02	9.28E-02
0.00E+00	9.28E-06	0.00E+00	0.00E+00

Table A8. ABAQUS 6.10 CAE. Output Field Data for Model 4

Stress (N/mm^2)	Strain (mm)	Reaction force (kN)	Displacement (mm)
3.17E+02	1.32E-03	6.69E+03	8.66E-01
2.91E+02	1.21E-03	6.13E+03	7.94E-01
2.65E+02	1.10E-03	5.57E+03	7.21E-01
2.39E+02	9.89E-04	5.02E+03	6.49E-01
2.12E+02	8.80E-04	4.46E+03	5.77E-01
1.86E+02	7.71E-04	3.90E+03	5.05E-01
1.60E+02	6.62E-04	3.34E+03	4.33E-01
1.34E+02	5.53E-04	2.79E+03	3.61E-01
1.08E+02	4.45E-04	2.23E+03	2.89E-01
8.14E+01	3.35E-04	1.67E+03	2.16E-01
5.52E+01	2.25E-04	1.11E+03	1.44E-01
2.90E+01	1.16E-04	5.57E+02	7.21E-02
2.82E+00	7.25E-06	0.00E+00	0.00E+00

Table A9. ABAQUS 6.10 CAE Output Field Data for Model 5

Stress (N/mm^2)	Strain (mm)	Reaction Force (kN)	Displacement (mm)
2.54E+02	1.32E-03	4.90E+03	7.61E-01
2.33E+02	1.21E-03	4.49E+03	6.98E-01
2.12E+02	1.10E-03	4.08E+03	6.34E-01
1.91E+02	9.89E-04	3.68E+03	5.71E-01
1.70E+02	8.80E-04	3.27E+03	5.07E-01
1.49E+02	7.70E-04	2.86E+03	4.44E-01
1.28E+02	6.61E-04	2.45E+03	3.81E-01
1.07E+02	5.52E-04	2.04E+03	3.17E-01
8.62E+01	4.43E-04	1.63E+03	2.54E-01
6.52E+01	3.34E-04	1.23E+03	1.90E-01
4.41E+01	2.25E-04	8.17E+02	1.27E-01
2.31E+01	1.16E-04	4.08E+02	6.34E-02
0.00E+00	6.65E-06	0.00E+00	0.00E+00

Table A10. ABAQUS 6.10 CAE. Output Field Data for Model 6

Stress (N/mm^2)	Strain (mm)	Reaction Force(kN)	Displacement (mm)
1.72E+02	1.19E-03	6.04E+03	6.72E-01
1.58E+02	1.09E-03	5.54E+03	6.16E-01
1.44E+02	9.90E-04	5.04E+03	5.60E-01
1.29E+02	8.92E-04	4.53E+03	5.04E-01
1.15E+02	7.94E-04	4.03E+03	4.48E-01
1.01E+02	6.96E-04	3.53E+03	3.92E-01
8.70E+01	5.97E-04	3.02E+03	3.36E-01
7.29E+01	4.99E-04	2.52E+03	2.80E-01
5.88E+01	4.01E-04	2.01E+03	2.24E-01
4.46E+01	3.03E-04	1.51E+03	1.68E-01
3.05E+01	2.05E-04	1.09E+03	1.12E-01
1.63E+01	1.07E-04	5.04E+02	5.60E-02
2.19E+00	8.94E-06	0.00E+00	0.00E+00

APPENDIX B

```
          PROGRAM  BULUS2
C     STOCHHASTIC SECTION MODULUS REQUIREMENT FOR CFRP
PULTRUDED BEAMS
C     X(1)=YIELD STRESS
C     X(2)=SECTION MODULUS
C     X(3)=IMPOSED LOAD
C     X(4)=SPAN
      IMPLICIT DOUBLE PRECISION (A-H,O-Z)
      EXTERNAL BENDING
      DIMENSION  X(4),EX(4),SX(4),VP(10,4),COV(4,4),ZES(3),
     +          UU(4),EIVEC(4,4),IV(2,4)
      CHARACTER*10 PRT
      COMMON/BENDING /ALPHA
      DATA EX/3.3D3,300D3,3.5D0,3.050D3/,
     +     SX/1.65D2,1.5D4,5.25D-1,8.2356D1/,
     +     N/4/,NC/4/,NE/4/,IRHO/1/
       WRITE(*,*)'ENTER VALUE OF ALPHA.......'
      READ(*,*)ALPHA
      WRITE(*,*)'INPUT VALUE OF SECTION MODULUS.....'
      READ(*,*)EX(2)
      SX(2)=0.5*EX(2)
      NAUS=7
      ICRT=0
      OPEN(7,FILE='BULUS2.RES',STATUS='OLD',ERR=10)
      GOTO 20
10    OPEN(7,FILE='BULUS2.RES',STATUS='NEW')
20    CALL YINIT (N,IV,VP,IRHO,COV,NC)
      IV(1,1)=3
      IV(1,2)=3
      IV(1,3)=3
      DO 100 I=1,N
100       X(I) = EX(I)
      CONTINUE
        V1=1.D0
      BETA=1.D0
      WRITE (NAUS,5000)
5000  FORMAT (////,5X,70('*'),/,30X,'F O R M 5',/,5X,70('*'),/,
     +   20X,'SAFETY LEVEL BENDING CHECK ON BULUS2')
      CALL YKOPF (NAUS, N, IV, EX, SX, VP, IRHO)
      WRITE (ICRT,*) ' START OF FORM5'
      WRITE (ICRT,*) ' STOCHASTIC MODEL :'
      CALL YKOPF (ICRT, N, IV, EX, SX, VP, IRHO)
      PRT='  COV  '
      CALL YMAUS (NAUS,NC,N,COV,PRT)
```

```
      CALL FORM5 (N, IV, EX, SX, VP, BENDING, IRHO, COV, NC,
     +           EIVEC, NE, V1, NAUS, BETA, X, UU, ZES, IER)
      PRT='  UU  '
      CALL YFAUS (NAUS,N,UU,PRT)
      PRT='  ZES  '
      CALL YFAUS (NAUS,3,ZES,PRT)
       WRITE(NAUS,504)
      write(NAUS,505)(uu(i)/beta,i=1,n)
504     FORMAT(/,3X,'ALPHA VECTOR:')
505     format(3x,/3X,6(2X,E8.2)/)
      WRITE (ICRT,*) ' END OF FORM5 : IER =',IER
      WRITE (ICRT,*) ' RESULTS SEE FILE BULUS2.RES'
      STOP
      END

      SUBROUTINE BENDING (N, X, FX, IER)
      IMPLICIT DOUBLE PRECISION (A-H,O-Z)
      DIMENSION X(N)
      COMMON /BENDING/ALPHA
C         G(X) = R-S
       R=0.75*X(1)*X(2)
          S= 0.125*X(3)*X(4)**2*(1.4*ALPHA+1.6)
C         CHECK FOR ERRORS, CALCULATE FX
      IF (R.NE.0..AND.S.NE.0)THEN
         FX = R-S
       IER = 0
      ELSE
       FX = 1.D+20
       IER = 1
      ENDIF
      RETURN
      END

        PROGRAM  BULUS3
C     STOCHHASTIC SECTION MODULUS REQUIREMENT FOR CFRP
PULTRUDED BEAMS
C     X(1)=YIELD STRESS
C     X(2)=SECTION MODULUS
C     X(3)=IMPOSED LOAD
C     X(4)=SPAN
      IMPLICIT DOUBLE PRECISION (A-H,O-Z)
      EXTERNAL BENDING
      DIMENSION  X(4),EX(4),SX(4),VP(10,4),COV(4,4),ZES(3),
     +          UU(4),EIVEC(4,4),IV(2,4)
      CHARACTER*10 PRT
      COMMON/BENDING /ALPHA
```

```
      DATA EX/3.3D3,300D3,3.5D0,3.050D3/,
     +     SX/1.65D2,1.5D4,5.25D-1,8.2356D1/,
     +     N/4/,NC/4/,NE/4/,IRHO/1/
       WRITE(*,*)'ENTER VALUE OF ALPHA.......'
      READ(*,*)ALPHA
      WRITE(*,*)'INPUT VALUE OF SECTION MODULUS.....'
      READ(*,*)EX(2)
      SX(2)=0.5*EX(2)
      NAUS=7
      ICRT=0
      OPEN(7,FILE='BULUS3.RES',STATUS='OLD',ERR=10)
      GOTO 20
10    OPEN(7,FILE='BULUS3.RES',STATUS='NEW')
20    CALL YINIT (N,IV,VP,IRHO,COV,NC)
      IV(1,1)=3
      IV(1,2)=3
      IV(1,3)=3
      DO 100 I=1,N
100       X(I) = EX(I)
      CONTINUE
        V1=1.D0
      BETA=1.D0
      WRITE (NAUS,5000)
5000  FORMAT (////,5X,70('*'),/,30X,'F O R M 5',/,5X,70('*'),/,
     +   20X,'SAFETY LEVEL BENDING CHECK ON BULUS3')
      CALL YKOPF (NAUS, N, IV, EX, SX, VP, IRHO)
      WRITE (ICRT,*) ' START OF FORM5'
      WRITE (ICRT,*) ' STOCHASTIC MODEL :'
      CALL YKOPF (ICRT, N, IV, EX, SX, VP, IRHO)
      PRT='  COV  '
      CALL YMAUS (NAUS,NC,N,COV,PRT)
      CALL FORM5 (N, IV, EX, SX, VP, BENDING, IRHO, COV, NC,
     +           EIVEC, NE, V1, NAUS, BETA, X, UU, ZES, IER)
      PRT='  UU  '
      CALL YFAUS (NAUS,N,UU,PRT)
      PRT='  ZES  '
      CALL YFAUS (NAUS,3,ZES,PRT)
        WRITE(NAUS,504)
       write(NAUS,505)(uu(i)/beta,i=1,n)
504     FORMAT(/,3X,'ALPHA VECTOR:')
505     format(3x,/3X,6(2X,E8.2)/)
      WRITE (ICRT,*) ' END OF FORM5 : IER =',IER
      WRITE (ICRT,*) ' RESULTS SEE FILE BULUS3.RES'
      STOP
      END
```

```
      SUBROUTINE BENDING (N, X, FX, IER)
      IMPLICIT DOUBLE PRECISION (A-H,O-Z)
      DIMENSION X(N)
      COMMON /BENDING/ALPHA
C        G(X) = R-S
       R=0.65*X(1)*X(2)
          S= 0.125*X(3)*X(4)**2*(1.4*ALPHA+1.6)
C        CHECK FOR ERRORS, CALCULATE FX
      IF (R.NE.0..AND.S.NE.0)THEN
         FX = R-S
       IER = 0
      ELSE
       FX = 1.D+20
       IER = 1
      ENDIF
      RETURN
      END
```

APPENDIX C

Abaqus 6.10-1 MODEL 1 Date 26-Nov-2014 Time 11:06:53
For use by TEAM TBE under license from Dassault Systemes or its subsidiary.

The Abaqus Software is a product of:

Dassault Systemes Simulia Corp.
Rising Sun Mills
166 Valley Street
Providence, RI 02909-2499, USA

On machine Bulus-PC
you are authorized to run
Abaqus/Standard until 11-Nov-2017

Your site id is: 20111111

* *
PROCESSING PART, INSTANCE, AND ASSEMBLY INFORMATION
****
END PROCESSING PART, INSTANCE, AND ASSEMBLY INFORMATION
****
OPTIONS BEING PROCESSED
****

```
*Heading
*Node
*Element, type=C3D8R
*Nset, nset="ASSEMBLY_MODEL 1-1__PICKEDSET2"
*Elset, elset="ASSEMBLY_MODEL 1-1__PICKEDSET2"
*Nset, nset=ASSEMBLY__PICKEDSET4
*Elset, elset=ASSEMBLY__PICKEDSET4
*Elset, elset=ASSEMBLY___PICKEDSURF5_S4
*Elset, elset=ASSEMBLY___PICKEDSURF5_S6
*surface, type=ELEMENT, name=ASSEMBLY__PICKEDSURF5
*surface, type=ELEMENT, name=ASSEMBLY__PICKEDSURF5
*material, name=CFRPBEAM
*density
*elastic
*solidsection, elset="ASSEMBLY_MODEL 1-1__PICKEDSET2",
material=CFRPBEAM
*boundary
*solidsection, elset="ASSEMBLY_MODEL 1-1__PICKEDSET2",
material=CFRPBEAM
*surface, type=ELEMENT, name=ASSEMBLY__PICKEDSURF5
*output, field, variable=PRESELECT
```

*output, history, variable=PRESELECT
*output, field, variable=PRESELECT
*output, history, variable=PRESELECT
*output, field, variable=PRESELECT
*output, history, variable=PRESELECT
*Step, name=loadbeam
*output, field, variable=PRESELECT
*output, history, variable=PRESELECT
*Step, name=loadbeam
*Step, name=loadbeam
*static
*boundary
*dsload
*output, field, variable=PRESELECT
*output, history, variable=PRESELECT
*endstep
*Step, name=loadbeam
*static
*boundary
*output, field, variable=PRESELECT
*output, history, variable=PRESELECT
*endstep

- (RAMP) OR (STEP) - INDICATE USE OF DEFAULT AMPLITUDES ASSOCIATED WITH THE STEP

P R O B L E M S I Z E

NUMBER OF ELEMENTS IS 27720
NUMBER OF NODES IS 42660
NUMBER OF NODES DEFINED BY THE USER 42660
TOTAL NUMBER OF VARIABLES IN THE MODEL 127980
(DEGREES OF FREEDOM PLUS MAX NO. OF ANY LAGRANGE MULTIPLIER
VARIABLES. INCLUDE *PRINT,SOLVE=YES TO GET THE ACTUAL NUMBER.)

END OF USER INPUT PROCESSING

JOB TIME SUMMARY
USER TIME (SEC) = 3.9000
SYSTEM TIME (SEC) = 0.30000
TOTAL CPU TIME (SEC) = 4.2000
WALLCLOCK TIME (SEC) = 10

STEP 1 INCREMENT 1

TIME COMPLETED IN THIS STEP 0.00

S T E P 1 S T A T I C A N A L Y S I S

AUTOMATIC TIME CONTROL WITH -
A SUGGESTED INITIAL TIME INCREMENT OF 1.00
AND A TOTAL TIME PERIOD OF 1.00
THE MINIMUM TIME INCREMENT ALLOWED IS 1.000E-05
THE MAXIMUM TIME INCREMENT ALLOWED IS 1.00

LINEAR EQUATION SOLVER TYPE DIRECT SPARSE

M E M O R Y E S T I M A T E

PROCESS	FLOATING PT OPERATIONS PER ITERATION	MINIMUM MEMORY REQUIRED (MBYTES)	MEMORY TO MINIMIZE I/O (MBYTES)
1	1.42E+010	104	460

NOTE:
(1) SINCE ABAQUS DOES NOT PRE-ALLOCATE MEMORY AND ONLY ALLOCATES MEMORY AS NEEDED DURING THE ANALYSIS,
THE MEMORY REQUIREMENT PRINTED HERE CAN ONLY BE VIEWED AS A GENERAL GUIDELINE BASED ON THE BEST
KNOWLEDGE AVAILABLE AT THE BEGINNING OF A STEP BEFORE THE SOLUTION PROCESS HAS BEGUN.
(2) THE ESTIMATE IS NORMALLY UPDATED AT THE BEGINNING OF EVERY STEP. IT IS THE MAXIMUM VALUE OF THE
ESTIMATE FROM THE CURRENT STEP TO THE LAST STEP OF THE ANALYSIS, WITH UNSYMMETRIC SOLUTION TAKEN
INTO ACCOUNT IF APPLICABLE.
(3) SINCE THE ESTIMATE IS BASED ON THE ACTIVE DEGREES OF FREEDOM IN THE FIRST ITERATION OF THE
CURRENT STEP, THE MEMORY ESTIMATE MIGHT BE SIGNIFICANTLY DIFFERENT THAN ACTUAL USAGE FOR
PROBLEMS WITH SUBSTANTIAL CHANGES IN ACTIVE DEGREES OF FREEDOM BETWEEN STEPS (OR EVEN WITHIN
THE SAME STEP). EXAMPLES ARE: PROBLEMS WITH SIGNIFICANT CONTACT CHANGES, PROBLEMS WITH MODEL
CHANGE, PROBLEMS WITH BOTH STATIC STEP AND STEADY STATE DYNAMIC PROCEDURES WHERE ACOUSTIC
ELEMENTS WILL ONLY BE ACTIVATED IN THE STEADY STATE DYNAMIC STEPS.

(4) FOR MULTI-PROCESS EXECUTION, THE ESTIMATED VALUE OF FLOATING POINT OPERATIONS FOR EACH PROCESS
IS BASED ON AN INITIAL SCHEDULING OF OPERATIONS AND MIGHT NOT REFLECT THE ACTUAL FLOATING
POINT OPERATIONS COMPLETED ON EACH PROCESS. OPERATIONS ARE DYNAMICALY BALANCED DURING EXECUTION,
SO THE ACTUAL BALANCE OF OPERATIONS BETWEEN PROCESSES IS EXPECTED TO BE BETTER THAN THE ESTIMATE
PRINTED HERE.
(5) THE UPPER LIMIT OF MEMORY THAT CAN BE ALLOCATED BY ABAQUS WILL IN GENERAL DEPEND ON THE VALUE OF
THE "MEMORY" PARAMETER AND THE AMOUNT OF PHYSICAL MEMORY AVAILABLE ON THE MACHINE. PLEASE SEE
THE "ABAQUS ANALYSIS USER'S MANUAL" FOR MORE DETAILS. THE ACTUAL USAGE OF MEMORY AND OF DISK
SPACE FOR SCRATCH DATA WILL DEPEND ON THIS UPPER LIMIT AS WELL AS THE MEMORY REQUIRED TO MINIMIZE
I/O. IF THE MEMORY UPPER LIMIT IS GREATER THAN THE MEMORY REQUIRED TO MINIMIZE I/O, THEN THE ACTUAL
MEMORY USAGE WILL BE CLOSE TO THE ESTIMATED "MEMORY TO MINIMIZE I/O" VALUE, AND THE SCRATCH DISK
USAGE WILL BE CLOSE-TO-ZERO; OTHERWISE, THE ACTUAL MEMORY USED WILL BE CLOSE TO THE PREVIOUSLY
MENTIONED MEMORY LIMIT, AND THE SCRATCH DISK USAGE WILL BE ROUGHLY PROPORTIONAL TO THE DIFFERENCE
BETWEEN THE ESTIMATED "MEMORY TO MINIMIZE I/O" AND THE MEMORY UPPER LIMIT. HOWEVER ACCURATE
ESTIMATE OF THE SCRATCH DISK SPACE IS NOT POSSIBLE.
(6) USING "*RESTART, WRITE" CAN GENERATE A LARGE AMOUNT OF DATA WRITTEN IN THE WORK DIRECTORY.

THE ANALYSIS HAS BEEN COMPLETED

ANALYSIS COMPLETE

JOB TIME SUMMARY
USER TIME (SEC) = 10.800
SYSTEM TIME (SEC) = 0.60000
TOTAL CPU TIME (SEC) = 11.400
WALLCLOCK TIME (SEC) = 19

Abaqus 6.10-1 MODEL 2 Date 26-Nov-2014 Time 11:39:06
For use by TEAM TBE under license from Dassault Systemes or its subsidiary.

The Abaqus Software is a product of:

Dassault Systemes Simulia Corp.
Rising Sun Mills
166 Valley Street
Providence, RI 02909-2499, USA

On machine Bulus-PC
you are authorized to run
Abaqus/Standard until 11-Nov-2017

Your site id is: 20111111

* *

PROCESSING PART, INSTANCE, AND ASSEMBLY INFORMATION
****

END PROCESSING PART, INSTANCE, AND ASSEMBLY INFORMATION
****

OPTIONS BEING PROCESSED
****

*Heading
*Node
*Element, type=C3D8R
*Nset, nset=ASSEMBLY_MODEL2-1__PICKEDSET2
*Elset, elset=ASSEMBLY_MODEL2-1__PICKEDSET2
*Nset, nset=ASSEMBLY__PICKEDSET4
*Elset, elset=ASSEMBLY__PICKEDSET4
*Elset, elset=ASSEMBLY___PICKEDSURF5_S4
*Elset, elset=ASSEMBLY___PICKEDSURF5_S6
*surface, type=ELEMENT, name=ASSEMBLY__PICKEDSURF5
*surface, type=ELEMENT, name=ASSEMBLY__PICKEDSURF5
*material, name=MATERIAL-1
*density
*elastic
*solidsection, elset=ASSEMBLY_MODEL2-1__PICKEDSET2, material=MATERIAL-1
*boundary
*solidsection, elset=ASSEMBLY_MODEL2-1__PICKEDSET2, material=MATERIAL-1
*surface, type=ELEMENT, name=ASSEMBLY__PICKEDSURF5
*output, field, variable=PRESELECT
*output, history, variable=PRESELECT
*output, field, variable=PRESELECT

*output, history, variable=PRESELECT
*output, field, variable=PRESELECT
*output, history, variable=PRESELECT
*Step, name=Step-1
*output, field, variable=PRESELECT
*output, history, variable=PRESELECT
*Step, name=Step-1
*Step, name=Step-1
*static
*boundary
*dsload
*output, field, variable=PRESELECT
*output, history, variable=PRESELECT
*endstep
*Step, name=Step-1
*static
*boundary
*output, field, variable=PRESELECT
*output, history, variable=PRESELECT
*endstep

- (RAMP) OR (STEP) - INDICATE USE OF DEFAULT AMPLITUDES ASSOCIATED WITH THE STEP

P R O B L E M S I Z E

NUMBER OF ELEMENTS IS 37800
NUMBER OF NODES IS 57828
NUMBER OF NODES DEFINED BY THE USER 57828
TOTAL NUMBER OF VARIABLES IN THE MODEL 173484
(DEGREES OF FREEDOM PLUS MAX NO. OF ANY LAGRANGE MULTIPLIER
VARIABLES. INCLUDE *PRINT,SOLVE=YES TO GET THE ACTUAL NUMBER.)

END OF USER INPUT PROCESSING

JOB TIME SUMMARY
USER TIME (SEC) = 4.8000
SYSTEM TIME (SEC) = 0.50000
TOTAL CPU TIME (SEC) = 5.3000
WALLCLOCK TIME (SEC) = 10
1
STEP 1 INCREMENT 1
TIME COMPLETED IN THIS STEP 0.00

S T E P 1 S T A T I C A N A L Y S I S

AUTOMATIC TIME CONTROL WITH -
A SUGGESTED INITIAL TIME INCREMENT OF 1.00
AND A TOTAL TIME PERIOD OF 1.00
THE MINIMUM TIME INCREMENT ALLOWED IS 1.000E-05
THE MAXIMUM TIME INCREMENT ALLOWED IS 1.00

LINEAR EQUATION SOLVER TYPE DIRECT SPARSE

M E M O R Y E S T I M A T E

PROCESS	FLOATING PT OPERATIONS PER ITERATION	MINIMUM MEMORY REQUIRED (MBYTES)	MEMORY TO MINIMIZE I/O (MBYTES)
1	2.47E+010	144	653

NOTE:
(1) SINCE ABAQUS DOES NOT PRE-ALLOCATE MEMORY AND ONLY ALLOCATES MEMORY AS NEEDED DURING THE ANALYSIS,
THE MEMORY REQUIREMENT PRINTED HERE CAN ONLY BE VIEWED AS A GENERAL GUIDELINE BASED ON THE BEST
KNOWLEDGE AVAILABLE AT THE BEGINNING OF A STEP BEFORE THE SOLUTION PROCESS HAS BEGUN.
(2) THE ESTIMATE IS NORMALLY UPDATED AT THE BEGINNING OF EVERY STEP. IT IS THE MAXIMUM VALUE OF THE
ESTIMATE FROM THE CURRENT STEP TO THE LAST STEP OF THE ANALYSIS, WITH UNSYMMETRIC SOLUTION TAKEN
INTO ACCOUNT IF APPLICABLE.
(3) SINCE THE ESTIMATE IS BASED ON THE ACTIVE DEGREES OF FREEDOM IN THE FIRST ITERATION OF THE
CURRENT STEP, THE MEMORY ESTIMATE MIGHT BE SIGNIFICANTLY DIFFERENT THAN ACTUAL USAGE FOR
PROBLEMS WITH SUBSTANTIAL CHANGES IN ACTIVE DEGREES OF FREEDOM BETWEEN STEPS (OR EVEN WITHIN
THE SAME STEP). EXAMPLES ARE: PROBLEMS WITH SIGNIFICANT CONTACT CHANGES, PROBLEMS WITH MODEL
CHANGE, PROBLEMS WITH BOTH STATIC STEP AND STEADY STATE DYNAMIC PROCEDURES WHERE ACOUSTIC
ELEMENTS WILL ONLY BE ACTIVATED IN THE STEADY STATE DYNAMIC STEPS.
(4) FOR MULTI-PROCESS EXECUTION, THE ESTIMATED VALUE OF FLOATING POINT OPERATIONS FOR EACH PROCESS

IS BASED ON AN INITIAL SCHEDULING OF OPERATIONS AND MIGHT NOT REFLECT THE ACTUAL FLOATING
POINT OPERATIONS COMPLETED ON EACH PROCESS. OPERATIONS ARE DYNAMICALY BALANCED DURING EXECUTION,
SO THE ACTUAL BALANCE OF OPERATIONS BETWEEN PROCESSES IS EXPECTED TO BE BETTER THAN THE ESTIMATE
PRINTED HERE.
(5) THE UPPER LIMIT OF MEMORY THAT CAN BE ALLOCATED BY ABAQUS WILL IN GENERAL DEPEND ON THE VALUE OF
THE "MEMORY" PARAMETER AND THE AMOUNT OF PHYSICAL MEMORY AVAILABLE ON THE MACHINE. PLEASE SEE
THE "ABAQUS ANALYSIS USER'S MANUAL" FOR MORE DETAILS. THE ACTUAL USAGE OF MEMORY AND OF DISK
SPACE FOR SCRATCH DATA WILL DEPEND ON THIS UPPER LIMIT AS WELL AS THE MEMORY REQUIRED TO MINIMIZE
I/O. IF THE MEMORY UPPER LIMIT IS GREATER THAN THE MEMORY REQUIRED TO MINIMIZE I/O, THEN THE ACTUAL
MEMORY USAGE WILL BE CLOSE TO THE ESTIMATED "MEMORY TO MINIMIZE I/O" VALUE, AND THE SCRATCH DISK
USAGE WILL BE CLOSE-TO-ZERO; OTHERWISE, THE ACTUAL MEMORY USED WILL BE CLOSE TO THE PREVIOUSLY
MENTIONED MEMORY LIMIT, AND THE SCRATCH DISK USAGE WILL BE ROUGHLY PROPORTIONAL TO THE DIFFERENCE
BETWEEN THE ESTIMATED "MEMORY TO MINIMIZE I/O" AND THE MEMORY UPPER LIMIT. HOWEVER ACCURATE
ESTIMATE OF THE SCRATCH DISK SPACE IS NOT POSSIBLE.
(6) USING "*RESTART, WRITE" CAN GENERATE A LARGE AMOUNT OF DATA WRITTEN IN THE WORK DIRECTORY.

THE ANALYSIS HAS BEEN COMPLETED

ANALYSIS COMPLETE

JOB TIME SUMMARY
USER TIME (SEC) = 15.900
SYSTEM TIME (SEC) = 0.70000
TOTAL CPU TIME (SEC) = 16.600
WALLCLOCK TIME (SEC) = 27

Abaqus 6.10-1 MODEL 3 Date 26-Nov-2014 Time 16:14:05
For use by TEAM TBE under license from Dassault Systemes or its subsidiary.

The Abaqus Software is a product of:

Dassault Systemes Simulia Corp.
Rising Sun Mills
166 Valley Street
Providence, RI 02909-2499, USA

On machine Bulus-PC
you are authorized to run
Abaqus/Standard until 11-Nov-2017

Your site id is: 20111111

* *
PROCESSING PART, INSTANCE, AND ASSEMBLY INFORMATION
****
END PROCESSING PART, INSTANCE, AND ASSEMBLY INFORMATION
****
OPTIONS BEING PROCESSED
****
*Heading
*Node
*Element, type=C3D8R
*Nset, nset="ASSEMBLY_MODEL 3-1__PICKEDSET2"
*Elset, elset="ASSEMBLY_MODEL 3-1__PICKEDSET2"
*Nset, nset=ASSEMBLY__PICKEDSET4
*Nset, nset=ASSEMBLY__PICKEDSET5
*Elset, elset=ASSEMBLY__PICKEDSET4
*Elset, elset=ASSEMBLY__PICKEDSET5
*Elset, elset=ASSEMBLY___PICKEDSURF6_S3
*Elset, elset=ASSEMBLY___PICKEDSURF6_S4
*Elset, elset=ASSEMBLY___PICKEDSURF6_S5
*Elset, elset=ASSEMBLY___PICKEDSURF6_S6
*surface, type=ELEMENT, name=ASSEMBLY__PICKEDSURF6
*surface, type=ELEMENT, name=ASSEMBLY__PICKEDSURF6
*material, name=MATERIAL-1
*density
*elastic
*solidsection, elset="ASSEMBLY_MODEL 3-1__PICKEDSET2", material=MATERIAL-1
*boundary
*boundary

*solidsection, elset="ASSEMBLY_MODEL 3-1__PICKEDSET2", material=MATERIAL-1
*surface, type=ELEMENT, name=ASSEMBLY__PICKEDSURF6
*output, field, variable=PRESELECT
*output, history, variable=PRESELECT
*output, field, variable=PRESELECT
*output, history, variable=PRESELECT
*output, field, variable=PRESELECT
*output, history, variable=PRESELECT
*Step, name=Step-1
*output, field, variable=PRESELECT
*output, history, variable=PRESELECT
*Step, name=Step-1
*Step, name=Step-1
*static
*boundary
*boundary
*dsload
*output, field, variable=PRESELECT
*output, history, variable=PRESELECT
*endstep
*Step, name=Step-1
*static
*boundary
*boundary
*output, field, variable=PRESELECT
*output, history, variable=PRESELECT
*endstep

- (RAMP) OR (STEP) - INDICATE USE OF DEFAULT AMPLITUDES ASSOCIATED WITH THE STEP

P R O B L E M S I Z E

NUMBER OF ELEMENTS IS 11600
NUMBER OF NODES IS 23718
NUMBER OF NODES DEFINED BY THE USER 23718
TOTAL NUMBER OF VARIABLES IN THE MODEL 71154
(DEGREES OF FREEDOM PLUS MAX NO. OF ANY LAGRANGE MULTIPLIER
VARIABLES. INCLUDE *PRINT,SOLVE=YES TO GET THE ACTUAL NUMBER.)

END OF USER INPUT PROCESSING

JOB TIME SUMMARY
USER TIME (SEC) = 1.8000
SYSTEM TIME (SEC) = 0.30000
TOTAL CPU TIME (SEC) = 2.1000
WALLCLOCK TIME (SEC) = 6
1

STEP 1 INCREMENT 1
TIME COMPLETED IN THIS STEP 0.00

S T E P 1 S T A T I C A N A L Y S I S

AUTOMATIC TIME CONTROL WITH -
A SUGGESTED INITIAL TIME INCREMENT OF 1.00
AND A TOTAL TIME PERIOD OF 1.00
THE MINIMUM TIME INCREMENT ALLOWED IS 1.000E-05
THE MAXIMUM TIME INCREMENT ALLOWED IS 1.00

LINEAR EQUATION SOLVER TYPE DIRECT SPARSE

M E M O R Y E S T I M A T E

PROCESS	FLOATING PT OPERATIONS PER ITERATION	MINIMUM MEMORY REQUIRED (MBYTES)	MEMORY TO MINIMIZE I/O (MBYTES)
1	4.15E+009	55	210

NOTE:
(1) SINCE ABAQUS DOES NOT PRE-ALLOCATE MEMORY AND ONLY ALLOCATES MEMORY AS NEEDED DURING THE ANALYSIS,
THE MEMORY REQUIREMENT PRINTED HERE CAN ONLY BE VIEWED AS A GENERAL GUIDELINE BASED ON THE BEST
KNOWLEDGE AVAILABLE AT THE BEGINNING OF A STEP BEFORE THE SOLUTION PROCESS HAS BEGUN.
(2) THE ESTIMATE IS NORMALLY UPDATED AT THE BEGINNING OF EVERY STEP. IT IS THE MAXIMUM VALUE OF THE
ESTIMATE FROM THE CURRENT STEP TO THE LAST STEP OF THE ANALYSIS, WITH UNSYMMETRIC SOLUTION TAKEN
INTO ACCOUNT IF APPLICABLE.
(3) SINCE THE ESTIMATE IS BASED ON THE ACTIVE DEGREES OF FREEDOM IN THE FIRST ITERATION OF THE
CURRENT STEP, THE MEMORY ESTIMATE MIGHT BE SIGNIFICANTLY DIFFERENT THAN ACTUAL USAGE FOR
PROBLEMS WITH SUBSTANTIAL CHANGES IN ACTIVE DEGREES OF FREEDOM BETWEEN STEPS (OR EVEN WITHIN

THE SAME STEP). EXAMPLES ARE: PROBLEMS WITH SIGNIFICANT CONTACT CHANGES, PROBLEMS WITH MODEL
CHANGE, PROBLEMS WITH BOTH STATIC STEP AND STEADY STATE DYNAMIC PROCEDURES WHERE ACOUSTIC
ELEMENTS WILL ONLY BE ACTIVATED IN THE STEADY STATE DYNAMIC STEPS.
(4) FOR MULTI-PROCESS EXECUTION, THE ESTIMATED VALUE OF FLOATING POINT OPERATIONS FOR EACH PROCESS
IS BASED ON AN INITIAL SCHEDULING OF OPERATIONS AND MIGHT NOT REFLECT THE ACTUAL FLOATING
POINT OPERATIONS COMPLETED ON EACH PROCESS. OPERATIONS ARE DYNAMICALY BALANCED DURING EXECUTION,
SO THE ACTUAL BALANCE OF OPERATIONS BETWEEN PROCESSES IS EXPECTED TO BE BETTER THAN THE ESTIMATE
PRINTED HERE.
(5) THE UPPER LIMIT OF MEMORY THAT CAN BE ALLOCATED BY ABAQUS WILL IN GENERAL DEPEND ON THE VALUE OF
THE "MEMORY" PARAMETER AND THE AMOUNT OF PHYSICAL MEMORY AVAILABLE ON THE MACHINE. PLEASE SEE
THE "ABAQUS ANALYSIS USER'S MANUAL" FOR MORE DETAILS. THE ACTUAL USAGE OF MEMORY AND OF DISK
SPACE FOR SCRATCH DATA WILL DEPEND ON THIS UPPER LIMIT AS WELL AS THE MEMORY REQUIRED TO MINIMIZE
I/O. IF THE MEMORY UPPER LIMIT IS GREATER THAN THE MEMORY REQUIRED TO MINIMIZE I/O, THEN THE ACTUAL
MEMORY USAGE WILL BE CLOSE TO THE ESTIMATED "MEMORY TO MINIMIZE I/O" VALUE, AND THE SCRATCH DISK
USAGE WILL BE CLOSE-TO-ZERO; OTHERWISE, THE ACTUAL MEMORY USED WILL BE CLOSE TO THE PREVIOUSLY
MENTIONED MEMORY LIMIT, AND THE SCRATCH DISK USAGE WILL BE ROUGHLY PROPORTIONAL TO THE DIFFERENCE
BETWEEN THE ESTIMATED "MEMORY TO MINIMIZE I/O" AND THE MEMORY UPPER LIMIT. HOWEVER ACCURATE
ESTIMATE OF THE SCRATCH DISK SPACE IS NOT POSSIBLE.
(6) USING "*RESTART, WRITE" CAN GENERATE A LARGE AMOUNT OF DATA WRITTEN IN THE WORK DIRECTORY.

THE ANALYSIS HAS BEEN COMPLETED

ANALYSIS COMPLETE

JOB TIME SUMMARY
USER TIME (SEC) = 4.5000
SYSTEM TIME (SEC) = 0.10000
TOTAL CPU TIME (SEC) = 4.6000
WALLCLOCK TIME (SEC) = 8

Abaqus 6.10-1 MODEL 4 Date 26-Nov-2014 Time 12:32:01
For use by TEAM TBE under license from Dassault Systemes or its subsidiary.

The Abaqus Software is a product of:

Dassault Systemes Simulia Corp.
Rising Sun Mills
166 Valley Street
Providence, RI 02909-2499, USA

On machine Bulus-PC
you are authorized to run
Abaqus/Standard until 11-Nov-2017

Your site id is: 20111111

* *

PROCESSING PART, INSTANCE, AND ASSEMBLY INFORMATION

END PROCESSING PART, INSTANCE, AND ASSEMBLY INFORMATION

OPTIONS BEING PROCESSED

*Heading
*Node
*Element, type=C3D8R
*Nset, nset="ASSEMBLY_MODEL 4-1__PICKEDSET2"
*Elset, elset="ASSEMBLY_MODEL 4-1__PICKEDSET2"
*Nset, nset=ASSEMBLY__PICKEDSET4
*Elset, elset=ASSEMBLY__PICKEDSET4
*Elset, elset=ASSEMBLY___PICKEDSURF5_S3
*Elset, elset=ASSEMBLY___PICKEDSURF5_S4
*Elset, elset=ASSEMBLY___PICKEDSURF5_S5
*Elset, elset=ASSEMBLY___PICKEDSURF5_S6
*surface, type=ELEMENT, name=ASSEMBLY__PICKEDSURF5
*surface, type=ELEMENT, name=ASSEMBLY__PICKEDSURF5
*material, name=MATERIAL-1
*density
*elastic
*solidsection, elset="ASSEMBLY_MODEL 4-1__PICKEDSET2", material=MATERIAL-1
*boundary
*solidsection, elset="ASSEMBLY_MODEL 4-1__PICKEDSET2", material=MATERIAL-1
*surface, type=ELEMENT, name=ASSEMBLY__PICKEDSURF5
*output, field, variable=PRESELECT

*output, history, variable=PRESELECT
*output, field, variable=PRESELECT
*output, history, variable=PRESELECT
*output, field, variable=PRESELECT
*output, history, variable=PRESELECT
*Step, name=Step-1
*output, field, variable=PRESELECT
*output, history, variable=PRESELECT
*Step, name=Step-1
*Step, name=Step-1
*static
*boundary
*dsload
*output, field, variable=PRESELECT
*output, history, variable=PRESELECT
*endstep
*Step, name=Step-1
*static
*boundary
*output, field, variable=PRESELECT
*output, history, variable=PRESELECT
*endstep

- (RAMP) OR (STEP) - INDICATE USE OF DEFAULT AMPLITUDES ASSOCIATED WITH THE STEP

P R O B L E M S I Z E

NUMBER OF ELEMENTS IS 26800
NUMBER OF NODES IS 41004
NUMBER OF NODES DEFINED BY THE USER 41004
TOTAL NUMBER OF VARIABLES IN THE MODEL 123012
(DEGREES OF FREEDOM PLUS MAX NO. OF ANY LAGRANGE MULTIPLIER
VARIABLES. INCLUDE *PRINT,SOLVE=YES TO GET THE ACTUAL NUMBER.)

END OF USER INPUT PROCESSING

JOB TIME SUMMARY
USER TIME (SEC) = 3.5000
SYSTEM TIME (SEC) = 0.30000
TOTAL CPU TIME (SEC) = 3.8000
WALLCLOCK TIME (SEC) = 9
1

STEP 1 INCREMENT 1

TIME COMPLETED IN THIS STEP 0.00

S T E P 1 S T A T I C A N A L Y S I S

AUTOMATIC TIME CONTROL WITH -
A SUGGESTED INITIAL TIME INCREMENT OF 1.00
AND A TOTAL TIME PERIOD OF 1.00
THE MINIMUM TIME INCREMENT ALLOWED IS 1.000E-05
THE MAXIMUM TIME INCREMENT ALLOWED IS 1.00

LINEAR EQUATION SOLVER TYPE DIRECT SPARSE

M E M O R Y E S T I M A T E

PROCESS	FLOATING PT OPERATIONS PER ITERATION	MINIMUM MEMORY REQUIRED (MBYTES)	MEMORY TO MINIMIZE I/O (MBYTES)
1	2.05E+010	107	493

NOTE:
(1) SINCE ABAQUS DOES NOT PRE-ALLOCATE MEMORY AND ONLY ALLOCATES MEMORY AS NEEDED DURING THE ANALYSIS,
THE MEMORY REQUIREMENT PRINTED HERE CAN ONLY BE VIEWED AS A GENERAL GUIDELINE BASED ON THE BEST
KNOWLEDGE AVAILABLE AT THE BEGINNING OF A STEP BEFORE THE SOLUTION PROCESS HAS BEGUN.
(2) THE ESTIMATE IS NORMALLY UPDATED AT THE BEGINNING OF EVERY STEP. IT IS THE MAXIMUM VALUE OF THE
ESTIMATE FROM THE CURRENT STEP TO THE LAST STEP OF THE ANALYSIS, WITH UNSYMMETRIC SOLUTION TAKEN
INTO ACCOUNT IF APPLICABLE.
(3) SINCE THE ESTIMATE IS BASED ON THE ACTIVE DEGREES OF FREEDOM IN THE FIRST ITERATION OF THE
CURRENT STEP, THE MEMORY ESTIMATE MIGHT BE SIGNIFICANTLY DIFFERENT THAN ACTUAL USAGE FOR
PROBLEMS WITH SUBSTANTIAL CHANGES IN ACTIVE DEGREES OF FREEDOM BETWEEN STEPS (OR EVEN WITHIN
THE SAME STEP). EXAMPLES ARE: PROBLEMS WITH SIGNIFICANT CONTACT CHANGES, PROBLEMS WITH MODEL
CHANGE, PROBLEMS WITH BOTH STATIC STEP AND STEADY STATE DYNAMIC PROCEDURES WHERE ACOUSTIC
ELEMENTS WILL ONLY BE ACTIVATED IN THE STEADY STATE DYNAMIC STEPS.

(4) FOR MULTI-PROCESS EXECUTION, THE ESTIMATED VALUE OF FLOATING POINT OPERATIONS FOR EACH PROCESS
IS BASED ON AN INITIAL SCHEDULING OF OPERATIONS AND MIGHT NOT REFLECT THE ACTUAL FLOATING
POINT OPERATIONS COMPLETED ON EACH PROCESS. OPERATIONS ARE DYNAMICALY BALANCED DURING EXECUTION,
SO THE ACTUAL BALANCE OF OPERATIONS BETWEEN PROCESSES IS EXPECTED TO BE BETTER THAN THE ESTIMATE
PRINTED HERE.
(5) THE UPPER LIMIT OF MEMORY THAT CAN BE ALLOCATED BY ABAQUS WILL IN GENERAL DEPEND ON THE VALUE OF
THE "MEMORY" PARAMETER AND THE AMOUNT OF PHYSICAL MEMORY AVAILABLE ON THE MACHINE. PLEASE SEE
THE "ABAQUS ANALYSIS USER'S MANUAL" FOR MORE DETAILS. THE ACTUAL USAGE OF MEMORY AND OF DISK
SPACE FOR SCRATCH DATA WILL DEPEND ON THIS UPPER LIMIT AS WELL AS THE MEMORY REQUIRED TO MINIMIZE
I/O. IF THE MEMORY UPPER LIMIT IS GREATER THAN THE MEMORY REQUIRED TO MINIMIZE I/O, THEN THE ACTUAL
MEMORY USAGE WILL BE CLOSE TO THE ESTIMATED "MEMORY TO MINIMIZE I/O" VALUE, AND THE SCRATCH DISK
USAGE WILL BE CLOSE-TO-ZERO; OTHERWISE, THE ACTUAL MEMORY USED WILL BE CLOSE TO THE PREVIOUSLY
MENTIONED MEMORY LIMIT, AND THE SCRATCH DISK USAGE WILL BE ROUGHLY PROPORTIONAL TO THE DIFFERENCE
BETWEEN THE ESTIMATED "MEMORY TO MINIMIZE I/O" AND THE MEMORY UPPER LIMIT. HOWEVER ACCURATE
ESTIMATE OF THE SCRATCH DISK SPACE IS NOT POSSIBLE.
(6) USING "*RESTART, WRITE" CAN GENERATE A LARGE AMOUNT OF DATA WRITTEN IN THE WORK DIRECTORY.

THE ANALYSIS HAS BEEN COMPLETED

ANALYSIS COMPLETE

JOB TIME SUMMARY
USER TIME (SEC) = 11.700
SYSTEM TIME (SEC) = 0.60000
TOTAL CPU TIME (SEC) = 12.300
WALLCLOCK TIME (SEC) = 15

Abaqus 6.10-1 MODEL 5 Date 26-Nov-2014

Time 12:57:30
For use by TEAM TBE under license from Dassault Systemes or its subsidiary.

The Abaqus Software is a product of:

Dassault Systemes Simulia Corp.
Rising Sun Mills
166 Valley Street
Providence, RI 02909-2499, USA

On machine Bulus-PC
you are authorized to run
Abaqus/Standard until 11-Nov-2017

Your site id is: 20111111

* *
PROCESSING PART, INSTANCE, AND ASSEMBLY INFORMATION
****
END PROCESSING PART, INSTANCE, AND ASSEMBLY INFORMATION
****
OPTIONS BEING PROCESSED
****
*Heading
*Node
*Element, type=C3D8R
*Nset, nset="ASSEMBLY_MODEL 5-1__PICKEDSET2"
*Elset, elset="ASSEMBLY_MODEL 5-1__PICKEDSET2"
*Nset, nset=ASSEMBLY__PICKEDSET4
*Elset, elset=ASSEMBLY__PICKEDSET4
*Elset, elset=ASSEMBLY___PICKEDSURF5_S3
*Elset, elset=ASSEMBLY___PICKEDSURF5_S4
*Elset, elset=ASSEMBLY___PICKEDSURF5_S5
*Elset, elset=ASSEMBLY___PICKEDSURF5_S6
*surface, type=ELEMENT, name=ASSEMBLY__PICKEDSURF5
*surface, type=ELEMENT, name=ASSEMBLY__PICKEDSURF5
*material, name=MATERIAL-1
*density
*elastic
*solidsection, elset="ASSEMBLY_MODEL 5-1__PICKEDSET2",

material=MATERIAL-1
*boundary

*solidsection, elset="ASSEMBLY_MODEL 5-1__PICKEDSET2",

material=MATERIAL-1
*surface, type=ELEMENT, name=ASSEMBLY__PICKEDSURF5
*output, field, variable=PRESELECT
*output, history, variable=PRESELECT
*output, field, variable=PRESELECT
*output, history, variable=PRESELECT
*output, field, variable=PRESELECT
*output, history, variable=PRESELECT
*Step, name=Step-1
*output, field, variable=PRESELECT
*output, history, variable=PRESELECT
*Step, name=Step-1
*Step, name=Step-1
*static
*boundary
*dsload
*output, field, variable=PRESELECT
*output, history, variable=PRESELECT
*endstep
*Step, name=Step-1
*static
*boundary
*output, field, variable=PRESELECT
*output, history, variable=PRESELECT
*endstep

- (RAMP) OR (STEP) - INDICATE USE OF DEFAULT AMPLITUDES ASSOCIATED

WITH THE STEP

P R O B L E M S I Z E

NUMBER OF ELEMENTS IS 30800
NUMBER OF NODES IS 47034
NUMBER OF NODES DEFINED BY THE USER 47034
TOTAL NUMBER OF VARIABLES IN THE MODEL 141102
(DEGREES OF FREEDOM PLUS MAX NO. OF ANY LAGRANGE MULTIPLIER
VARIABLES. INCLUDE *PRINT,SOLVE=YES TO GET THE ACTUAL

NUMBER.)

END OF USER INPUT PROCESSING

JOB TIME SUMMARY
USER TIME (SEC) = 3.9000
SYSTEM TIME (SEC) = 0.30000
TOTAL CPU TIME (SEC) = 4.2000
WALLCLOCK TIME (SEC) = 7
1

STEP 1 INCREMENT 1

TIME COMPLETED IN THIS STEP 0.00

S T E P 1 S T A T I C A N A L Y S I S

AUTOMATIC TIME CONTROL WITH -
A SUGGESTED INITIAL TIME INCREMENT OF 1.00
AND A TOTAL TIME PERIOD OF 1.00
THE MINIMUM TIME INCREMENT ALLOWED IS 1.000E-05
THE MAXIMUM TIME INCREMENT ALLOWED IS 1.00

LINEAR EQUATION SOLVER TYPE DIRECT SPARSE

M E M O R Y E S T I M A T E

PROCESS	FLOATING PT OPERATIONS PER ITERATION	MINIMUM MEMORY REQUIRED (MBYTES)	MEMORY TO MINIMIZE I/O (MBYTES)
1	2.21E+010	121	549

NOTE:
(1) SINCE ABAQUS DOES NOT PRE-ALLOCATE MEMORY AND ONLY ALLOCATES

MEMORY AS NEEDED DURING THE ANALYSIS,
THE MEMORY REQUIREMENT PRINTED HERE CAN ONLY BE VIEWED AS A

GENERAL GUIDELINE BASED ON THE BEST
KNOWLEDGE AVAILABLE AT THE BEGINNING OF A STEP BEFORE THE

SOLUTION PROCESS HAS BEGUN.
(2) THE ESTIMATE IS NORMALLY UPDATED AT THE BEGINNING OF EVERY

STEP. IT IS THE MAXIMUM VALUE OF THE

ESTIMATE FROM THE CURRENT STEP TO THE LAST STEP OF THE

ANALYSIS, WITH UNSYMMETRIC SOLUTION TAKEN
INTO ACCOUNT IF APPLICABLE.
(3) SINCE THE ESTIMATE IS BASED ON THE ACTIVE DEGREES OF FREEDOM

IN THE FIRST ITERATION OF THE
CURRENT STEP, THE MEMORY ESTIMATE MIGHT BE SIGNIFICANTLY

DIFFERENT THAN ACTUAL USAGE FOR
PROBLEMS WITH SUBSTANTIAL CHANGES IN ACTIVE DEGREES OF FREEDOM

BETWEEN STEPS (OR EVEN WITHIN
THE SAME STEP). EXAMPLES ARE: PROBLEMS WITH SIGNIFICANT

CONTACT CHANGES, PROBLEMS WITH MODEL
CHANGE, PROBLEMS WITH BOTH STATIC STEP AND STEADY STATE

DYNAMIC PROCEDURES WHERE ACOUSTIC
ELEMENTS WILL ONLY BE ACTIVATED IN THE STEADY STATE DYNAMIC

STEPS.
(4) FOR MULTI-PROCESS EXECUTION, THE ESTIMATED VALUE OF FLOATING

POINT OPERATIONS FOR EACH PROCESS
IS BASED ON AN INITIAL SCHEDULING OF OPERATIONS AND MIGHT NOT

REFLECT THE ACTUAL FLOATING
POINT OPERATIONS COMPLETED ON EACH PROCESS. OPERATIONS ARE

DYNAMICALY BALANCED DURING EXECUTION,
SO THE ACTUAL BALANCE OF OPERATIONS BETWEEN PROCESSES IS

EXPECTED TO BE BETTER THAN THE ESTIMATE
PRINTED HERE.
(5) THE UPPER LIMIT OF MEMORY THAT CAN BE ALLOCATED BY ABAQUS WILL

IN GENERAL DEPEND ON THE VALUE OF

THE "MEMORY" PARAMETER AND THE AMOUNT OF PHYSICAL MEMORY

AVAILABLE ON THE MACHINE. PLEASE SEE
THE "ABAQUS ANALYSIS USER'S MANUAL" FOR MORE DETAILS. THE

ACTUAL USAGE OF MEMORY AND OF DISK
SPACE FOR SCRATCH DATA WILL DEPEND ON THIS UPPER LIMIT AS WELL

AS THE MEMORY REQUIRED TO MINIMIZE
I/O. IF THE MEMORY UPPER LIMIT IS GREATER THAN THE MEMORY

REQUIRED TO MINIMIZE I/O, THEN THE ACTUAL
MEMORY USAGE WILL BE CLOSE TO THE ESTIMATED "MEMORY TO

MINIMIZE I/O" VALUE, AND THE SCRATCH DISK
USAGE WILL BE CLOSE-TO-ZERO; OTHERWISE, THE ACTUAL MEMORY USED

WILL BE CLOSE TO THE PREVIOUSLY
MENTIONED MEMORY LIMIT, AND THE SCRATCH DISK USAGE WILL BE

ROUGHLY PROPORTIONAL TO THE DIFFERENCE
BETWEEN THE ESTIMATED "MEMORY TO MINIMIZE I/O" AND THE MEMORY

UPPER LIMIT. HOWEVER ACCURATE
ESTIMATE OF THE SCRATCH DISK SPACE IS NOT POSSIBLE.
(6) USING "*RESTART, WRITE" CAN GENERATE A LARGE AMOUNT OF DATA

WRITTEN IN THE WORK DIRECTORY.

THE ANALYSIS HAS BEEN COMPLETED

ANALYSIS COMPLETE

JOB TIME SUMMARY
USER TIME (SEC) = 13.000
SYSTEM TIME (SEC) = 0.60000
TOTAL CPU TIME (SEC) = 13.600
WALLCLOCK TIME (SEC) = 17

Abaqus 6.10-1 MODEL 6 Date 26-Nov-2014 Time 11:06:53
For use by TEAM TBE under license from Dassault Systemes or its subsidiary.

The Abaqus Software is a product of:

Dassault Systemes Simulia Corp.
Rising Sun Mills
166 Valley Street
Providence, RI 02909-2499, USA

On machine Bulus-PC
you are authorized to run
Abaqus/Standard until 11-Nov-2017

Your site id is: 20111111

* *

PROCESSING PART, INSTANCE, AND ASSEMBLY INFORMATION
****

END PROCESSING PART, INSTANCE, AND ASSEMBLY INFORMATION
****

OPTIONS BEING PROCESSED
****

*Heading
*Node
*Element, type=C3D8R
*Nset, nset="ASSEMBLY_MODEL 6-1__PICKEDSET2"
*Elset, elset="ASSEMBLY_MODEL 1-1__PICKEDSET2"
*Nset, nset=ASSEMBLY__PICKEDSET4
*Elset, elset=ASSEMBLY__PICKEDSET4
*Elset, elset=ASSEMBLY___PICKEDSURF5_S4
*Elset, elset=ASSEMBLY___PICKEDSURF5_S6
*surface, type=ELEMENT, name=ASSEMBLY__PICKEDSURF5
*surface, type=ELEMENT, name=ASSEMBLY__PICKEDSURF5
*material, name=CFRPBEAM
*density
*elastic
*solidsection, elset="ASSEMBLY_MODEL6 1-1__PICKEDSET2", material=CFRPBEAM
*boundary
*solidsection, elset="ASSEMBLY_MODEL6 1-1__PICKEDSET2", material=CFRPBEAM
*surface, type=ELEMENT, name=ASSEMBLY__PICKEDSURF5
*output, field, variable=PRESELECT
*output, history, variable=PRESELECT
*output, field, variable=PRESELECT

*output, history, variable=PRESELECT
*output, field, variable=PRESELECT
*output, history, variable=PRESELECT
*Step, name=loadbeam
*output, field, variable=PRESELECT
*output, history, variable=PRESELECT
*Step, name=loadbeam
*Step, name=loadbeam
*static
*boundary
*dsload
*output, field, variable=PRESELECT
*output, history, variable=PRESELECT
*endstep
*Step, name=loadbeam
*static
*boundary
*output, field, variable=PRESELECT
*output, history, variable=PRESELECT
*endstep

- (RAMP) OR (STEP) - INDICATE USE OF DEFAULT AMPLITUDES ASSOCIATED WITH THE STEP

P R O B L E M S I Z E

NUMBER OF ELEMENTS IS 27720
NUMBER OF NODES IS 42660
NUMBER OF NODES DEFINED BY THE USER 42660
TOTAL NUMBER OF VARIABLES IN THE MODEL 127980
(DEGREES OF FREEDOM PLUS MAX NO. OF ANY LAGRANGE MULTIPLIER
VARIABLES. INCLUDE *PRINT,SOLVE=YES TO GET THE ACTUAL NUMBER.)

USER INPUT PROCESSING

JOB TIME SUMMARY
USER TIME (SEC) = 3.9000
SYSTEM TIME (SEC) = 0.30000
TOTAL CPU TIME (SEC) = 4.2000
WALLCLOCK TIME (SEC) = 10
1

STEP 1 INCREMENT 1
TIME COMPLETED IN THIS STEP 0.00

S T E P 1 S T A T I C A N A L Y S I S

AUTOMATIC TIME CONTROL WITH -
A SUGGESTED INITIAL TIME INCREMENT OF 1.00
AND A TOTAL TIME PERIOD OF 1.00
THE MINIMUM TIME INCREMENT ALLOWED IS 1.000E-05
THE MAXIMUM TIME INCREMENT ALLOWED IS 1.00

LINEAR EQUATION SOLVER TYPE DIRECT SPARSE

M E M O R Y E S T I M A T E

PROCESS	FLOATING PT OPERATIONS PER ITERATION	MINIMUM MEMORY REQUIRED (MBYTES)	MEMORY TO MINIMIZE I/O (MBYTES)
1	1.42E+010	104	460

NOTE:
(1) SINCE ABAQUS DOES NOT PRE-ALLOCATE MEMORY AND ONLY ALLOCATES MEMORY AS NEEDED DURING THE ANALYSIS,
THE MEMORY REQUIREMENT PRINTED HERE CAN ONLY BE VIEWED AS A GENERAL GUIDELINE BASED ON THE BEST
KNOWLEDGE AVAILABLE AT THE BEGINNING OF A STEP BEFORE THE SOLUTION PROCESS HAS BEGUN.
(2) THE ESTIMATE IS NORMALLY UPDATED AT THE BEGINNING OF EVERY STEP. IT IS THE MAXIMUM VALUE OF THE
ESTIMATE FROM THE CURRENT STEP TO THE LAST STEP OF THE ANALYSIS, WITH UNSYMMETRIC SOLUTION TAKEN
INTO ACCOUNT IF APPLICABLE.
(3) SINCE THE ESTIMATE IS BASED ON THE ACTIVE DEGREES OF FREEDOM IN THE FIRST ITERATION OF THE
CURRENT STEP, THE MEMORY ESTIMATE MIGHT BE SIGNIFICANTLY DIFFERENT THAN ACTUAL USAGE FOR
PROBLEMS WITH SUBSTANTIAL CHANGES IN ACTIVE DEGREES OF FREEDOM BETWEEN STEPS (OR EVEN WITHIN
THE SAME STEP). EXAMPLES ARE: PROBLEMS WITH SIGNIFICANT CONTACT CHANGES, PROBLEMS WITH MODEL
CHANGE, PROBLEMS WITH BOTH STATIC STEP AND STEADY STATE DYNAMIC PROCEDURES WHERE ACOUSTIC
ELEMENTS WILL ONLY BE ACTIVATED IN THE STEADY STATE DYNAMIC STEPS.
(4) FOR MULTI-PROCESS EXECUTION, THE ESTIMATED VALUE OF FLOATING POINT OPERATIONS FOR EACH PROCESS

IS BASED ON AN INITIAL SCHEDULING OF OPERATIONS AND MIGHT NOT REFLECT THE ACTUAL FLOATING
POINT OPERATIONS COMPLETED ON EACH PROCESS. OPERATIONS ARE DYNAMICALY BALANCED DURING EXECUTION,
SO THE ACTUAL BALANCE OF OPERATIONS BETWEEN PROCESSES IS EXPECTED TO BE BETTER THAN THE ESTIMATE
PRINTED HERE
(5) THE UPPER LIMIT OF MEMORY THAT CAN BE ALLOCATED BY ABAQUS WILL IN GENERAL DEPEND ON THE VALUE OF
THE "MEMORY" PARAMETER AND THE AMOUNT OF PHYSICAL MEMORY AVAILABLE ON THE MACHINE. PLEASE SEE
THE "ABAQUS ANALYSIS USER'S MANUAL" FOR MORE DETAILS. THE ACTUAL USAGE OF MEMORY AND OF DISK
SPACE FOR SCRATCH DATA WILL DEPEND ON THIS UPPER LIMIT AS WELL AS THE MEMORY REQUIRED TO MINIMIZE
I/O. IF THE MEMORY UPPER LIMIT IS GREATER THAN THE MEMORY REQUIRED TO MINIMIZE I/O, THEN THE ACTUAL
MEMORY USAGE WILL BE CLOSE TO THE ESTIMATED "MEMORY TO MINIMIZE I/O" VALUE, AND THE SCRATCH DISK
USAGE WILL BE CLOSE-TO-ZERO; OTHERWISE, THE ACTUAL MEMORY USED WILL BE CLOSE TO THE PREVIOUSLY
MENTIONED MEMORY LIMIT, AND THE SCRATCH DISK USAGE WILL BE ROUGHLY PROPORTIONAL TO THE DIFFERENCE
BETWEEN THE ESTIMATED "MEMORY TO MINIMIZE I/O" AND THE MEMORY UPPER LIMIT. HOWEVER ACCURATE
ESTIMATE OF THE SCRATCH DISK SPACE IS NOT POSSIBLE.
(6) USING "*RESTART, WRITE" CAN GENERATE A LARGE AMOUNT OF DATA WRITTEN IN THE WORK DIRECTORY.

THE ANALYSIS HAS BEEN COMPLETED

ANALYSIS COMPLETE

JOB TIME SUMMARY
USER TIME (SEC) = 10.800
SYSTEM TIME (SEC) = 0.60000
TOTAL CPU TIME (SEC) = 11.400
WALLCLOCK TIME (SEC) = 19